

Margins for Uncertainty in the Predicted Spent Fuel Isotopic Inventories for BWR Burnup Credit

AVAILABILITY OF REFERENCE MATERIALS IN NRC PUBLICATIONS

NRC Reference Material

As of November 1999, you may electronically access NUREG-series publications and other NRC records at NRC's Library at www.nrc.gov/reading-rm.html. Publicly released records include, to name a few, NUREG-series publications; *Federal Register* notices; applicant, licensee, and vendor documents and correspondence; NRC correspondence and internal memoranda; bulletins and information notices; inspection and investigative reports; licensee event reports; and Commission papers and their attachments.

NRC publications in the NUREG series, NRC regulations, and Title 10, "Energy," in the *Code of Federal Regulations* may also be purchased from one of these two sources.

1. The Superintendent of Documents

U.S. Government Publishing Office
Washington, DC 20402-0001
Internet: bookstore.gpo.gov
Telephone: (202) 512-1800
Fax: (202) 512-2104

2. The National Technical Information Service

5301 Shawnee Road
Alexandria, VA 22312-0002
www.ntis.gov
1-800-553-6847 or, locally, (703) 605-6000

A single copy of each NRC draft report for comment is available free, to the extent of supply, upon written request as follows:

Address: **U.S. Nuclear Regulatory Commission**
Office of Administration
Multimedia, Graphics, and Storage &
Distribution Branch
Washington, DC 20555-0001
E-mail: distribution.resource@nrc.gov
Facsimile: (301) 415-2289

Some publications in the NUREG series that are posted at NRC's Web site address www.nrc.gov/reading-rm/doc-collections/nuregs are updated periodically and may differ from the last printed version. Although references to material found on a Web site bear the date the material was accessed, the material available on the date cited may subsequently be removed from the site.

Non-NRC Reference Material

Documents available from public and special technical libraries include all open literature items, such as books, journal articles, transactions, *Federal Register* notices, Federal and State legislation, and congressional reports. Such documents as theses, dissertations, foreign reports and translations, and non-NRC conference proceedings may be purchased from their sponsoring organization.

Copies of industry codes and standards used in a substantive manner in the NRC regulatory process are maintained at—

The NRC Technical Library

Two White Flint North
11545 Rockville Pike
Rockville, MD 20852-2738

These standards are available in the library for reference use by the public. Codes and standards are usually copyrighted and may be purchased from the originating organization or, if they are American National Standards, from—

American National Standards Institute

11 West 42nd Street
New York, NY 10036-8002
www.ansi.org
(212) 642-4900

Legally binding regulatory requirements are stated only in laws; NRC regulations; licenses, including technical specifications; or orders, not in NUREG-series publications. The views expressed in contractor prepared publications in this series are not necessarily those of the NRC.

The NUREG series comprises (1) technical and administrative reports and books prepared by the staff (NUREG-XXXX) or agency contractors (NUREG/CR-XXXX), (2) proceedings of conferences (NUREG/CP-XXXX), (3) reports resulting from international agreements (NUREG/IA-XXXX), (4) brochures (NUREG/BR-XXXX), and (5) compilations of legal decisions and orders of the Commission and Atomic and Safety Licensing Boards and of Directors' decisions under Section 2.206 of NRC's regulations (NUREG-0750).

DISCLAIMER: This report was prepared as an account of work sponsored by an agency of the U.S. Government. Neither the U.S. Government nor any agency thereof, nor any employee, makes any warranty, expressed or implied, or assumes any legal liability or responsibility for any third party's use, or the results of such use, of any information, apparatus, product, or process disclosed in this publication, or represents that its use by such third party would not infringe privately owned rights.

Margins for Uncertainty in the Predicted Spent Fuel Isotopic Inventories for BWR Burnup Credit

Manuscript Completed: June 2018
Date Published: December 2018

Prepared by:
I. Gauld
U. Mertyurek

Oak Ridge National Laboratory
Bethel Valley Road
Oak Ridge, TN 37831

Mourad Aissa, NRC Project Manager

ABSTRACT

US Nuclear Regulatory Commission staff guidance on burnup credit for spent fuel storage and transportation is currently limited to spent fuel assemblies from pressurized water reactors. This report describes research to develop a technical basis to expand burnup credit to boiling water reactors (BWRs). One of the largest components of uncertainty in burnup credit analyses is the predicted isotopic inventories of spent fuel as applied to the criticality safety analysis application model. The analysis of BWR fuel inventories is challenging due to the complexity of BWR assembly designs, the lack of publicly available radiochemical assay measurements, and limited access to documentation on fuel design and operating conditions. This study has compiled and evaluated experimental data on measured nuclide concentrations in commercial spent fuel for more than 75 fuel samples that cover a wide range of modern assembly designs and operating conditions. These data were applied to predict the net effect of isotopic uncertainties on the effective neutron multiplication factor for a representative spent nuclear fuel storage system. The experimental data, uncertainty analysis methodology, and results for a dry storage cask application system are described. The uncertainty analysis methodology presented in this report is independent of the depletion analysis code and the application model and can be easily adopted to estimate margins of uncertainty for other codes, nuclear data libraries, and application models. The results are only applicable to BWR burnup credit beyond peak reactivity where any initial gadolinium present in the fuel has been fully depleted.

TABLE OF CONTENTS

ABSTRACT	iii
LIST OF FIGURES	vii
LIST OF TABLES.....	ix
EXECUTIVE SUMMARY	xi
ABBREVIATIONS AND ACRONYMS	xiii
1 INTRODUCTION	1-1
2 BURNUP CREDIT ANALYSIS METHODOLOGY	2-1
3 NUCLIDES IMPORTANT TO BURNUP CREDIT.....	3-1
4 CODE AND MODELLING DESCRIPTIONS.....	4-1
4.1 Depletion Analyses.....	4-1
4.2 Criticality Analyses	4-2
4.3 Nuclear Data Libraries.....	4-3
5 EXPERIMENTAL ASSAY DATA	5-1
5.1 Dodewaard (6 × 6)	5-2
5.2 Forsmark 3 SVEA-100 (10 × 10)	5-5
5.3 Forsmark 3 GE14 (10 × 10).....	5-8
5.4 Fukushima Daini 1 (9 × 9-9).....	5-11
5.5 Fukushima Daini 2 (8 × 8-2).....	5-14
5.6 Fukushima Daini 2 GE9 (8 × 8-4)	5-17
5.7 Leibstadt SVEA-96 (10 × 10)	5-19
5.8 Limerick 1 GE11 (9 × 9-7).....	5-22
5.9 Quad Cities GE11 (9 × 9).....	5-25
6 CRITICALITY APPLICATION MODELS	6-1
6.1 GE14 Assembly.....	6-1
6.2 GBC-68 Cask	6-2
7 UNCERTAINTY ANALYSIS	7-1
7.1 Methodology.....	7-1
7.1.1 Measurements	7-1
7.1.2 Measurement dates	7-2
7.1.3 Partial Isotopic Datasets	7-3
7.2 Isotopic Bias and Uncertainty.....	7-4
7.3 Criticality Calculations	7-9
7.4 Experimental Correlations.....	7-16
7.5 Isotopic Model Uncertainties	7-16
7.5.1 Measurements	7-16
7.5.2 Void	7-16
7.5.3 Fuel Temperature.....	7-17
7.5.4 Sample Burnup	7-17
7.5.5 Summary of Model Uncertainties	7-18
7.6 Trending Analysis.....	7-18
7.6.1 Trends with Fuel Burnup.....	7-19

7.6.2 Trends with Moderator Void.....	7-21
7.6.3 Trends with Fuel Reactivity.....	7-21
7.7 Margins for Isotopic Uncertainty.....	7-24
8 SUMMARY AND CONCLUSIONS.....	8-1
9 REFERENCES	9-1
APPENDIX A MEASURED NUCLIDE CONCENTRATIONS IN SPENT FUEL SAMPLES	A-1
APPENDIX B COMPARISON OF POLARIS-CALCULATED NUCLIDE COMPOSITIONS WITH MEASUREMENTS	B-1
APPENDIX C POLARIS MODEL INPUT FILES	C-1

LIST OF FIGURES

Figure 1	Overview of the Burnup Credit Validation Process [6].....	2-2
Figure 2	Polaris Lattice Physics Calculation Flow [26]	4-2
Figure 3	Polaris Model of Dodewaard 6 × 6 Assembly.....	5-4
Figure 4	Polaris Model of Forsmark Unit 3 SVEA-100 Assembly.....	5-7
Figure 5	Polaris Model of Forsmark Unit 3 GE14 10 × 10 Assembly	5-10
Figure 6	Polaris Model of the Fukushima Daini-1 9 × 9-9 Assemblies	5-14
Figure 7	Polaris Model of the Fukushima Daini-2 8 × 8-2 Assemblies	5-16
Figure 8	Polaris Model of the Fukushima Daini-2 8 × 8-4 Assemblies	5-19
Figure 9	Polaris Model of Leibstadt SVEA-96 10 × 10 Assembly.....	5-21
Figure 10	Polaris Model of Limerick-1 GE11 9 × 9 Assembly	5-24
Figure 11	(a) DOM and (b) VAN Lattice of the GE14 Assembly (Shown in a Dry Cask Storage Cell).....	6-1
Figure 12	Radial View of the KENO V.a GBC-68 Cask Model (Elevation of Vanished Lattice).....	6-3
Figure 13	Uncertainty Analysis Methodology for Nuclide Compositions (Adapted from [19]).....	7-3
Figure 14	Box Plot of the Major Actinide Isotopes.....	7-6
Figure 15	Box Plot of the Minor Actinides and Fission Products (Mo, Tc, Ru, Ag, and Rh).....	7-7
Figure 16	Box Plot of the Fission Products (Nd, Cs, Sm, Eu, and Gd).....	7-8
Figure 17	k_{eff} Bias for Actinide-Only and Actinide-Plus-Fission Products Results	7-15
Figure 18	k_{eff} Bias for Actinide-Only (top) and Actinide-Plus-Fission Products (bottom) Results as a Function of fuel Burnup Showing Mean (red) and 95% LTL Band (blue)	7-20
Figure 19	k_{eff} Bias for Actinide-Only (bottom) and Actinide-Plus-Fission Products (top) Results as a Function of Moderator Void Showing Mean (red) and 95% LTL Band (blue).....	7-22
Figure 20	k_{eff} Bias for Actinide-Only (bottom) and Actinide-Plus-Fission Products (top) Results as a Function of Application k_{eff} Showing Mean (red) and 95% LTL Band (blue).....	7-23

LIST OF TABLES

Table 1	Major Actinides Considered in Burnup Credit Criticality Analyses.....	3-1
Table 2	Actinides and Fission Products Important to Burnup Credit Criticality Analyses	3-1
Table 3	Summary of BWR Spent Fuel Samples	5-1
Table 4	Summary of Dodewaard 6 × 6 Assembly Fuel Sample Measurements	5-3
Table 5	Dodewaard 6 × 6 Assembly Parameters.....	5-5
Table 6	Summary of Forsmark Unit 3 SVEA-100 10 × 10 Assembly Fuel Sample Measurements.....	5-6
Table 7	Forsmark 3 SVEA-100 Assembly Parameters	5-8
Table 8	Summary of Forsmark Unit 3 GE14 10 × 10 Assembly Fuel Sample Measurements.....	5-9
Table 9	Forsmark 3 GE14 10 × 10 Assembly Parameters [41].....	5-11
Table 10	Summary of Fukushima Daini-1 9 × 9-9 Assembly Fuel Sample Measurements	5-12
Table 11	Fukushima Daini-1 9 × 9-9 Assembly Parameters	5-13
Table 12	Summary of Fukushima Daini-1 8 × 8-2 Assembly Fuel Sample Measurements	5-15
Table 13	Fukushima Daini-2 8 × 8-2 and 8 × 8-4 Assembly Parameters.....	5-17
Table 14	Summary of Fukushima Daini-2 8 × 8-4 Assembly Fuel Sample Measurements	5-18
Table 15	Summary of Leibstadt SVEA-96 10 × 10 Assembly Fuel Sample Measurements.....	5-20
Table 16	Leibstadt SVEA-96 10 × 10 Assembly Parameters.....	5-22
Table 17	Summary of Limerick GE11 9 × 9 Assembly Measurements	5-23
Table 18	Limerick-1 GE11 9 × 9 Assembly Parameters.....	5-25
Table 19	Statistical Analysis of Predicted Isotopic Concentrations (C/M-1) (%)	7-5
Table 20	Criticality Results for the GBC-68 Cask Model for Major Actinide-Only Compositions.....	7-11
Table 21	Criticality Results for the GBC-68 Cask Criticality Analysis Model for Actinide and Fission Product Spent Fuel Compositions.....	7-13
Table 22	Summary of Uncertainties	7-18
Table 23	Summary of Bias and Uncertainties for Trending Parameters	7-24

EXECUTIVE SUMMARY

Applicants for certificates of compliance for spent nuclear fuel transportation and dry storage systems perform analyses to demonstrate that these systems are adequately subcritical per the requirements of Title 10 of the Code of Federal Regulations (10 CFR) Parts 71 and 72. For spent fuel from pressurized water reactors, these analyses may credit the reduction in assembly reactivity caused by depletion of fissile nuclides and buildup of neutron-absorbing nuclides during power operation. This credit for reactivity reduction during depletion is commonly referred to as burnup credit. US Nuclear Regulatory Commission (NRC) staff review burnup credit analyses according to the guidance in the Division of Spent Fuel Storage and Transportation Interim Staff Guidance (ISG) 8, Revision 3, Burnup Credit in the Criticality Safety Analyses of PWR Spent Fuel in Transportation and Storage Casks. However, currently no equivalent guidance exists for boiling water reactor (BWR) spent fuel.

The technical basis for BWR burnup credit, beyond the burnup region of peak reactivity, is presently being evaluated by the NRC. A key element of the burnup credit analysis methodology is the validation of the depletion codes used to calculate the nuclide compositions of the spent fuel that are used in the criticality safety calculations. This step is usually performed by comparing calculated nuclide concentrations with measured values obtained from destructive assay of spent fuel samples. These comparisons can be used to develop margins for uncertainty in the criticality calculation that are associated with the calculated nuclide compositions.

Previous studies to validate nuclide predictions for BWR fuels have been limited by a lack of well-documented destructive assay data and measurements for modern BWR assembly designs. Spent fuel measurements previously considered for BWR isotopic validation included early 6×6 and 7×7 BWR assemblies with low enrichments and designs that lacked the heterogeneity of modern BWR assemblies. Moreover, the void conditions for these older assemblies were not reported. The restricted availability of public sources of BWR data is due in part to the proprietary nature of the newer assembly designs, enrichment configurations, and operating conditions in the reactor.

The present analysis uses an expanded experimental database of destructive radiochemical assay measurements that include detailed design and operating history information. Most of these data were made publicly available by the Japan Atomic Energy Agency (JAEA) and the Japan Nuclear Regulation Authority (NRA). These data and reference reports have been documented in a recently released database of spent fuel compositions developed through international cooperation activities of the Organisation for Economic Co-operation and Development (OECD) Nuclear Energy Agency (NEA). These data cover several 8×8 and 9×9 fuel assembly designs.

In addition to the data contributed by Japan, this work applies measurements for a modern General Electric (GE) GE14 10×10 fuel assembly made under a proprietary experimental program coordinated by the Spanish fuel manufacturer ENUSA Industrias Avanzadas, S.A. and the Spanish Nuclear Safety Council, Consejo de Seguridad Nuclear (CSN). Data were obtained for a SVEA-96 10×10 assembly from the proprietary MALIBU experimental program coordinated by the Belgian Nuclear Research Center (SCK•CEN), and additional data for a GE11 9×9 assembly design were obtained from measurements made under the US Department of Energy Office of Civilian Radioactive Waste Management (OCRWM) Yucca Mountain project. These data provide an improved experimental basis for the evaluation of BWR nuclide compositions uncertainties by including modern heterogeneous assembly designs, expanded isotopic measurements, and more complete reactor operating history information.

These experimental data are applied in this report to develop margins for uncertainty in burnup credit criticality calculations associated with the calculation of nuclide compositions for BWR spent fuel. A total of 77 spent fuel measurements are used in this analysis that cover a wide range of assembly designs including 8 × 8-2, 8 × 8-4, 9 × 9-7, 9 × 9-9, GE11 9 × 9, GE14 10 × 10, SVEA-96 and SVEA-100 10 × 10 designs. The void fractions extend to 74% with a burnup range from 7 to 68 GWd/MTU.

The uncertainty analysis methodology applied in the present research is based on the direct application of measured nuclide concentrations to a criticality application model for each measured spent fuel sample. Separately, nuclide concentrations are calculated for each sample and applied to the same application model. Margins for uncertainty are then developed by a statistical analysis of the distributions of the difference in measured and calculated k_{eff} results for all samples. This validation approach is largely independent of the depletion and criticality computational methods and safety analysis application model.

This analysis approach is demonstrated in this report using SCALE 6.2.2. with ENDF/B-VII.1 cross section data. Specifically, depletion calculations were performed using the Polaris code and criticality calculations were performed using KENO V.a. Margins for uncertainty associated with the predicted nuclide compositions are developed for a GBC-68 dry storage cask model. Therefore, the results presented here are specific to this code system and application model but are expected to be similar for other comparable dry storage and transportation cask designs, when using same computer codes and cross section data.

A margin for uncertainty is developed using the 95% one-sided lower tolerance limit (LTL) for the population of data, and trending analysis is performed for sample burnup, average void, and k_{eff} of the application model. For the Polaris calculations and the GBC-68 application model used in the present study, the k_{eff} bias for actinide-only calculations is determined to be 253 pcm with a maximum margin for isotopic uncertainty of 2,170 pcm for the range of fuel samples included in the current analysis. This margin is observed to be largely independent of fuel burnup or void fraction based on the analysis of available experimental data. For actinide-plus-fission product calculations, the k_{eff} bias is 161 pcm and the maximum margin for isotopic uncertainty is 2,390 pcm.

These results are similar to those seen in previous studies for PWR burnup credit, where average biases for a dry storage cask of 320 to 720 pcm and uncertainties of 1,430 to 2,050 pcm were reported for fuel with a burnup less than 50 GWd/MTU. The larger uncertainties seen in the present study are likely attributed to the increased complexity of the BWR fuel and larger uncertainties in the reactor operating data used in the models.

ABBREVIATIONS AND ACRONYMS

ARIANE	Actinides Research In A Nuclear Element
BWR	boiling water reactor
C/M	calculated-to-measurement (ratio)
CSN	Consejo de Seguridad Nuclear (Spanish Nuclear Safety Council)
DOE	US Department of Energy
DOM	full lattice
ENUSA	Spanish fuel manufacturer ENUSA Industrias Avanzadas, S.A
ESSM	embedded self-shielding method
GBC	generic burnup credit (cask design)
GE	General Electric
HPLC	high performance liquid chromatography
ICPMS	inductively coupled plasma mass spectrometry
IDA	isotopic dilution analysis
IDMS	isotope dilution mass spectrometry
JAEA	Japan Atomic Energy Agency
JAERI	Japanese Atomic Energy Research Institute
JNES	Japan Nuclear Energy Safety Organization
JPDR	Japanese Power Demonstration Reactor
LCE	laboratory critical experiment
LTL	lower tolerance limit
LWR	light water reactor
MALIBU	MOX and UOX LWR Fuels Irradiated to High Burnup
MG	multi-group
MOC	method of characteristics
MOX	mixed oxide fuel
MS	mass spectrometry
MTU	metric ton uranium (10^6 grams)
NEA	Nuclear Energy Agency
NRA	Nuclear Regulation Authority of Japan
NRC	US Nuclear Regulatory Commission
OCRWM	Office of Civilian Radioactive Waste Management
OECD	Organization for Economic Cooperation and Development
ORNL	Oak Ridge National Laboratory
PNNL	Pacific Northwest National Laboratory
PSI	Paul Scherrer Institute
PWR	pressurized water reactor
RCA	radiochemical assay
SCALE	Nuclear analysis modeling and simulation code suite
SCK•CEN	Studiecentrum voor Kernenergie - Centre d'étude de l'Energie Nucléaire
SFCOMPO	Spent Fuel Isotopic Composition Database
TEPCO	Tokyo Electric Power Company
TIMS	thermal ionization mass spectrometry

VAN vanished lattice
WPNCS Working Party on Nuclear Criticality Safety
YMP Yucca Mountain Project

1 INTRODUCTION

Interim Staff Guidance 8 [1] on the implementation of burnup credit for storage and transportation systems (ISG-8 rev. 3) issued in 2012 by the US Nuclear Regulatory Commission (NRC) applies only to pressurized water reactor (PWR) fuel assemblies. There has been less incentive to take credit for fuel burnup in criticality safety analyses for boiling water reactor (BWR) assembly designs in dry storage and transportation casks because the benefit of burnup credit in increasing cask loading capacity is less significant and the assembly designs and reactor operations of BWRs are more complex compared to PWR assemblies. However, as the enrichments of BWR assemblies have increased from a median of about 2.8 wt% ^{235}U in 1990 to more than 4.0 wt% in 2013 [2], application of burnup credit in criticality safety analyses can provide increased enrichment capacity and/or reduced neutron absorber concentration, and it can also demonstrate subcriticality of reconfigured spent fuel in transportation packages.

Consequently, criticality safety bases for BWR spent fuel transportation/storage casks using burnup credit are currently being developed by the nuclear industry.

Burnup credit requires, as part of the analysis methodology, that the concentrations of the spent fuel nuclides being credited in the criticality safety analysis be calculated using isotopic depletion codes. This step of the analysis procedure introduces uncertainties that must be accurately quantified using measurement data in order to develop conservative margins in the analysis that account for this uncertainty. The uncertainty due to predicted nuclide concentrations represents an important component of the total uncertainty in criticality calculations using burnup credit.

The purpose of this report is to present a general methodology to assess the uncertainties associated with calculated nuclide compositions and develop margins for the associated aggregate uncertainty in the neutron multiplication factor (k_{eff}) for criticality calculations. Other components of k_{eff} uncertainty in BWR burnup credit criticality safety calculations are addressed in separate reports [3].

Previous studies to validate nuclide predictions for BWR fuels [4]–[7] have been limited by a lack of well-documented measurements of spent fuel compositions and representative assembly designs and operating information. The restricted availability of public sources of BWR spent fuel assay data for validation for modern assembly designs and enrichments is due in part to the commercial proprietary nature of the newer assembly designs, enrichment configurations, and operating conditions in the reactor. Spent fuel measurements previously considered for BWR isotopic validation included early 6×6 and 7×7 BWR assemblies with low enrichments and designs that lacked the heterogeneity of modern BWR assemblies. Moreover, the axial void conditions for these older assemblies were not reported. Measurements of an 8×8 BWR assembly from the Fukushima Daini-2 reactor were reported by the Japan Atomic Energy Agency (JAEA) with void information included [8]; these data were also used in the earlier studies.

The present analysis uses an expanded experimental database obtained using destructive radiochemical assay measurements and more detailed operating history information. Extensive measurements from experiments performed in Japan were recently made publicly available by the Japan Nuclear Regulation Authority (NRA) through international cooperation activities of the Organisation for Economic Co-operation and Development (OECD) Nuclear Energy Agency (NEA) Working Party on Nuclear Criticality Safety (WPNCs) [9]. These data and experimental references are documented in an OECD/NEA database of spent fuel compositions [10].

In addition to the public data contributed by Japan, this work applies measurements for a modern General Electric (GE) GE14 10 × 10 fuel assembly made under a proprietary experimental program coordinated by the Spanish fuel manufacturer ENUSA Industrias Avanzadas, S.A. and the Spanish Nuclear Safety Council, Consejo de Seguridad Nuclear (CSN) [11]. Data were obtained for a SVEA-96 10 × 10 assembly from the proprietary MALIBU experimental program coordinated by the Belgian Nuclear Research Center (SCK•CEN) [12]. Additional data for a GE11 9 × 9 assembly design were obtained from measurements made under the US Department of Energy Office of Civilian Radioactive Waste Management (OCRWM) Yucca Mountain project [13]. These data provide an improved experimental basis for the evaluation of BWR isotopic uncertainties by including modern heterogeneous assembly designs, expanded isotopic measurements, and more complete reactor operating history information.

The validation approach in this report is independent of the depletion and criticality computational methods and safety analysis application model. The range of application includes fuel burnup beyond peak reactivity that is associated with the use of fuel containing gadolinium oxide (Gd_2O_3) or other integral neutron absorbers. Analyses are included that take credit in the criticality safety calculations for the major actinides in spent fuel with and without the addition of minor actinides and principal fission products. The uncertainty in k_{eff} due to biases and uncertainties in calculated nuclide concentrations is presented based on analyses performed with the Polaris lattice physics code [14] in SCALE 6.2.2 [15] and Evaluated Nuclear Data File/B Version VII.1 (ENDF/B-VII.1) nuclear cross section and decay data [16]. Criticality calculations were performed using the KENO V.a Monte Carlo neutron transport code and the 252-energy group ENDF/B-VII.1 cross section library available in SCALE 6.2.2.

This report presents an overview of the burnup credit analysis methodology in Section 2 that identifies the main components of the depletion and criticality validation methodology. The isotopes that are considered in burnup credit are discussed in Section 3. Section 4 describes the computational methods and nuclear data used in the depletion calculations applied in this report. The experimental isotopic assay data used to validate the computational codes are presented in Section 5. Representative application models for BWR spent fuel assemblies and a dry storage cask are described in Section 6. Section 7 presents an analysis of k_{eff} bias and uncertainty results based on SCALE 6.2.2 for the application model. Conclusions are provided in Section 8. Appendices A, B and C provide measured nuclide concentrations used in this report, comparisons of measurements to Polaris calculated concentrations, and sample Polaris input files for different lattice types.

2 BURNUP CREDIT ANALYSIS METHODOLOGY

Criticality safety analyses are performed to demonstrate that a proposed fuel storage or transport configuration meets the applicable requirements of Title 10, Code of Federal Regulations (CFR), Parts 71 and 72 [17]. A general overview of the process for implementing burnup credit for criticality safety analyses is outlined in Figure 1. The process includes development of safety analysis models considering a range of parameters important to criticality safety and isotopic and criticality validation analyses to demonstrate that the proposed configuration will meet the maximum k_{eff} limits specified in the applicable requirements and guidance.

This report addresses only the uncertainty component associated with the predicted isotopic inventory used in burnup credit calculations beyond peak reactivity.

The methods used to calculate the burnup credit nuclide compositions are usually validated through comparisons to measured radiochemical assay (RCA) data. The validation steps addressed in this report cover items (5) through (7) in Figure 1. The criticality validation addresses items (8) through (15) in Figure 1. In this report, the consensus terminology from ANSI/ANS-8.27 [18] is used.

The criterion for establishing subcriticality with credit for the reactivity decrease due to fuel burnup requires the calculated multiplication factor k_p plus allowances for biases and uncertainties shall be equal to or less than an established, allowable neutron multiplication factor; that is,

$$k_p + \Delta k_p + \beta_i + \Delta k_i + \beta + \Delta k_\beta + \Delta k_x + \Delta k_m \leq k_{limit}, \quad (1)$$

where

k_p is the calculated multiplication factor of the model for the system being evaluated;

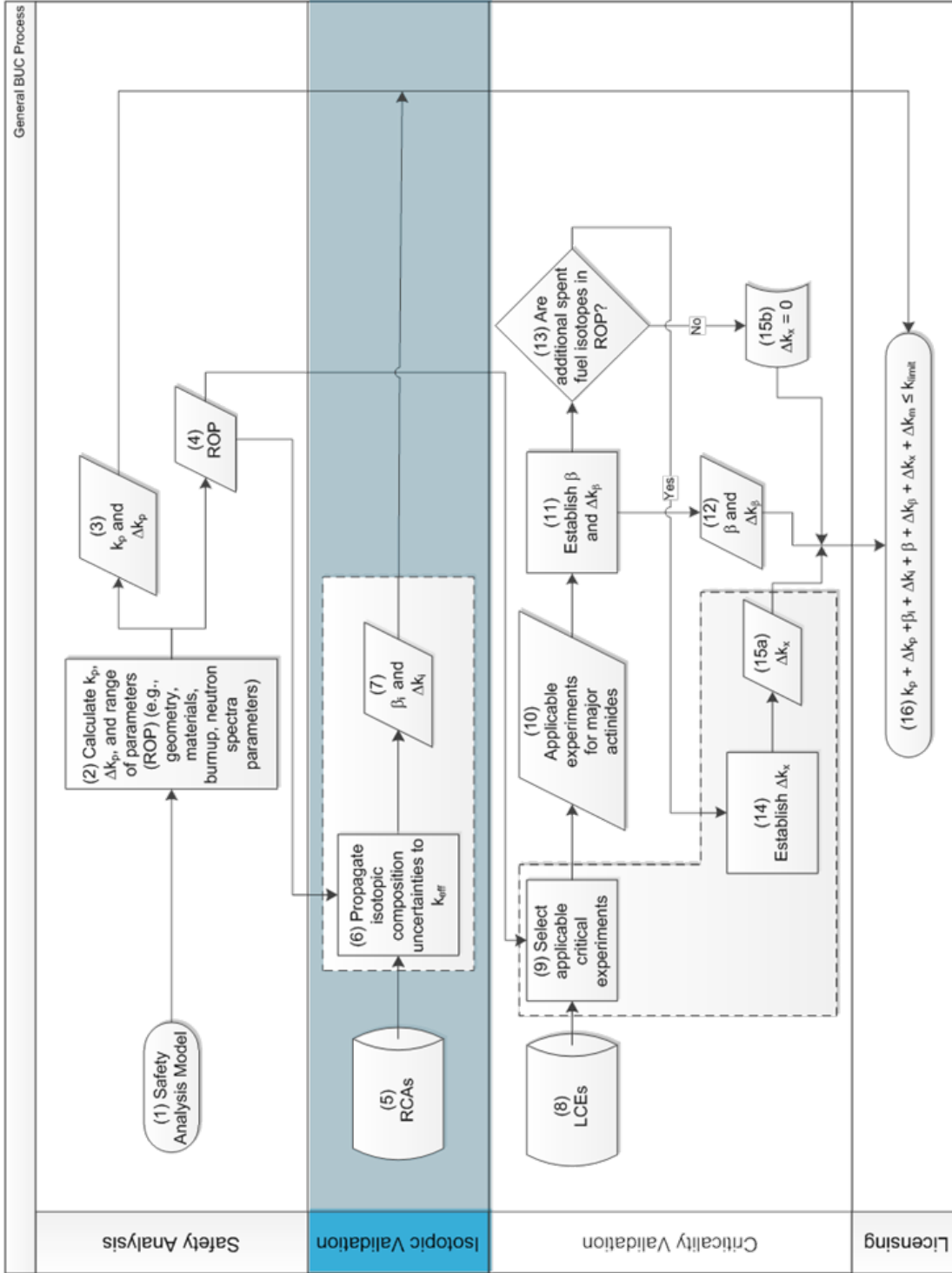
Δk_p is an allowance for

- statistical or convergence uncertainties, or both, in the determination of k_p ,
- material and fabrication tolerances, and
- uncertainties due to geometric or material representation limitations of the models used in the determination of k_p ;

β_i is the bias in k_p due to depletion code bias in the calculated nuclide concentrations;

Δk_i is the bias uncertainty in k_p due to depletion code bias uncertainty in the calculated nuclide concentrations;

β is the bias that results from using a particular calculation method and nuclear cross section data to calculate k_{eff} values for benchmark criticality experiments;



RCA: Radiochemical Assay
 LCE: Laboratory Critical Experiment

Figure 1 Overview of the Burnup Credit Validation Process [6]

Δk_β is the criticality bias uncertainty, which includes

- statistical or convergence uncertainties, or both, in the computation of β ,
- uncertainties in the benchmark criticality experiments,
- uncertainty in the bias resulting from application of the linear least-squares fitting technique to the critical experiment results, and
- tolerance interval multiplier to yield a single-sided 95% probability and 95% confidence level;

Δk_x is a supplement to β and Δk_β that may be included to provide an allowance for the bias and uncertainty from nuclide cross section data that might not be adequately accounted for in the benchmark criticality experiments used for calculating β ;

Δk_m is a margin for unknown uncertainties deemed to be adequate to ensure subcriticality of the physical system being modeled (this term is typically referred to as an administrative margin); and

k_{limit} is the upper limit on the k_{eff} value for which the system is considered safe.

The validation approach using measured nuclide concentrations requires that fuel samples are available for representative assembly designs and operating conditions and that measured nuclide concentrations are available for the actinide and/or fission products being credited in the criticality safety application model.

Several approaches for propagating isotopic composition uncertainty to k_{eff} uncertainty have been developed and demonstrated [20], each involving different levels of analysis complexity and having different degrees of conservatism. The approach used in the present study analysis has three steps. In the first step, the calculated isotope concentrations for each measured fuel sample are used in the criticality application model to determine the k_{eff} . This step is performed without any adjustment of the model parameters for conservatism and with no accounting for bias or uncertainty in the calculated concentrations. In the second step, the measured isotopic concentrations for each sample are applied in the criticality model to obtain the k_{eff} . The difference between the k_{eff} values obtained using calculated nuclide compositions in the model, k_c , and measured nuclide composition in the model, k_m , is a direct measure of the k_{eff} bias, β_i , due to the depletion calculation code for that sample.

By analyzing a significant number of spent fuel samples with variable enrichments, burnup, and void conditions, the behavior of the k_{eff} bias can be statistically estimated for the range of fuel parameters and the k_{eff} bias, β_i , and uncertainty in the bias, Δk_i , can be determined for the application system. This last step is referred to as the propagation of isotopic composition uncertainties to k_{eff} and is identified as step (6) in Figure 1.

The significant benefit of this approach is that the bias and uncertainty in each individual nuclide do not need to be determined. Since nuclide concentrations as calculated from depletion codes and measured data are applied directly in criticality calculations, correlations in the nuclide bias associated with both the measurements and the calculations for each sample are implicitly addressed by this approach. This method also avoids the complexity of Monte Carlo sampling of individual nuclide uncertainties that has been applied previously [6]. A limitation of the present

approach is that criticality calculations are restricted to the fuel compositions for each sample that have been measured. Therefore, this approach does not address cases of variability of fuel compositions in the models, such as axial burnup distributions variations due to zoned assembly enrichments.

This methodology is similar to an approach applied previously under the Department of Energy OCRWM in support of post-closure criticality safety assessments for the Yucca Mountain Project [19]. However, these previous studies applied bounding input parameters in the depletion analysis in order to provide conservative estimates of the nuclide compositions. The current work performs the depletion calculations for each sample using the best available design and operating parameters without conservatism. In addition, the previous work did not account for burnup credit nuclides that were not measured in some spent fuel samples, resulting in a different set of nuclides being credited in different samples. The current work applies estimates of the concentrations for isotopes that were not measured based on results for samples that did measure those isotopes. Additional uncertainty introduced by this procedure is estimated.

A limitation of the approach of using isotopic destructive RCA measurements to validate the depletion calculations is that the calculations require, as input, data that can have large uncertainties. In particular, unlike PWR assemblies where the properties of the water moderator are relatively well known, the moderator void fractions for BWR assemblies are not well known. Void fraction is not measured directly but is obtained from core follow codes that predict the neutronic and thermal-hydraulic behavior of the reactor. These codes provide data on a spatial average (nodal) level sufficient to model core behavior and fuel management. However, when applied to the analysis of individual fuel rods, larger uncertainties may be introduced. Average nodal data do not account for spatial variations of void fraction within an assembly and average void fractions may not be representative of the moderator environment in the proximity of the measured fuel samples. Consequently, the modeling uncertainties for BWR fuel are expected to be larger than for PWR fuel.

Other uncertainties in the methodology include the burnup of the measured fuel sample and the accuracy of the assay measurements themselves. The sample burnup is estimated using measured burnup indicator nuclides that can have large measurement uncertainties. Additionally, there can be inconsistencies between different burnup indicators. The impact of these modeling uncertainties is discussed further in the report.

In practice, criticality calculations are usually performed using spent fuel nuclide compositions calculated using conservative depletion (operational) parameters to ensure conservative estimates of the nuclide inventory. The purpose of this report is to develop additional margins for the uncertainty associated with the code calculations themselves by using experiments with well documented operating parameters.

3 NUCLIDES IMPORTANT TO BURNUP CREDIT

The burnup credit analysis methodology presented in this report considers spent fuel compositions consisting of 12 actinide and 16 fission product nuclides selected on the basis of their importance to fuel reactivity (i.e., nuclides with the largest macroscopic neutron fission cross sections and neutron absorption cross sections) and on the basis of the chemical volatility of the isotope that may cause it to be released from the fuel. These nuclides are frequently categorized as the nine major actinides (Table 1) and 28 major actinides, minor actinides, and major fission product nuclides (Table 2). The burnup credit nuclides have been identified in previous studies as having the most significant effects on k_{eff} for burnup credit analyses related to dry cask storage and transportation of PWR and BWR fuel assemblies [21].

These 28 nuclides are commonly considered in burnup credit criticality safety analyses that base validation of calculated nuclide concentrations on comparisons to available assay data. Of the 16 fission products listed in Table 2, ^{149}Sm , ^{151}Sm , ^{143}Nd , ^{103}Rh , ^{133}Cs , and ^{155}Gd have the largest reactivity impact. Credit for fission product nuclides has been limited in the past by the relatively small number of measurements available for BWR fuel. The burnup credit nuclides are stable or very long lived with the exception of ^{151}Sm ($T_{1/2} = 90$ years), ^{238}Pu ($T_{1/2} = 87.7$ years), ^{241}Pu ($T_{1/2} = 14.4$ years), and ^{241}Am ($T_{1/2} = 432.7$ years).

The reactivity of commercial spent fuel increases immediately after discharge due to the reduction in ^{135}Xe and other short-lived fission products. Starting at approximately 3 days after discharge, the reactivity decreases largely due to the decay of the fissile nuclide ^{241}Pu leading to ^{241}Am (neutron absorber) and to the formation of ^{155}Gd (a strong large neutron absorber) from the decay of ^{155}Eu ($T_{1/2} = 4.75$ years). After approximately 100 years, the reactivity begins to increase due primarily to the decay of ^{241}Am and ^{240}Pu ($T_{1/2} = 6,560$ years).

Table 1 Major Actinides Considered in Burnup Credit Criticality Analyses

^{234}U	^{235}U	^{238}U	^{238}Pu	^{239}Pu	^{240}Pu	^{241}Pu	^{242}Pu	^{241}Am
------------------	------------------	------------------	-------------------	-------------------	-------------------	-------------------	-------------------	-------------------

Table 2 Actinides and Fission Products Important to Burnup Credit Criticality Analyses

^{234}U	^{235}U	^{236}U	^{238}U	^{237}Np	^{238}Pu	^{239}Pu
^{240}Pu	^{241}Pu	^{242}Pu	^{241}Am	^{243}Am	^{95}Mo	^{99}Tc
^{101}Ru	^{103}Rh	^{109}Ag	^{133}Cs	^{143}Nd	^{145}Nd	^{147}Sm
^{149}Sm	^{150}Sm	^{151}Sm	^{152}Sm	^{151}Eu	^{153}Eu	^{155}Gd

4 CODE AND MODELLING DESCRIPTIONS

A variety of computer codes and nuclear data libraries can be used to perform burnup credit criticality safety analyses. Fuel depletion calculations are typically performed by industry using two-dimensional (2D) lattice physics models of an assembly to calculate fuel compositions. Widely used codes in the United States include SCALE [15], CASMO [22], and PARAGON [23]. Spent fuel compositions obtained with these codes are then used in criticality codes such as KENO in SCALE or MCNP [24] to determine the k_{eff} for the application system.

All depletion and criticality calculations in the present study were performed using codes and nuclear data libraries in SCALE 6.2.2, which is available publicly through the Radiation Safety Information Computational Center (RSICC) as package CCC-834. SCALE 6.2.2 is the first version that contains BWR modeling capabilities in the Polaris code for a large variety of assembly designs.

4.1 Depletion Analyses

Polaris is a new module introduced in SCALE 6.2 that provides 2D lattice physics analysis with pin-by-pin depletion capability for production calculations of light water reactor (LWR) fuel assembly designs. A detailed description of the methods and calculational approach of Polaris is provided by Jesse et al. [14]. Polaris provides a multigroup (MG) neutron transport capability coupled with the ORIGEN module to solve the time-dependent transmutation equations and isotopic evolution of materials during irradiation and decay.

Polaris was developed as a more efficient transport and depletion code for LWR analyses, compared to the general-purpose TRITON depletion capability in SCALE that uses one-dimensional (XS DRN), 2D (NEWT), or three-dimensional (KENO) neutron transport solutions. For the neutron transport calculation, Polaris employs the method of characteristics (MOC) which solves the characteristic transport equation over a set of equally spaced particle tracks across the lattice geometry. Polaris also provides an easy-to-use input format allowing users to set up lattice models with a minimal amount of input compared to TRITON requirements.

An efficient embedded self-shielding method (ESSM) is used in Polaris for resonance self-shielding of all fuel rods in an assembly [25]. ESSM is similar to the subgroup method where self-shielding effects due to neighboring fuel pins, guide tubes, water rods, and assembly structures are accounted for in the calculation. ESSM neglects resonance interference between resonance-absorbing nuclides in the same material. Cross section self-shielding is performed automatically to account for changes in the moderator void fraction and other operating conditions during the depletion analysis. In previous depletion studies for BWR fuel performed using TRITON, Dancoff factors used for resonance cross section corrections had to be calculated externally, usually with the MCDANCOFF code in SCALE, or an equivalent code, and applied manually as input to the model. When the Dancoff factors changed during irradiation due to variations in the moderator void and burnup, updating the factors required halting the calculation, saving the intermediate nuclide concentrations, inputting new Dancoff factors, and restarting the case. This procedure is performed internally in Polaris.

Within Polaris, the ORIGEN code is used to calculate time-dependent concentrations, activities, and radiation source terms for a large number of isotopes simultaneously generated or depleted by neutron transmutation, fission, and radioactive decay.

Polaris has been validated for reactor physics lattice calculations [26]. Comparisons of Polaris and TRITON results generally show consistent accuracies. The present study represents the first application of Polaris for extensive BWR isotopic validation.

The Polaris calculation flow is shown in Figure 2.

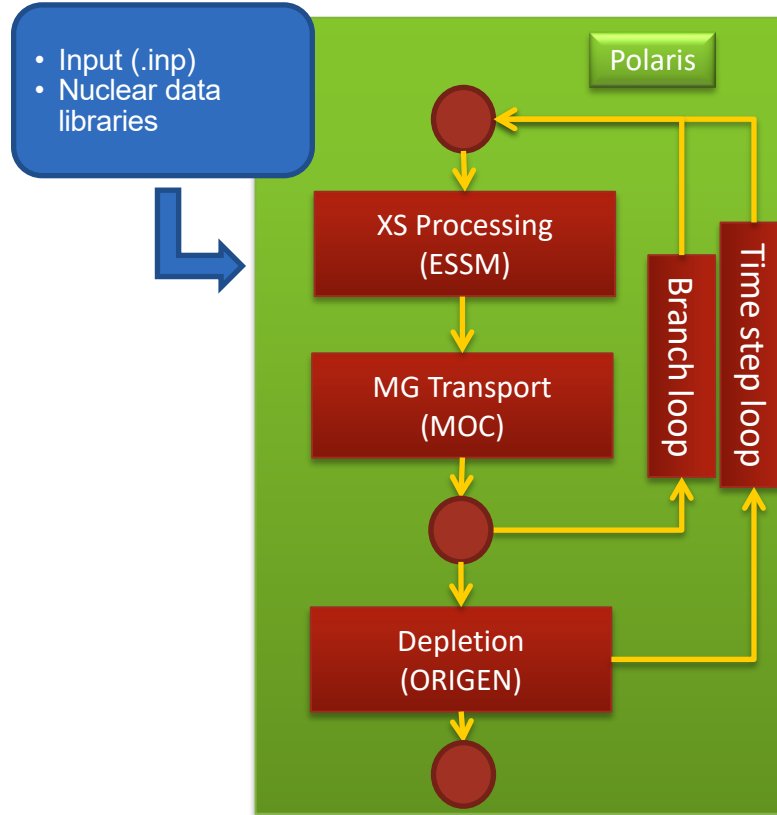


Figure 2 Polaris Lattice Physics Calculation Flow [26]

4.2 Criticality Analyses

Criticality calculations were performed using the SCALE KENO V.a three-dimensional (3D) Monte Carlo neutron transport code with MG cross sections. The KENO V.a calculations are accessed through the criticality safety analysis sequence (CSAS). This criticality sequence was used to perform automated problem-dependent cross section processing followed by KENO V.a calculations to solve the k_{eff} eigenvalue problem.

Criticality calculations were performed using the two sets of nuclides considered for fuel modeling in burnup credit: (1) major actinides only and (2) major and minor actinides and major fission products, as listed in Tables 1 and 2. Note that although not explicitly listed as a burnup credit isotope, oxygen is included in the fuel compositions, as it is a major constituent of the fuel matrix.

4.3 Nuclear Data Libraries

Neutron transport calculations in Polaris are performed using the 56-group ENDF/B-VII.1 cross section library for all analyses in this report.

Following each transport calculation performed by Polaris, these cross sections are collapsed and applied directly to the ORIGEN calculation to determine reaction rates and the nuclide transmutation inventories. ENDF/B-VII.1 [16] provides the cross sections for 388 individual isotopes. Cross sections for 386 isotopes not available in ENDF/B-VII.1 are taken from a MG library based on the JEFF-3.1/A, a special-purpose activation library [27], and are collapsed using the same procedures. Due to their negligible self-shielding and impact on transport calculations, nuclides obtained from the JEFF-3.1/A cross sections are not processed through the ESSM module and are applied as unshielded (infinitely dilute) cross sections.

All decay data used by ORIGEN are adopted from ENDF/B-VII.1. Independent fission product yields are developed from England and Rider [28] as included in ENDF/B-VII.0. The independent yields used by ORIGEN [29] have been adjusted to account for changes in the decay data and provide greater consistency in the cumulative fission yields in the England and Rider evaluation.

KENO V.a criticality calculations of the application model were performed using the 252-group ENDF/B-VII.1 neutron transport cross section library in SCALE.

5 EXPERIMENTAL ASSAY DATA

Measured BWR nuclide compositions are obtained from destructive RCA experiments of spent fuel rods selected from assemblies irradiated in eight different reactors operated in five countries. These assemblies include 6 × 6, 8 × 8, 9 × 9, and 10 × 10 lattice designs. A total of 77 measured samples were evaluated. More than 80% of the samples are from Fukushima Daini Units 1 and 2 in Japan. The measured data used in the present study are summarized in Table 3.

Table 3 Summary of BWR Spent Fuel Samples

Reactor and Unit	Country	Assembly Design	Number of Samples	Enrichments (wt % ²³⁵ U)	Burnup (GWd/MTU)
Dodewaard	Belgium	6 × 6	1	4.94	55
Forsmark 3	Sweden	10 × 10 (SVEA-96)	1	3.97	61
Forsmark 3 ^a	Sweden	10 × 10 (GE14)	8	3.95	38–50
Fukushima Daini 1	Japan	9 × 9-9	13	2.1, 4.9, 3.0 (Gd)	35–68
Fukushima Daini 2	Japan	8 × 8-4	25	3.4, 4.5, 3.4 (Gd)	9–59
Fukushima Daini 2	Japan	8 × 8-2	18	3.9, 3.4 (Gd)	7–44
Leibstadt 3 ^b	Switzerland	10 × 10 (SVEA-96)	3	3.9	56–63
Limerick 1 ^c	United States	9 × 9 (GE11)	8	3.95, 3.6 (Gd)	37–65

^a Spanish Nuclear Safety Council (CSN) (Proprietary data)

^b MALIBU International Program (Proprietary data)

^c US DOE Yucca Mountain Project (Proprietary data)

Measurements of the major actinide isotopes were available for all samples. Minor actinide and fission product measurements are available for many of the samples.

Several experimental datasets analyzed in previous studies [4]–[7] were not used in the current study due to insufficient documentation on the reactor operating conditions, most notably the local void fractions for the samples. The datasets that were not considered here included measurements from the Cooper reactor [30], Gundremmingen reactor [31], and the Japanese Power Demonstration Reaction (JPDR) [32] and [33]. Previous studies used semiempirical correlations of assembly power and axial void distributions from other assemblies to estimate the local void for measured assemblies. In the present study, only experimental datasets with reported axial void fractions were considered.

Many public sources of isotopic assay data are currently compiled as part of the OECD/NEA Spent Nuclear Fuel Isotopic database SFCOMPO 2.0 [10], maintained and distributed by the NEA Data Bank. The experimental data in SFCOMPO has been compiled from international contributions through the Expert Group on Assay Data for Spent Nuclear Fuel, under the auspices of the OECD/NEA WPNCs. All primary experimental reports on each dataset are maintained and made available as part of the database.

SFCOMPO 2.0 includes isotopic measurements for spent fuel samples from the following BWR reactors and assembly designs:

- Cooper (US) 7 × 7
- Dodewaard (Belgium) 6 × 6

- Forsmark 3 (Sweden) 10 × 10
- Fukushima Daiichi 3 (Japan) 8 × 8
- Fukushima Daini 1 (Japan) 9 × 9
- Fukushima Daini 2 (Japan) 8 × 8
- Garigliano (Italy) 8 × 8 and 9 × 9
- Gundremmingen (Germany) 6 × 6
- Japanese Power Demonstration Reaction (Japan) 6 × 6
- Monticello (US) 8 × 8
- Quad Cities (US) 8 × 8
- Tsuruga (Japan) 7 × 7

Only the measurements from Dodewaard, Forsmark 3, Fukushima Daini 1, and Fukushima Daini 2 reactors were used in this study since they include relatively complete design and operating history data.

Additional data used in this report were obtained from commercial proprietary programs that measured fuel samples from the Forsmark 3, Leibstadt 3, and Limerick 1 reactors, but information on these datasets is restricted. Descriptive data included in this report are limited to information available from public sources. Additional proprietary information required for modeling and simulation of these fuel assemblies is only available through a nondisclosure agreement.

Each experimental dataset used in the present study is described in the following sections. This information includes a general description of the measurements and the assembly design data. Because of the complexity of BWR design and operating history data, the information presented here is not intended to provide a complete description necessary for modeling purposes; rather, only a summary of the general assembly characteristics is given. Detailed information is available in the primary experimental reports cited in this report.

The burnup of the measured samples is a critical parameter in the modeling and simulation of the nuclide compositions. Burnup is not measured directly but is usually estimated from the measured concentration of one or more fission product burnup indicators. In this work ^{148}Nd was used as the primary indicator of the sample burnup. Depletion calculations were performed by adjusting the specific power of the sample to obtain agreement with the measured ^{148}Nd inventory within 1% or better. Cases where ^{148}Nd was not used for burnup determination are clearly indicated in the report.

5.1 Dodewaard (6 × 6)

Dodewaard was a BWR nuclear power plant that operated in the Netherlands until 1997. Destructive RCA measurements of fuel samples were performed as part of the ARIANE (Actinide Research in a Nuclear Element) international project [34]. ARIANE was an experimental program coordinated by Belgonucleaire with participants from institutions and companies in Belgium, Germany, Japan, the Netherlands, Switzerland, United Kingdom, and the United States. The objective of the ARIANE program was to obtain an accurate radiochemical post-irradiation examination of mixed oxide (MOX) and UO_2 fuel samples in PWR and BWR operating conditions. Experimental data from ARIANE were released publicly to the OECD/NEA Expert Group on Assay Data for Spent Nuclear Fuel, under the WPNCS. Measurement data and experimental reports are available through the SFCOMPO database.

The Dodewaard UO₂ sample, designated DU1, had an initial ²³⁵U enrichment of 4.941% and was irradiated for five cycles to about 55 GWd/MTU in fuel assembly Y013. This assembly was discharged in January 7, 1993. The assembly was manufactured by the Japan Nuclear Fuels Co., Ltd. (JNF), as a lead test assembly of an early BWR 6 × 6 lattice design containing one water rod and five gadolinium oxide (Gd₂O₃) rods. The DU1 sample was cut from a segmented rod located in position B2 of the assembly lattice. Sample DU1 was located in the third fuel segment from the bottom (four total segments) of segmented rod B2 at a height of 1,111 mm from the bottom end of the active fuel. The reported average void fraction was 50%. The basic fuel sample characteristics are listed in Table 4.

Table 4 Summary of Dodewaard 6 × 6 Assembly Fuel Sample Measurements

Assembly ID	Rod ID	Sample ID	Fuel type	Axial height (mm)	Avg. Void (%)	Enrichment (wt % ²³⁵ U)	Gd content (wt % Gd ₂ O ₃)	Burnup (GWd/MTU)
Y013	B2	DU1	UO ₂	1,111	50	4.941	0	55.5

The other fuel rods in assembly Y013 were standard UO₂ rods (full length) with variable enrichments (3.2, 2.6, and 1.8 wt %) except for two other experimental rods located in positions D5 and E4 that contained MOX with 6.43 wt% plutonium content. The MOX rods were positioned well away from the measured DU1 sample. Two gadolinium rods with 2.7 wt% Gd₂O₃ content in fuel and 3.2% enriched in ²³⁵U were adjacent to the measured rod. The Y013 assembly layout is shown in the Polaris model in Figure 3.

Assembly Y013 was irradiated for five cycles and achieved an operation-estimated assembly average burnup of 35.24 GWd/MTU. The large difference between the assembly and sample burnup is due to the high initial ²³⁵U content of the sample rod, while the other UO₂ fuel rods in the assembly had a maximum enrichment of 3.2%.

Assembly Y013 is not highly representative of modern designs, and it contained a segmented test rod from which sample DU1 was obtained. However, detailed design and operating history information was available from the operator at the sample axial location and extensive nuclide measurements were reported. Applicability of the DU1 sample for validation has been independently evaluated [35], and it was concluded that these data are suitable for validating isotopic depletion codes.

Independent measurements of the DU1 sample were performed at laboratories of the Belgian Nuclear Research Center, Studiecentrum voor Kernenergie (SCK•CEN) in 1996, and also at the Paul Scherrer Institute (PSI) in Switzerland in 1999 [34]. These measurements were conducted as part of the same experimental program to provide a cross check of the nuclide concentrations and verification of the estimated measurement uncertainties. Extensive isotopic data obtained using destructive RCA measurements are reported for 53 nuclides. The measurements at SCK•CEN were made using high precision Thermal Ionization Mass Spectrometry (TIMS) coupled to the Isotopic Dilution Analysis (IDA) technique. The measurements by PSI were performed using a multi-collector Inductively Coupled Plasma Mass Spectrometer (ICPMS) also with ID analysis. Measurement data are available for all 28 burnup credit isotopes listed in Table 2. In this report, analyses were performed using both sets of measurements to provide an estimate of the impact of isotope measurement uncertainties.

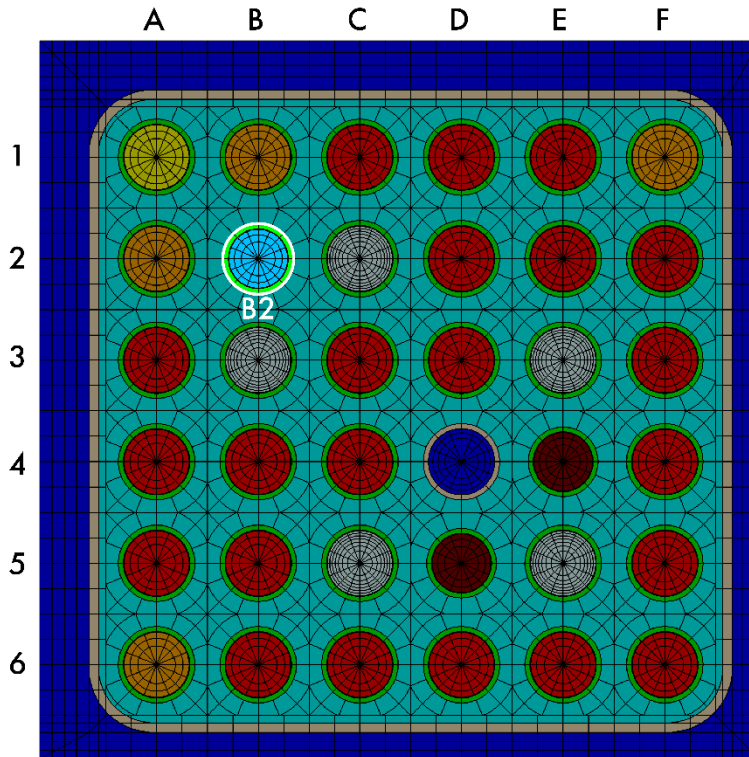


Figure 3 Polaris Model of Dodewaard 6 × 6 Assembly

Detailed core follow data for the measured sample are included in the ARIANE report [34]. Time-dependent void fraction, burnup, center and surface fuel temperatures are provided for all five cycles. These time-dependent operating data were applied in the Polaris model. An effective fuel temperature was calculated from the fuel center and surface temperatures using Rowlands's formulation [36]. The main fuel and assembly characteristics are summarized in Table 5.

The sample burnup was determined by matching the ^{148}Nd concentration predicted by Polaris with the measurement data, estimated by the laboratory to have an accuracy of better than 1% (95% confidence).

Table 5 Dodewaard 6 × 6 Assembly Parameters

Reactor and Assembly Data	
Reactor	Dodewaard
Operating pressure (bar)	75.5
Assembly type	6 × 6 GE/RDM
Fuel assembly pitch (cm)	12.7
Number of fuel rods	35
Number of gadolinia rods	5
Number of water rods	1
Fuel rod pitch (cm)	1.793
Channel bypass gap (cm)	0.872 / 0.476
Channel thickness (cm)	0.17
Channel corner radius ^a (cm)	0.9652
Channel material	Zirc-2
Channel temperature ^b (K)	564
Active fuel length (cm)	179.3
Fuel Rod Data	
Pellet radius ^c (cm)	0.5740 / 0.5176
Pellet material	UO ₂
Pellet density ^d (% theoretical density)	95.46
Fuel temperature (K)	1052
Clad inner radius (cm) ^c	0.5855 / 0.5275
Clad outer radius (cm) ^c	0.6745 / 0.6135
Clad material	Zirc-2
Clad temperature ^b (K)	564
Water Rod Data	
Inner radius ^e (cm)	0.5855
Outer radius ^e (cm)	0.6745
Water rod material	Zirc-2
Water rod temperature ^b (K)	564

^a Assumed to be the same as the 8 × 8 assembly [37]

^b Assumed to be at core average coolant temperature

^c Standard and segmented rod dimensions

^d Segmented UO₂ rod

^e Assumed to be identical to fuel rod cladding dimensions

5.2 Forsmark 3 SVEA-100 (10 × 10)

Measurements of fuel samples from SVEA-100 10 × 10 fuel assembly 14595, irradiated in the Forsmark Unit 3 reactor located in Sweden, were performed at the Studsvik Nuclear Laboratory. A 10 mm sample (identified as sample FFBU) from the central part of the UO₂ rod located at position F6 of assembly 14595 was dissolved at Studsvik. Aliquots of the fuel solution were shipped to two other laboratories in 1996, Harwell in the UK and Dimitrovgrad in Russia, for independent radiochemical determination of the isotopic composition and burnup analysis. Another sample was analyzed by Studsvik. These measurements and the experimental report were published in 2008 by Zwicky [38] and are available through the SFCOMPO database.

The Studsvik sample used in this study, identified as F3F6, was adjacent to FFBU and was 2 mm in length. It was dissolved and analyzed at Studsvik in 2003, and an aliquot of the same fuel solution was reanalyzed with new equipment in 2006. Results of these measurements and detailed assembly design and operating history information are published. The F3F6

measurements were used in this study. The Harwell and Dimitrovgrad measurements (FFBU) were used by Studsvik as cross checks of measurement accuracy.

Assembly 14595 was irradiated for six cycles and achieved a reactor-operator estimated burnup of 58 MWd/kgU. The assembly was discharged on June 6, 1993. The measured rod F6 had an enriched zone height of 3450 mm and natural uranium blanket zones that were 150 mm high at the top and bottom of the rod, resulting in a total active fuel height of 3750 mm. Sample F3F6 was obtained at an axial position 2004 mm from the bottom of the fuel rod and experienced an average void fraction of 58%. The fuel sample characteristics are listed in Table 6. The F3F6 sample burnup was estimated by Studsvik based on the measurements performed in 2006 using weighted burnup values based on measurements of neodymium isotopes, ^{235}U , and ^{239}Pu .

Table 6 Summary of Forsmark Unit 3 SVEA-100 10 × 10 Assembly Fuel Sample Measurements

Assembly ID	Rod ID	Sample ID	Fuel type	Axial height (mm)	Avg. Void (%)	Enrichment (wt % ^{235}U)	Gd content (wt % Gd_2O_3)	Burnup (GWd/MTU)
14595	F6	F3F6	UO ₂	2004	58	3.97	0	55.8

The layout of the Forsmark-3 assembly 14595 is shown in Figure 4 with the location of the measured rod F6 at the inner corner of the assembly subchannel and the subchannel structure (water cross) shown. The assembly used 10 different enrichments in the fuel rods, and five rods had a Gd_2O_3 content of 3.15 wt%. The general design specifications for the SVEA-100 assembly 14595 are listed in Table 7. Detailed time-dependent void fractions, fuel temperature, and specific power for the measured sample are provided in the reference report [38].

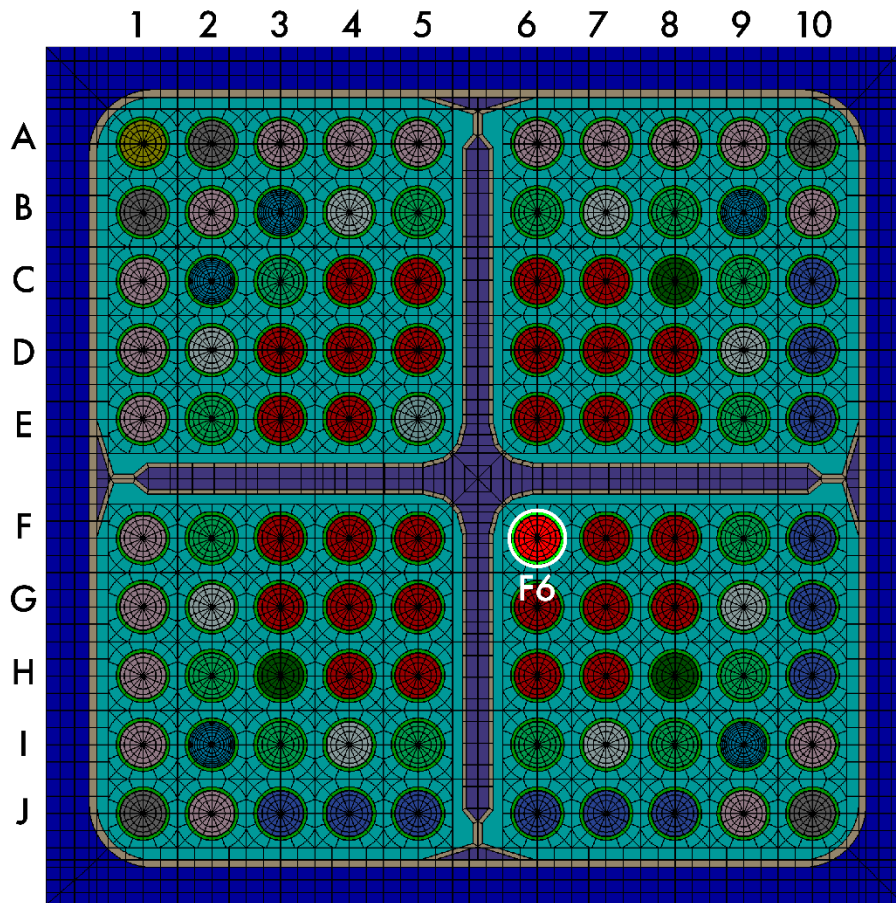


Figure 4 Polaris Model of Forsmark Unit 3 SVEA-100 Assembly

Measurements used in this study were part of the December 2006 analysis campaign of the F3F6 sample at Studsvik and were made using a High Performance Liquid Chromatography (HPLC) system for the chemical separations. Mass spectrometry was performed using an ICPMS. Measurements are reported for isotopes of uranium, plutonium, cerium, and neodymium. IDA was used with spike solutions of ^{233}U , ^{242}Pu , ^{140}Ce , and ^{148}Nd .

Table 7 Forsmark 3 SVEA-100 Assembly Parameters

Reactor and Assembly Data	
Reactor	Forsmark Unit 3
Operating pressure (bar)	70.0
Assembly type	10 × 10 SVEA-100
Fuel assembly pitch (cm)	15.475
Number of fuel rods	100
Number of gadolinia rods	5
Number of water rods	0
Fuel rod pitch (cm)	1.24
Channel bypass gap (cm)	0.6775 / 0.7775
Channel thickness (cm)	0.14
Channel corner radius (cm)	1.01
Channel material	Zirc-2
Channel temperature ^a (K)	560
Active fuel length (cm)	375
Fuel Rod Data	
Pellet radius (cm)	0.481
Pellet material	UO ₂
Pellet density (% theoretical density)	96.9
Clad inner radius (cm)	0.5275
Fuel temperature (K)	792
Clad outer radius (cm)	0.6135
Clad material	Zirc-2
Clad temperature ^a (K)	560
Water Rod Data	
Inner radius (cm)	N/A
Outer radius (cm)	N/A
Water rod material	N/A
Water rod temperature (K)	N/A

^a Assumed to be at core average coolant temperature

5.3 Forsmark 3 GE14 (10 × 10)

Under a proprietary Spanish experimental program [11] coordinated by the Spanish fuel vendor ENUSA, isotopic measurements were made on a modern GE14 10 × 10 assembly from the Forsmark Unit 3 reactor operated in Sweden. The program involved the Spanish safety council for nuclear activities, CSN, and the organization responsible for waste management in Spain, ENRESA, with support provided by the US NRC and Oak Ridge National Laboratory (ORNL). The program provided extensive isotopic composition data for benchmarking codes and computational models used in reactor safety studies as well as for interim storage, transportation, and final disposal of spent nuclear fuel.

Fuel samples of rod J8 from GE14 assembly GN592 were measured at the Studsvik Nuclear Laboratory. A total of eight fuel samples from fuel rod J8 were measured over the entire rod length to provide data on burnup and void variations. Samples 1 and 2, and samples 3 and 7, were selected from adjacent axial positions of the rod to verify measurement repeatability and uncertainty. The measurements provided isotopic data at six unique axial positions.

Measured fuel rod J8 was located at the periphery of the assembly, on a side away from the control blades. All samples from rod J8 were from the enriched zone of the rod with an initial

enrichment of 3.95 wt % ²³⁵U. The fuel assembly was irradiated for five consecutive operating cycles (cycles 16–20) and was discharged on May 28, 2005. The measured fuel rod attained an estimated rod average burnup of 41 GWd/MTU and peak burnup of about 56 GWd/MTU.

Table 8 provides a summary of sample identification names, the elevation of each sample, and the estimated void at the sample locations. Sample elevations are measured from the lower end plug of the fuel rod. The distance from the lower end plug to the start of the active fuel region is about 40 mm.

Table 8 Summary of Forsmark Unit 3 GE14 10 × 10 Assembly Fuel Sample Measurements

Assembly ID	Rod ID	Sample ID	Fuel type	Axial height (mm)	Avg. Void (%)	Enrichment (wt % ²³⁵ U)	Gd content (wt % Gd ₂ O ₃)	Burnup (GWd/MTU)
GN592	J8	ENUSA-1	UO ₂	1,847	51	3.95	0	50.4
		ENUSA-2	UO ₂	1,858	51	3.95	0	50.7
		ENUSA-3	UO ₂	718	13	3.95	0	49.0
		ENUSA-4	UO ₂	2,508	61	3.95	0	51.1
		ENUSA-5	UO ₂	3,282	67	3.95	0	43.6
		ENUSA-6	UO ₂	403	2.2	3.95	0	43.5
		ENUSA-7	UO ₂	707	13	3.95	0	49.0
		ENUSA-8	UO ₂	3,389	67	3.95	0	38.3

The layout of assembly GN592 is shown in Figure 5. This assembly has 92 fuel rods including 12 part-length rods; nine of the rods contained Gd₂O₃ in fuel. Seven different uranium enrichments are used in the assembly design. The enriched zone of the rods is 323.4 cm in length, with natural uranium axial blankets of 29.4 cm on the top and 15.2 cm on the bottom, resulting in a total active rod length of 368 cm. The general design specifications for the GE14 assembly GN592 are listed in Table 9.

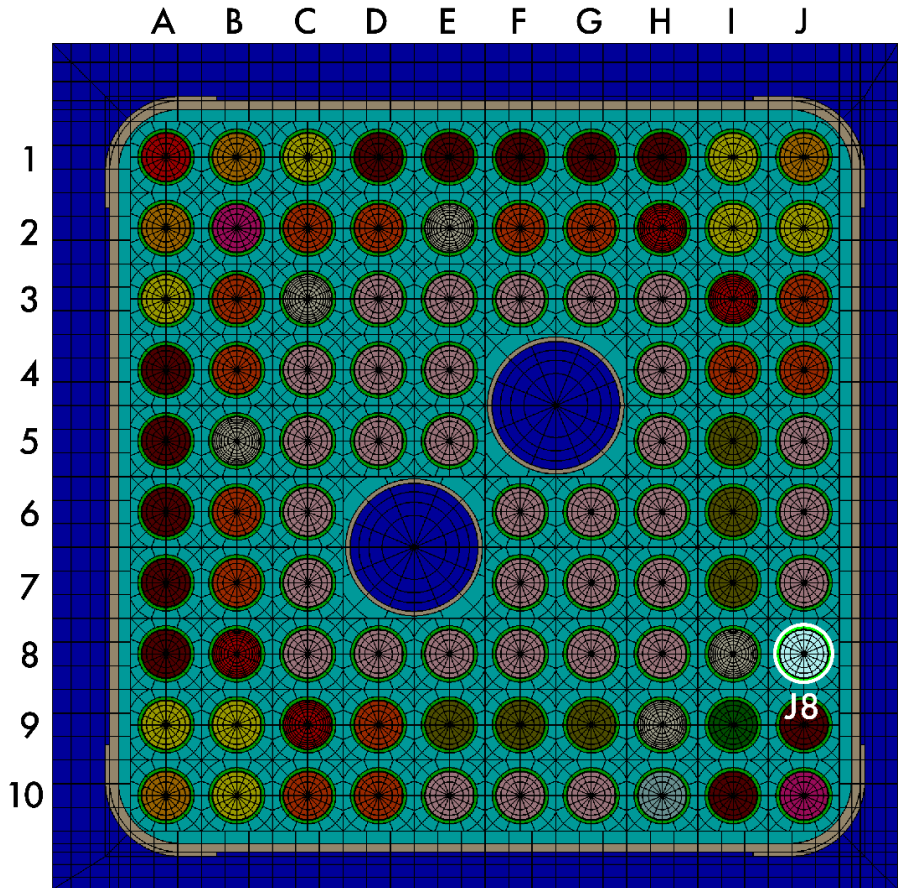


Figure 5 Polaris Model of Forsmark Unit 3 GE14 10 × 10 Assembly

Detailed time-dependent reactor operating data, including void fraction, fuel temperature, and power for the measured samples, are documented in reference reports prepared by Vattenfall in Sweden [39].

Destructive and nondestructive assay measurements of fuel rod J8 were performed at the Studsvik Nuclear [40] Laboratory in 2009. HPLC was used for chemical separations for the analysis of individual isotopes of more than 10 different elements. Mass spectrometry was performed using ICPMS with ID analysis for most isotopes. Nuclides without any isobaric overlap were measured by ICPMS with external calibration analysis. Gamma-emitting nuclides were analyzed by gamma spectrometry. The measurements include more than 60 isotopes and include most of the burnup credit isotopes listed in Table 2.

Table 9 Forsmark 3 GE14 10 × 10 Assembly Parameters [41]

Reactor and Assembly Data	
Reactor	Forsmark Unit 3
Operating pressure (bar)	70.0
Assembly type	10 × 10 GE14
Fuel assembly pitch ^a (cm)	[]
Number of fuel rods	92
Number of gadolinia rods	9
Number of water rods	2
Fuel rod pitch (cm)	1.295
Channel bypass gap ^a (cm)	[]
Channel thickness ^a (cm)	[]
Channel corner radius ^a (cm)	[]
Channel material	Zirc-2
Channel temperature ^b (K)	560
Active fuel length (cm)	368
Fuel Rod Data	
Pellet radius (cm)	0.438
Pellet material	UO ₂
Pellet density (g/cm ³)	10.50
Fuel temperature (K)	792
Clad inner radius (cm)	0.447
Clad outer radius (cm)	0.513
Clad material	Zirc-2
Clad temperature ^b (K)	560
Water Rod Data	
Inner radius ^a (cm)	[]
Outer radius ^a (cm)	[]
Water rod material	Zirc-2
Water rod temperature ^b (K)	560

^a Proprietary value^b Assumed to be at core average coolant temperature

5.4 Fukushima Daini 1 (9 × 9-9)

As part of a validation study of burnup calculations of BWR cores conducted by the Japan Nuclear Energy Safety (JNES) organization, now the Japan Regulation Authority (NRA), physics and depletion analyses were performed using post-irradiation measurements of burnup and isotopic inventories of eight samples taken from two 9 × 9-9 BWR lead test fuel assemblies irradiated in the Fukushima Daini Unit 1 reactor (2F1). Assembly 2F1ZN2 was discharged on May 9, 2000, after three cycles of irradiation. Assembly 2F1ZN3 was irradiated for five cycles and discharged on January 7, 2003. This assembly design is similar to the ATRIUM-9 design.

Measurements for isotopes of uranium, plutonium, and neodymium for eight samples selected from five different fuel rods of the two assemblies were reported by Yamamoto [42]. An additional five samples from the same rods were later reported by Suzuki [43] that included measurements of additional fission products. Supplementary design and operating information necessary to model the 9 × 9-9 assemblies was provided by Yamamoto [44] through the OECD/NEA coordinated activity on spent fuel assay data; these data and reports are currently included in the

SFCOMPO database. The additional data included the fuel rod enrichment layout, time-dependent void fractions, and accumulated burnup for the assemblies at the axial locations (nodes) of all measured samples.

The measurements included both UO₂ and UO₂-Gd₂O₃ type fuel rods with initial enrichments of 2.1, 3.0, and 4.9 wt% ²³⁵U. The C2 fuel rods contained Gd₂O₃ with a content of 5 wt% in the fuel. Sample burnup values ranged from 29 GWd/MTU (UO₂-Gd₂O₃) to 68.4 GWd/MTU (UO₂). The sample burnup was estimated using the measured ¹⁴⁸Nd concentration. Measurements were obtained for the bottom, middle, and top elevations of the rods. A summary of the measured sample characteristics is given in Table 10. The axial elevations of each sample are relative to the bottom of the active region of the fuel rod.

Table 10 Summary of Fukushima Daini-1 9 × 9-9 Assembly Fuel Sample Measurements

Assembly ID	Rod ID	Sample ID	Fuel type	Axial height (mm)	Avg. Void (%)	Enrichment (wt % ²³⁵ U)	Gd content (wt % Gd ₂ O ₃)	Burnup (GWd/MTU)
2F1ZN2	C2	GDB	UO ₂ -Gd ₂ O ₃	757	18	3.0	5.0	35.6
		GDT	UO ₂ -Gd ₂ O ₃	2,922	74	3.0	5.0	29.0
	C3	UB	UO ₂	788	18	4.9	0	46.5
		UT	UO ₂	2,922	74	4.9	0	38.9
2F1ZN3	A9	UB	UO ₂	788	18	2.1	0	61.2
		UM	UO ₂	1,654	38	2.1	0	68.0
		UT	UO ₂	2,844	60	2.1	0	55.7
	C2	GDB	UO ₂ -Gd ₂ O ₃	804	18	3.0	5.0	55.6
		GDM	UO ₂ -Gd ₂ O ₃	1,654	38	3.0	5.0	57.7
		GDT	UO ₂ -Gd ₂ O ₃	2,875	60	3.0	5.0	46.8
	C3	UB	UO ₂	788	11	4.9	0	68.3
		UM	UO ₂	1,639	38	4.9	0	68.4
		UT	UO ₂	2,844	60	4.9	0	58.0

The configuration of assemblies 2F1ZN2 and 2F1ZN3 is shown in Figure 6 with the measured rod locations C2, C3, and A9 highlighted. The measured assemblies use five different ²³⁵U enrichments and contain 12 Gd₂O₃ fuel rods, as indicated by the different colored rods in the figure. The general design specifications of the 9 × 9-9 assemblies are listed in Table 11.

Post-irradiation examination and destructive radiochemical analysis of the fuel samples were performed at the JAEA and resulted in high-accuracy isotopic inventory data for the irradiated samples. Measurements for isotopes of uranium (²³⁴U, ²³⁵U, ²³⁶U, ²³⁸U), plutonium (²³⁸Pu, ²³⁹Pu, ²⁴⁰Pu, ²⁴¹Pu, ²⁴²Pu) and neodymium (¹⁴²Nd, ¹⁴³Nd, ¹⁴⁴Nd, ¹⁴⁵Nd, ¹⁴⁶Nd, ¹⁴⁸Nd, ¹⁵⁰Nd) were performed using TIMS with ID analysis. Isotopes of samarium, europium, and gadolinium were measured using ID and ICPMS. The metallic fission product isotopes ⁹⁵Mo, ⁹⁹Tc, ¹⁰¹Ru, ¹⁰³Rh, ¹⁰⁹Ag, and ¹³³Cs were measured by ICPMS using the external calibration method. Measurements of assemblies 2F1ZN2 and 2F1ZN3 were made in 2002 and 2005, respectively.

Table 11 Fukushima Daini-1 9 × 9-9 Assembly Parameters

Reactor and Assembly Data	
Reactor	Fukushima Daini Unit 1
Operating pressure (bar)	70.7
Assembly type	9 × 9-9
Fuel assembly pitch (cm)	15.2
Number of fuel rods	72
Number of gadolinia rods	12
Number of water rods	1 (square channel)
Fuel rod pitch (cm)	1.45
Channel bypass gap (cm)	0.65
Channel thickness (cm)	0.25
Channel corner radius ^a (cm)	0.9652
Channel material ^b	Zirc-2
Channel temperature ^c (K)	559
Active fuel length (cm)	371
Fuel Rod Data	
Pellet radius (cm)	0.47
Pellet material	UO ₂ / Gd ₂ O ₃ -UO ₂
Pellet density (g/cm ³)	10.63 / 10.38
Fuel temperature (K)	900
Clad inner radius (cm)	0.49
Clad outer radius (cm)	0.55
Clad material	Zirc2
Clad temperature ^c (K)	559
Water Rod Data	
Inner width ^d (cm)	3.685
Outer width ^d (cm)	3.85
Water rod material	Zirc-2
Water rod temperature ^b (K)	559

^a Assumed to be same as 8 × 8 assembly [37]

^b Assumed value based on earlier designs

^c Assumed to be at core average coolant temperature

^d Assumed to be same as the ATRIUM-9 fuel design [45]

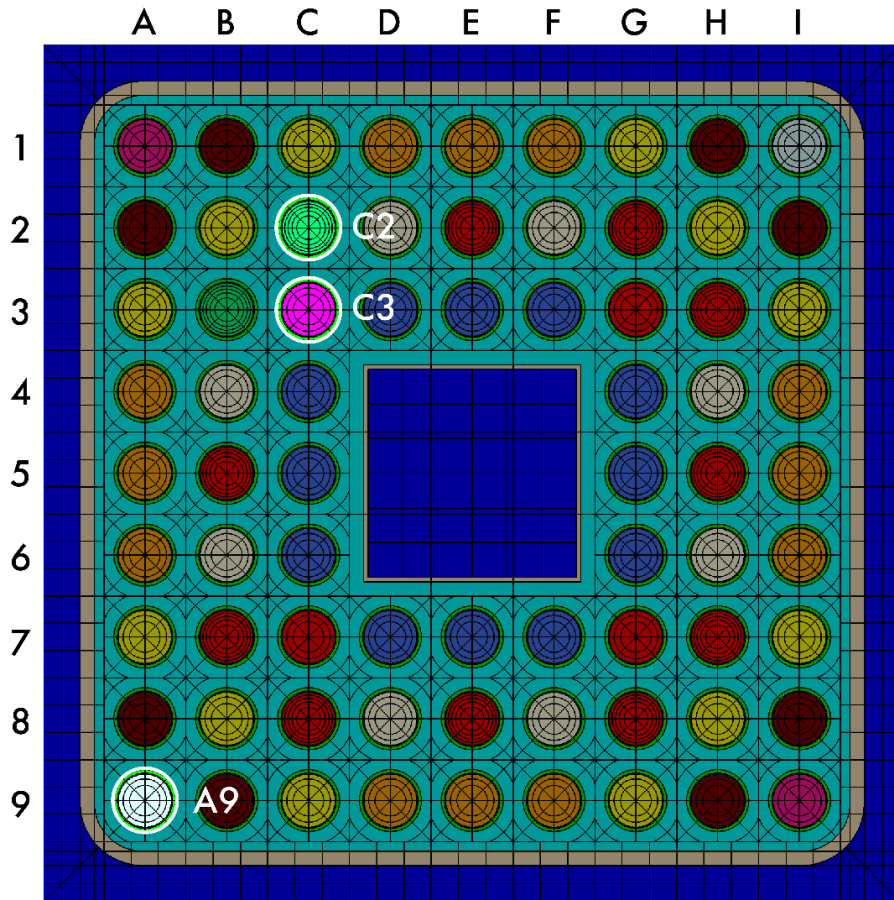


Figure 6 Polaris Model of the Fukushima Daini-1 9 × 9-9 Assemblies

5.5 Fukushima Daini 2 (8 × 8-2)

Under a burnup credit research project at the Japan Atomic Energy Research Institute (JAERI) and supported by the Science and Technology Agency of Japan in cooperation with the utilities, experiments were performed on spent fuel assemblies to obtain criticality data, and destructive and nondestructive measurements were made to determine the nuclide compositions of the fuel [46]. Analyses of these data by Japan have been reported by Nakahara [8] and Yamamoto [47]. The measurements and the reference reports have been compiled as part of the SFCOMPO database [48].

Measurements are reported for two fuel rods from lattice positions B2 and C2 of an 8 × 8 assembly identified as 2F2DN23 irradiated for three cycles in Unit 2 the Fukushima Daini Power Station 2 (2F2) reactor, operated by Tokyo Electric Power Company (TEPCO). Assembly 2F2DN23 was discharged on November 14, 1992. The measured fuel rods from assembly lattice positions B2 and C2 were identified as SF98 and SF99 in the research project. The rod designated SF98 was a UO₂ fuel with an enriched zone of 3.90 wt% ²³⁵U with natural uranium blankets having a nominal length of 155 mm at the top and bottom of the rod. Rod SF99 was a UO₂-Gd₂O₃ rod with two axial enrichment zones and two natural uranium blankets. The lower 2,937 mm section of the enriched zone had 3.40 wt% ²³⁵U and 4.5 wt% Gd₂O₃ enrichment whereas the upper section had 3.40 wt% ²³⁵U and 3.0 wt% Gd₂O₃ enrichment.

Isotope measurements were reported for 18 different samples obtained from different axial positions of the two rods. Three samples were selected from the natural uranium blanket regions of the rods. The sample characteristics are listed in Table 12. The sample axial locations in the fuel rods were measured from the bottom of the active fuel length. The burnup values were determined using the measured ^{148}Nd content in the fuel samples.

The configuration of assembly 2F2DN23 is shown in Figure 7. The 8×8 -2 assembly is similar to the GE7 design. There are six different enrichments (excluding the natural uranium regions) used in the assembly, as shown by the different colored rods in the figure. The experimental reports include assembly design information and provide time-dependent specific power for each sample location and the average void fraction as a function of axial location in the assembly. Time-dependent void data was not available for this assembly. The average void fractions are those provided by TEPCO and are standard values as written in the Application for Permission for the Installation of a Nuclear Reactor [8]. The impact of using average void compared to detailed void data was studied and found to be minor, as evaluated in Section 7 of this report. The general assembly design information is summarized in Table 13.

Destructive assay measurements of the fuel samples from rod B2 and C3 were performed at JAEA laboratories in May 1998 and July 1999, respectively. Fuel samples with a thickness of 0.5 mm were dissolved and measured using chemical separations and mass spectrometry with alpha counting. Isotopic compositions and absolute contents of uranium, plutonium, neodymium, and samarium isotopes were measured by isotopic dilution mass spectrometry (IDMS) using spikes of ^{150}Nd , ^{233}U , and ^{242}Pu . Concentrations of ^{234}U , ^{237}Np , ^{238}Pu , ^{241}Am , ^{243}Am , ^{242}Cm , and ^{244}Cm were measured as ratios to uranium by alpha spectrometry.

Table 12 Summary of Fukushima Daini-1 8×8 -2 Assembly Fuel Sample Measurements

Assembly ID	Rod ID	Sample ID	Fuel type	Axial height (mm) ^a	Avg. Void (%)	Enrichment (wt % ^{235}U)	Gd content (wt % Gd_2O_3)	Burnup (GWd/MTU)
2F2DN23	B2	SF98-1	UO_2	39	0	0.71	0	4.2
		SF98-2	UO_2	167	0	3.91	0	26.5
		SF98-3	UO_2	423	3	3.91	0	36.9
		SF98-4	UO_2	692	11	3.91	0	42.4
		SF98-5	UO_2	1,214	32	3.91	0	44.0
		SF98-6	UO_2	2,050	54.5	3.91	0	39.9
		SF98-7	UO_2	2,757	68	3.91	0	39.4
		SF98-8	UO_2	3,397	73	3.91	0	27.2
	C2	SF99-1	UO_2	134	0	0.71	0	7.5
		SF99-2	$\text{UO}_2\text{-Gd}_2\text{O}_3$	286	1.4	3.4	4.5	22.6
		SF99-3	$\text{UO}_2\text{-Gd}_2\text{O}_3$	502	5.8	3.4	4.5	32.4
		SF99-4	$\text{UO}_2\text{-Gd}_2\text{O}_3$	686	10.8	3.4	4.5	35.4
		SF99-5	$\text{UO}_2\text{-Gd}_2\text{O}_3$	1,189	27.7	3.4	4.5	37.4
		SF99-6	$\text{UO}_2\text{-Gd}_2\text{O}_3$	2,061	54.7	3.4	4.5	32.4
		SF99-7	$\text{UO}_2\text{-Gd}_2\text{O}_3$	2,744	66.5	3.4	4.5	32.1
		SF99-8	$\text{UO}_2\text{-Gd}_2\text{O}_3$	3,388	71.7	3.4	3.0	21.8
		SF99-9	$\text{UO}_2\text{-Gd}_2\text{O}_3$	3,540	72.9	3.4	3.0	16.7
		SF99-10	UO_2	3,676	74.3	0.71	0	7.2

^a Measured from the bottom of the active fuel length.

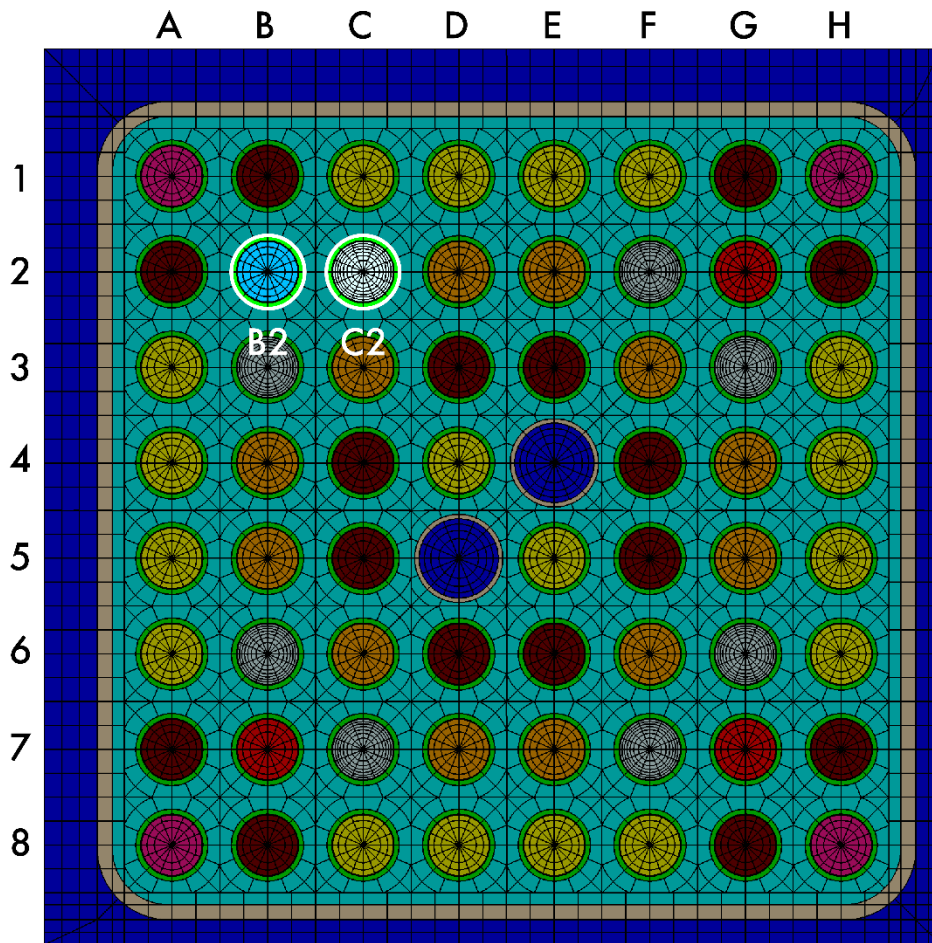


Figure 7 Polaris Model of the Fukushima Daini-2 8 × 8-2 Assemblies

Table 13 Fukushima Daini-2 8 × 8-2 and 8 × 8-4 Assembly Parameters

Reactor and Assembly Data		
Reactor	Fukushima Daini Unit 2	
Operating pressure (bar)	70.7	
Fuel assembly pitch (cm)	15.23	
Assembly type	8 × 8-2	8 × 8-4
Number of fuel rods	62	60
Number of gadolinia rods	8	8
Number of water rods	2	1
Fuel rod pitch (cm)	1.625	1.625
Channel bypass gap (cm)	0.65	0.65
Channel thickness (cm) ^a	0.2032	0.2032
Channel corner radius ^a (cm)	0.9652	0.9652
Channel material ^b	Zirc-2	Zirc-2
Channel temperature ^c (K)	559	559
Active fuel length (cm)	371	371
Fuel Rod Data		
Pellet radius ^c (cm)	0.515	0.519
Pellet material	UO ₂ / Gd ₂ O ₃ -UO ₂	UO ₂ / Gd ₂ O ₃ -UO ₂
Pellet density ^d (g/cm ³)	10.48	10.61
Fuel temperature (K)	900	900
Clad inner radius (cm)	0.527	0.529
Clad outer radius (cm)	0.613	0.615
Clad material	Zirc-2	Zirc-2
Clad temperature ^b (K)	559	559
Water Rod Data		
Inner radius ^d (cm)	0.6738	1.623
Outer radius (cm)	0.75	1.7
Water rod material	Zirc-2	
Water rod temperature ^{cb} (K)	559	

^a Assumed to be the same as for the 8 × 8 assembly [37]

^b Assumed value based on earlier designs

^c Assumed to be at core average coolant temperature

^d From IAEA TECDOC-849 [45]

5.6 Fukushima Daini 2 GE9 (8 × 8-4)

Isotopic measurements of four BWR 8 × 8-4 lead test assemblies, irradiated in Unit 2 of the Fukushima Daini Power Station 2 (2F2), were reported by the Japan NRA [47]. The assemblies, identified as 2F2D1, 2F2D2, 2F2D3, and 2F2D8, were discharged on March 8, 1990, August 24, 1991, November 14, 1992, and January 30, 1997, after one, two, three, and five cycles of irradiation, respectively, providing a wide range of sample burnups. Supplementary detailed design information necessary for modeling these assemblies was provided by Yamamoto [48]. This information included the enrichments of all fuel rods in the assembly. The measurements, design data, and reference reports are captured in the SFCOMPO database.

All assemblies have an 8 × 8-4 lattice arrangement with a large water rod that occupies the position of four lattice positions, similar to the GE9 assembly design. The assemblies used five different ²³⁵U enrichments and included eight UO₂-Gd₂O₃ rods with Gd₂O₃ contents of 3.0 and

4.5 wt% in fuel. Measurements for each assembly include both UO₂ and UO₂-Gd₂O₃ type fuel rods. The sample characteristics are given in Table 14. These data cover a wide range of burnup and void fraction values.

The configuration of the assembly is shown in Figure 8. All assemblies have the same layout and enrichment zoning. The general assembly design parameters for the 8 × 8-4 assembly are similar to the 8 × 8-2 design and are listed in Table 13.

Time-dependent void distributions for the 8 × 8-4 assemblies were not reported. However, the node average values of the channel void fractions of the 8 × 8-4 fuel assemblies were provided by the plant operator for all axial nodes of the assemblies which included the measured fuel samples [47].

Measurements made at laboratories of the Nippon Nuclear Fuel Development (NFD) Company are reported for isotopes of uranium, plutonium, and curium, as well as for ¹⁴⁸Nd, ²⁴¹Am and ²⁴³Am. The method of IDMS was applied to neodymium and uranium isotopes with spikes of ¹⁵⁰Nd and natural uranium, respectively. Alpha spectrometry and mass spectrometry were used for the plutonium isotopes, and alpha spectrometry was used to measure the americium isotopes. The sample burnups estimated by the laboratory were based on the ¹⁴⁸Nd method with the inventory data of uranium, plutonium. The ¹⁴⁸Nd measurement had a reported uncertainty of 6.4%. The burnup values used in this study used the measured ¹⁴⁸Nd content in each sample.

Table 14 Summary of Fukushima Daini-2 8 × 8-4 Assembly Fuel Sample Measurements

Assembly ID	Rod ID	Sample ID	Fuel type	Axial height (mm) ^a	Avg. Void (%)	Enrichment (wt % ²³⁵ U)	Gd content (wt % Gd ₂ O ₃)	Burnup (GWd/MTU)
2F2D1	F6	TU101	UO ₂	3,378	64.0	4.5	0	14.0
		TU102	UO ₂	642	12.9	4.5	0	18.2
	B3	TU103	UO ₂ -Gd ₂ O ₃	3,343	64.0	3.4	4.5	10.0
		TU104	UO ₂ -Gd ₂ O ₃	2,743	60.2	3.4	4.5	9.4
		TU105	UO ₂ -Gd ₂ O ₃	740	17.3	3.4	4.5	12.3
	F6	TU106	UO ₂	2,689	59.8	4.5	0	16.1
2F2D2	F6	TU201	UO ₂	3,178	63.1	4.5	0	29.1
		TU202	UO ₂	478	7.0	4.5	0	32.9
	B3	TU203	UO ₂ -Gd ₂ O ₃	3,178	63.1	3.4	4.5	24.5
		TU204	UO ₂ -Gd ₂ O ₃	2,592	58.5	3.4	4.5	23.5
		TU205	UO ₂ -Gd ₂ O ₃	578	10.4	3.4	4.5	22.8
2F2D3	H5	TU301	UO ₂	2,793	60.6	3.4	0	34.6
		TU302	UO ₂	423	5.2	3.4	0	31.4
	A4	TU304	UO ₂	2,856	61.0	3.4	0	37.8
		TU306	UO ₂	447	6.0	3.4	0	32.3
	B3	TU308	UO ₂ -Gd ₂ O ₃	3,242	63.5	3.4	4.5	30.2
		TU309	UO ₂ -Gd ₂ O ₃	2,780	60.5	3.4	4.5	34.8
TU311	UO ₂ -Gd ₂ O ₃	543	9.1	3.4	4.5	33.5		
2F2D8	H5	TU501	UO ₂	3,202	63.2	3.4	0	53.2
		TU502	UO ₂	2,453	58.0	3.4	0	58.9
		TU503	UO ₂	803	20.6	3.4	0	55.6
	A4	TU505	UO ₂	2,229	54.9	3.4	0	59.1
		TU506	UO ₂	850	23.0	3.4	0	57.5
	B3	TU510	UO ₂ -Gd ₂ O ₃	2,952	62.2	3.4	4.5	53.1
		TU511	UO ₂ -Gd ₂ O ₃	670	14.0	3.4	4.5	48.1

^a Measured from the bottom of the active fuel length.

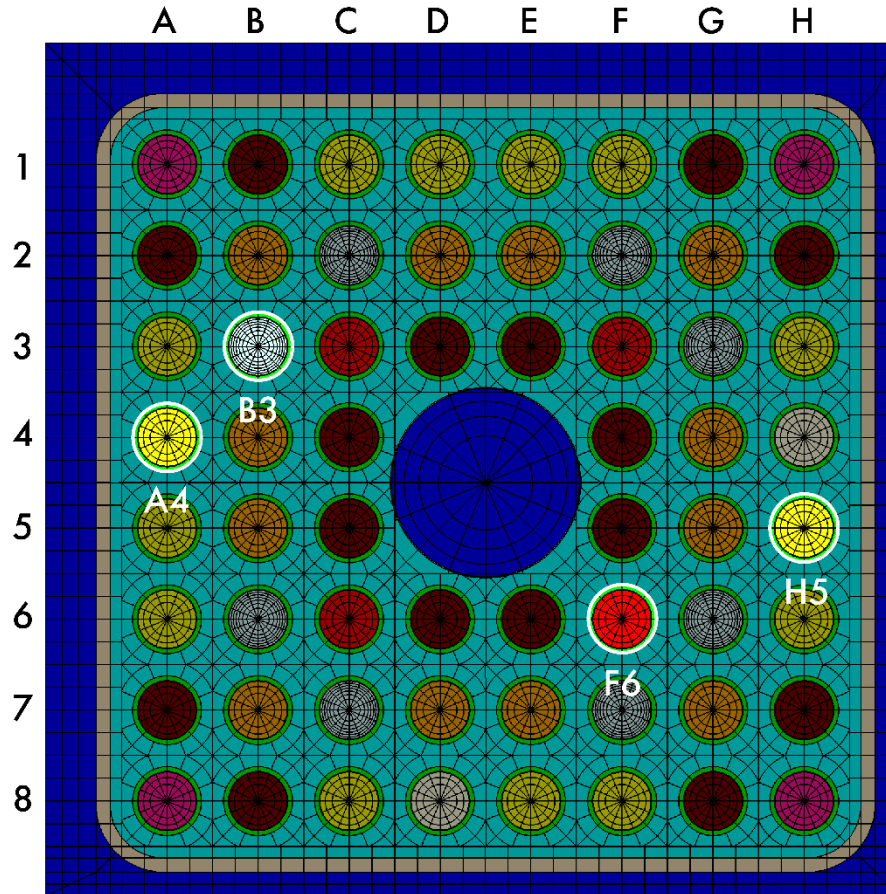


Figure 8 Polaris Model of the Fukushima Daini-2 8 × 8-4 Assemblies

5.7 Leibstadt SVEA-96 (10 × 10)

Measurements of isotopic concentrations from the MALIBU (MOX AND UOX LWR Fuels Irradiated to High Burnup) international experimental program [12] were analyzed in this study. MALIBU is a commercial proprietary program managed by the Belgian Nuclear Research Center, Studiecentrum voor Kernenergie–Centre d’Études de l’Énergie Nucleaire (SCK•CEN). This proprietary program included participants from Belgium, Sweden, Japan, France, Germany, Switzerland, and the United States. Measurements were performed at several radiochemical laboratories as a measurement cross check and to assess and reduce uncertainties.

Under an extension phase of the program, isotopic measurements were made on BWR fuel samples from a SVEA-96 Optima 10×10 assembly from the Kernkraftwerk Leibstadt reactor in Switzerland [49]. The measured assembly, identified as AIA003, was irradiated for seven cycles and was discharged in March 28, 2005.

Three samples were taken at different axial positions of rod H6 of assembly AIA003 to assess different void conditions. All samples had an initial enrichment of 3.90 wt% ²³⁵U. Characteristics of the measured samples are given in Table 15. The burnup values for samples KLU1 and KLU3 were determined using the ¹⁴⁸Nd concentration; this burnup was in good agreement with burnup

estimates based on other neodymium isotopes and ^{137}Cs . The KLU2 sample used $^{145+146}\text{Nd}$ and ^{137}Cs measurements to estimate the sample burnup, which was about 8% different from the burnup obtained using ^{148}Nd .

The SVEA-96 assembly design has a highly heterogeneous 10×10 lattice array with four subassembly regions similar to the SVEA-100 design. The fuel rod arrays are not exactly regular, with the outer fuel rods shifted slightly inwards from the edge of the assembly, and one fuel rod from the inner corner of each sub-assembly removed to accommodate a central square water channel. The assembly includes eight part-length rods located nearest the water channel. The fuel rods have seven different ^{235}U enrichments, and 12 of these rods contain Gd_2O_3 with a content of 4 wt% in the fuel. The fuel rods have two different diameters. The assembly design is shown in Figure 9 for the configuration of the dominant lattice (below the level of the part length rods) with different colors identifying different types of fuel rods in the assembly. The general assembly design parameters for the SVEA-96 assembly are listed in Table 16.

Detailed operating data including time-dependent specific power, void conditions, and fuel temperatures were provided by the Vattenfall Nuclear Fuel and Kernkraftwerk Leibstadt [50].

All samples were measured at Studsvik Nuclear Laboratory in Sweden during 2010. The sample at the lowest elevation, KLU1, was selected as a cross check sample and was also analyzed at the laboratories of SCK•CEN in Belgium and the PSI in Switzerland. Radiochemical analysis techniques were used to analyze more than 50 actinides and fission products. Mass spectrometry measurements at SCK•CEN were performed using TIMS in 2009 and 2010, and PSI used HPLC and ICPMS techniques and measurements were performed in 2010.

Table 15 Summary of Leibstadt SVEA-96 10×10 Assembly Fuel Sample Measurements

Assembly ID	Rod ID	Sample ID	Fuel type	Axial height (mm) ^a	Avg. Void (%)	Enrichment (wt % ^{235}U)	Gd content (wt % Gd_2O_3)	Burnup (GWd/MTU)
AIA003	H6	KLU1	UO ₂	588	8.4	3.90	0	60.5
		KLU2	UO ₂	1,922	51	3.90	0	65.0
		KLU3	UO ₂	3,302	70	3.90	0	58.4

^a Measured from the bottom of the active fuel length.

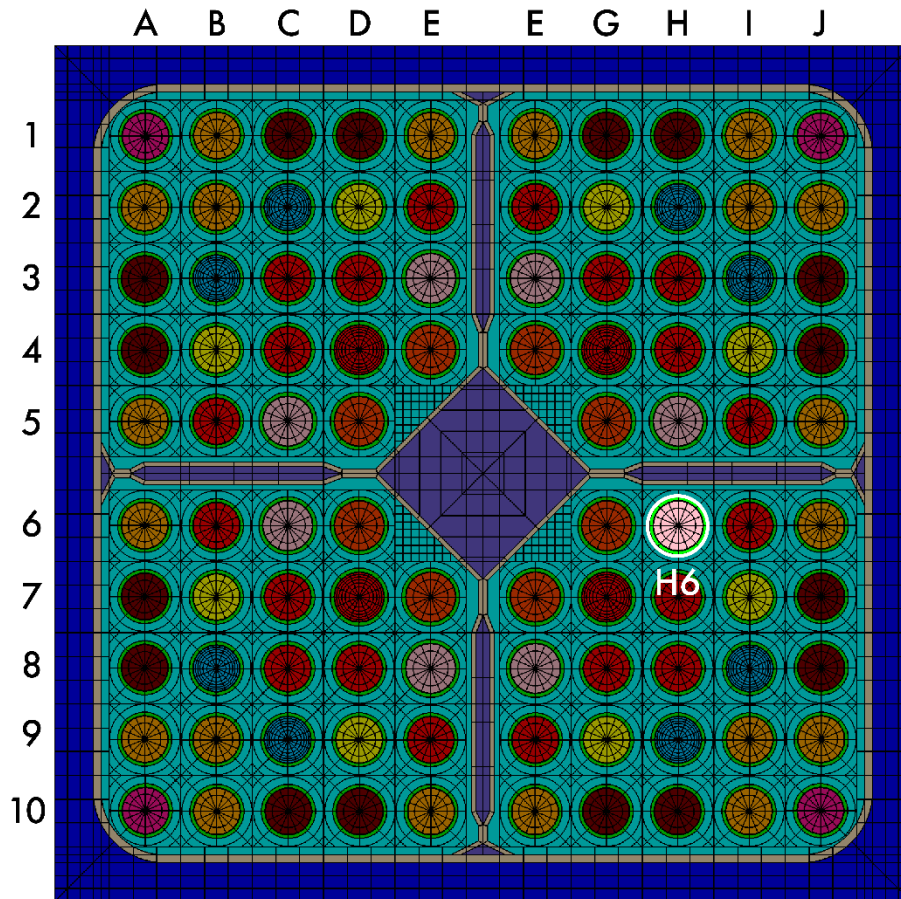


Figure 9 Polaris Model of Leibstadt SVEA-96 10 × 10 Assembly

Table 16 Leibstadt SVEA-96 10 × 10 Assembly Parameters

Reactor and Assembly Data	
Reactor	Leibstadt
Operating pressure (bar)	74
Assembly type	10 × 10 SVEA-96 Optima
Fuel assembly pitch (cm)	15.24
Number of fuel rods	96
Number of gadolinia rods	12
Number of water rods	1 (square channel)
Fuel rod pitch (cm) ^a	[]
Channel bypass gap (cm) ^d	0.69
Channel thickness (cm) ^a	[]
Channel corner radius (cm) ^a	[]
Channel material	Zirc-2
Channel temperature (K) ^b	562
Active fuel length (cm)	381
Fuel Rod Data	
Pellet radius (cm) ^d	0.4095
Pellet material	UO ₂
Pellet density (g/cm ³)	10.52
Fuel temperature (K) ^c	800
Clad inner radius (cm) ^d	0.418
Clad outer radius (cm) ^d	0.481
Clad material	Zirc-2
Clad temperature (K) ^b	562
Water Rod Data	
Inner width (cm) ^a	[]
Outer width (cm) ^a	[]
Water rod material	Zirc-2
Water rod temperature (K) ^b	562

^a Proprietary value^b Assumed to be at core average coolant temperature^c Average value^d Reference [51]

5.8 Limerick 1 GE11 (9 × 9-7)

Isotopic composition measurements of a spent fuel assembly from the Limerick Unit 1 reactor were measured in laboratories at GE Vallecitos Nuclear Center. These measurements have been analyzed in previous validation studies performed under the Yucca Mountain Project (YMP) in 2004 under the Office of Civilian Radioactive Waste Management [13]. Measurements were performed for eight samples selected from a high-burnup assembly identified as YJ1433 [52]. The reported measurement data include nuclide concentrations for 32 actinides and fission products.

Assembly YJ1433 is a GE11 9 × 9 design with two large water rods. There are five different ²³⁵U enrichments for the UO₂ rods, eight part-length rods, and nine rods containing Gd₂O₃ at 5 wt% in the fuel. The assembly configuration is shown in Figure 10. The assembly was irradiated for three cycles and was discharged after cycle 7 on May 27, 1998. The general design specifications for the GE11 assembly YJ1433 are listed in Table 18.

Three different fuel rods were measured, including a full length UO₂ rod from lattice location D9, a UO₂-Gd₂O₃ rod from location D8, and a part-length UO₂ rod from location H5. The characteristics of the measured samples are listed in Table 17.

The burnups assigned to these samples are based on values determined by GE Nuclear Energy [52]. These burnup values were determined using uranium, plutonium, and neodymium isotope ratios. However, for some samples, large deviations, of up to 7%, are observed between measured and calculated ¹⁴⁸Nd content, a common burnup indicator. Adjusting the calculations to match the measured ¹⁴⁸Nd resulted in inconsistencies in other nuclides, and this inconsistency in sample burnup has not been resolved. The impact of uncertainties in the estimated sample burnup values is assessed later in this report.

Table 17 Summary of Limerick GE11 9 × 9 Assembly Measurements

Assembly ID	Rod ID	Sample ID	Fuel type	Axial height (mm)	Avg. Void (%)	Enrichment (wt % ²³⁵ U)	Gd content (wt % Gd ₂ O ₃)	Burnup (GWd/MTU)
YJ1433	D8	D8-3D2	UO ₂ -Gd ₂ O ₃	823	54.8	3.6	5.0	54.4
		D8-4G3	UO ₂ -Gd ₂ O ₃	1,301	68.8	3.6	5.0	37.0
	D9	D9-1D2	UO ₂	308	12.1	3.95	0	62.1
		D9-2D2	UO ₂	623	44.1	3.95	0	65.5
		D9-4D4	UO ₂	823	65.4	3.95	0	64.9
		D9-4G1E1	UO ₂	1,305	69.1	3.95	0	56.5
	H5	H5-3A1C	UO ₂	308	54.8	3.95	0	57.9
		H5-3A1G	UO ₂	623	57.7	3.95	0	57.8

^a Measured from the bottom of the active fuel length.

Measurements performed by the laboratory at GE Vallecitos were made primarily using IDMS using TIMS. The measured nuclides include isotopes of U, Pu, Nd, Gd, Sm, Eu, Am, Cm, Np, and Cs. Alpha spectrometry and mass spectrometry were used to measure ²³⁸Pu, the americium isotopes, and ²³⁷Np.

The Limerick measurements were previously evaluated under the YMP project using depletion codes employing both 1D transport models [13] and 2D models [53]. The detailed design information for the GE11 assembly and operating history data for assembly YJ1433 are currently not public. The calculations reported in this study include restricted information that is only available under a nondisclosure agreement.

The void fraction data documented with the Limerick data are not based on detailed core simulation codes but were instead developed using core average void fractions and semiempirical correlations to estimate axial and time-dependent void levels for the measured assembly, potentially introducing additional uncertainty.

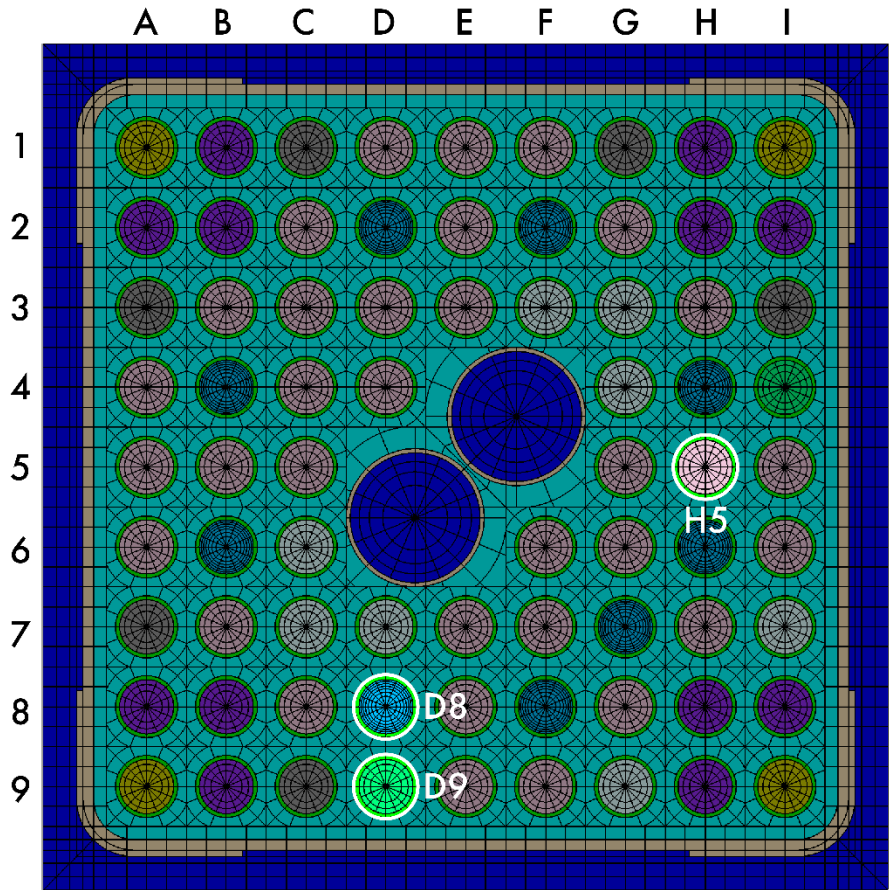


Figure 10 Polaris Model of Limerick-1 GE11 9 × 9 Assembly

Table 18 Limerick-1 GE11 9 × 9 Assembly Parameters

Reactor and Assembly Data	
Reactor	Limerick Unit 1
Operating pressure (bar)	70
Assembly type	GE11 9 × 9
Fuel assembly pitch (cm)	15.24
Number of fuel rods	74
Number of gadolinia rods	9
Number of water rods	2
Fuel rod pitch (cm) ^a	1.438
Channel bypass gap (cm) ^b	[]
Channel thickness (cm) ^b	[]
Channel corner radius (cm) ^b	[]
Channel material	Zirc-4
Channel temperature (K) ^c	560
Active fuel length (cm)	
Fuel Rod Data	
Pellet radius (cm) ^d	0.471
Pellet material	UO ₂ / Gd ₂ O ₃ -UO ₂
Pellet density (g/cm ³)	10.45
Fuel temperature (K)	1100
Clad inner radius (cm) ^a	0.4878
Clad outer radius (cm) ^a	0.559
Clad material	Zirc-2
Clad temperature (K) ^c	560
Water Rod Data	
Inner radius (cm) ^b	[]
Outer radius (cm) ^b	[]
Water rod material	Zirc-2
Water rod temperature (K)	560

^a Reference [54]

^b Proprietary value

^c Assumed to be at core average coolant temperature

^d Reference [55]

5.9 Quad Cities GE11 (9 × 9)

Measurements of fuel rods from lead test assembly LYD449X, a BP8 × 8R design irradiated in Quad Cities Unit 1, have been reported by the GE Vallecitos Laboratory [56][57] and by Argonne National Laboratory [58]. Extensive isotopic measurements were sponsored by the Office of Civilian Radioactive Waste Management to support burnup credit in post-closure criticality evaluations for the Yucca Mountain Project. Twelve samples from fuel rod segment numbers VW00101, ZB00113, and ZS00102 were measured by Argonne. Six samples from the same rod segments were measured by GE Vallecitos.

Detailed assembly design and operating data for the measured assembly however have not been made publicly available. Other information indicates that assembly LYD449X was reconstituted (rebuilt) with previously irradiated rods [59]. No additional information on the fuel rod reconfiguration has been identified. Due to the lack of operating information and assembly

reconfiguration details, these measurements were not used in the present study. The Quad Cities experiment is cited in this report only for completeness and to indicate that these measurements were considered for validation and could potentially be used in the future if additional irradiation data were made available.

6 CRITICALITY APPLICATION MODELS

Methods and experimental data described to this point are applicable to any criticality application model as long as diversity and availability of the selected measured isotopic compositions cover the application range.

The application model used in this report to assess the impact of predicted nuclide uncertainties on the system k_{eff} is based on a generic 68-assembly cask design containing GE14 10×10 assemblies. This section describes the assembly and cask models and the modeling assumptions. The methods and experimental data described in this report can be easily extended to other application models.

6.1 GE14 Assembly

The GE14 fuel assembly design was used as the reference design in the criticality analysis model. This assembly has a 10×10 array of fuel rods and contains two large central water rods that displace eight fuel rods from the array. The GE14 assembly uses varying fuel rod enrichments (Figure 5) and includes fuel rods containing gadolinium. In addition, enrichments can vary axially. The assembly uses part-length fuel rods, which terminate at approximately half the total height of the fuel assembly, resulting in two different fuel rod lattice configurations at different axial levels in the assembly. These two axial regions below and above the top end of the part-length rods are referred to as the dominant or full (DOM) lattice and vanished (VAN) lattice. The vanished lattice is located axially above the part-length rods, so these part-length rods are in effect removed from the lattice. Two-dimensional representations of the two lattice regions in the KENO V.a model are shown in Figure 11.

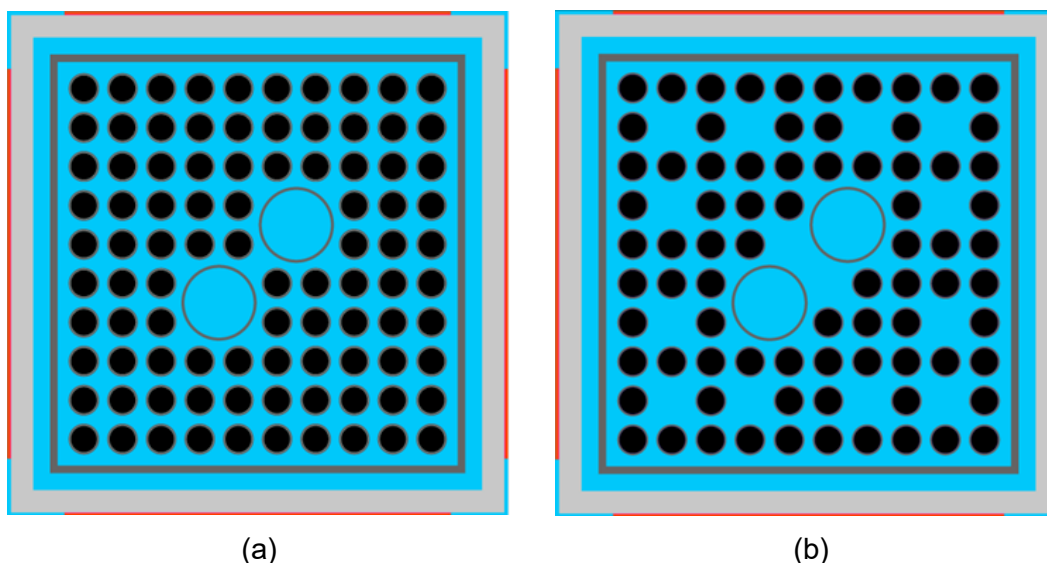


Figure 11 (a) DOM and (b) VAN Lattice of the GE14 Assembly (Shown in a Dry Cask Storage Cell)

The GE14 fuel assembly is used as the reference design for these studies since it is a common assembly type used in US BWRs and includes advanced geometry features seen in modern BWR fuel assemblies (e.g., large water rods, part-length rods, relatively high enrichment, and use of gadolinium-bearing fuel rods). A previous study [60] has shown that the GE14 10 × 10 assembly design is more reactive than smaller GE lattices (7 × 7, 8 × 8, and 9 × 9) for most burnups.

6.2 GBC-68 Cask

The computational benchmark model developed in Reference [41] as a generic burnup credit (GBC) cask containing 68 BWR assemblies (GBC-68 cask) was used to quantify the impact of isotopic bias and uncertainty in the criticality analysis. The cask is modeled using the KENO V.a Monte Carlo criticality code (Figure 12). This cask model is based on the same model used in previous BWR burnup credit studies [61].

The GBC-68 cask model uses GE14 assemblies with full-length and part-length fuel rods. The KENO V.a model of the GE14 assemblies explicitly represents each fuel rod, including the fuel-cladding gap and cladding. Part-length rods are truncated at the appropriate elevation so that both the full lattice (DOM) and the vanished lattice (VAN) are included explicitly in the KENO V.a model. The assembly channel is approximated in the model with constant thickness and square corners.

The GBC-68 cask model assumes that all fuel rods contain the same nuclide compositions both axially and radially. Similar assumptions were used previously in this application model [61]. Axial variations (i.e., the natural uranium blanket regions) or enrichment zoning of the fuel rods in the assembly were not included, but UO₂-Gd₂O₃ fuel rod compositions were explicitly modeled for the analysis of axial burnup distributions. Homogenization of the all fuel rods was also used previously in the analysis of void fraction and control blade effects [61].

The requirement to homogenize the fuel compositions in the KENO V.a calculations in the present analysis is imposed by the isotopic uncertainty analysis methodology. Criticality calculations are performed for the GE14 assembly design and GBC-68 application model using measured isotopic contents for the 77 spent fuel samples selected and described in Section 4. These samples span a wide range of enrichments, burnups, and void fractions and include measurements of both UO₂ and UO₂-Gd₂O₃ type fuels. However, the compositions are constrained to those of the measured samples, and therefore a more spatially detailed application model is not possible.

The present analysis does not model gadolinium-bearing fuel rods explicitly. Because of this, the results are only applicable to BWR burnup credit beyond peak reactivity where any initial gadolinium present in the fuel has been fully depleted. In addition, the lowest-burnup-measured UO₂-Gd₂O₃ fuel samples used in this study (Fukushima Daini 2 assembly 2F2D1 rod B3) did not measure gadolinium isotopes. Any initial ¹⁵⁵Gd or ¹⁵⁷Gd present in UO₂-Gd₂O₃ fuel rods is assumed to be fully depleted in these analyses.

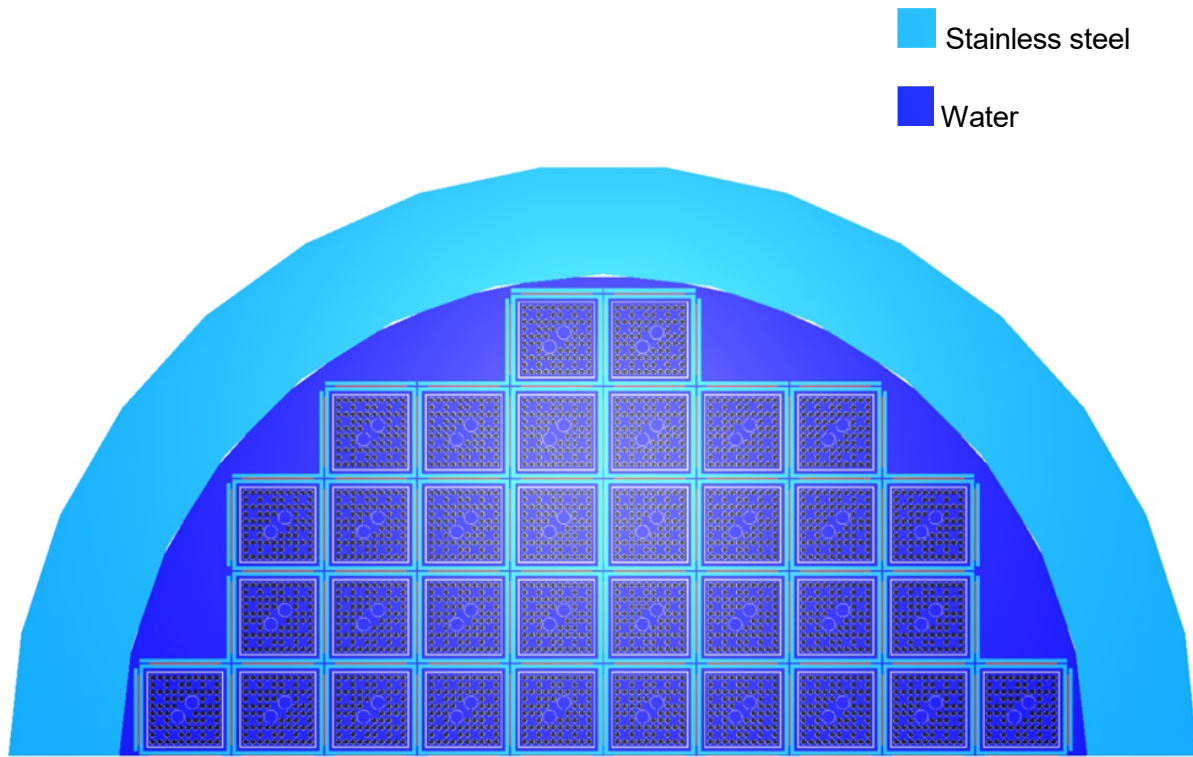


Figure 12 Radial View of the KENO V.a GBC-68 Cask Model (Elevation of Vanished Lattice)

7 UNCERTAINTY ANALYSIS

The most widely used approach to burnup credit validation involves validating the two separate components of the criticality safety analysis; components related to the prediction of nuclide compositions and components associated with the criticality calculation. Validation of the code prediction of nuclide compositions is routinely performed using experimental data from destructive radiochemical analysis of spent fuel samples and is the subject of this report. Validation of the criticality calculation itself is performed using applicable critical experiments and is reported separately [3].

7.1 Methodology

Several different approaches have been developed and used to assess the effect of uncertainties in predicted nuclide compositions on the k_{eff} of a criticality application model, each with different levels of complexity and conservatism. These methods include, but are not limited to: (1) the development of bounding factors [62] applied to adjust the calculated isotopic compositions for uncertainty to ensure conservative estimates of k_{eff} , (2) Monte Carlo sampling of the statistical distributions of the nuclide compositions [63] to obtain the uncertainty distribution of k_{eff} , and (3) direct application of measured and calculated nuclide compositions in the criticality model [7]. A review and comparison of these different approaches has been previously documented [20].

In the present study, the direct application of measured nuclide compositions in the criticality model is used. The basis for selecting this approach is discussed in more detail in Section 2 of this report. KENO V.a calculations are performed using the major actinide-only compositions (Table 1) and also actinide and fission product nuclide compositions (Table 2). Fuel compositions include the oxygen, which is part of the UO_2 fuel matrix. KENO V.a criticality calculations are performed using the measured nuclide concentrations for each fuel sample.

In parallel with these calculations, separate KENO V.a calculations are performed using isotopic concentrations obtained directly from the Polaris depletion calculation for the same samples. The Polaris calculations are performed using assembly design, irradiation history data and measurement dates as reported in the experimental references. No adjustment of the irradiation parameters is used in the Polaris calculations to obtain conservative isotopic values. Therefore, the nuclide concentrations calculated using Polaris represent best-estimate values. This procedure is illustrated in Figure 13.

7.1.1 Measurements

The measured isotopic concentrations are those reported by the laboratory as isotopic content or isotopic ratios that have been converted to mass units per initial metric ton of heavy metal (uranium). Measured concentration units have been converted to units of milligram per gram of initial uranium (mg/gUi) to provide a consistent basis for comparison with calculations. Most of the experimental datasets included in the SFCOMPO database store measurements in units as reported by the laboratory and also in mg/gUi units.

Measurements for the Limerick-1 samples are reported in units of mg per gram of ^{238}U in the measured sample. The reported units are converted to mg/gUi on the basis of the measurement data by the following formula:

$$\frac{m_i}{\frac{U}{U8} + \frac{Pu}{U8} + \frac{Np + Am + Cm}{U8} + \frac{F}{U8}} \quad (1)$$

where m_i is the mass of measured isotope i as reported in mg/g ^{238}U (U8), and the denominator is an experimental estimate of the initial uranium content derived from the sum of the heavy metal (uranium, plutonium, americium, curium) weights in the measured sample, corrected for the weight loss in initial uranium due to fission, F . In this equation the uranium mass U/U8 includes the contribution of ^{238}U of 1,000 mg/g ^{238}U . The reduction in the initial heavy metal mass during burnup is estimated from the total number of fissions as determined from measured ^{148}Nd by $F/U8 = m (238/148) / \bar{Y}$, where $\bar{Y} = 0.0170$ is the effective ^{148}Nd fission yield applied to UO_2 fuel [49], and m is the measured ^{148}Nd mass in mg/g ^{238}U .

The measured isotopic data of the burnup credit isotopes (Table 2) are listed in Appendix A for all samples, with the cooling time of the measurements indicated. Measured results for the Dodewaard sample DU1 are included for both the SCK•CEN and PSI measurements.

7.1.2 Measurement dates

The cooling times used to compare measured and calculated nuclide concentrations are those reported by the laboratory, generally corresponding to the actual date of the measurements. For several experiments, measurements of different isotopes in a sample are reported for different dates. Adjustment of measurements to a common reference date is possible using decay relationships and has been performed in previous studies [6] and recommended in earlier guidance [1]. However, in order to perform these adjustments, measurements of any decay precursor nuclides (production terms) are also required. Because most samples used in this report were measured on the same date or on dates that are very similar relative to the half-lives of the nuclides and/or precursors, no adjustment of the measurements was performed in this study to avoid potentially introducing additional uncertainty in the measured concentrations. The impact of not performing time corrections was analyzed for the specific samples used in this study and was found to be less than 30 pcm. This bias is insignificant relative to other uncertainties.

Measurements for Fukushima Daini 2 assembly 2F2DN23 were reported at the time of discharge from the reactor (no cooling time), with the exception of the samarium isotopes that were reported at the time of measurement (cooling time approximately 6 years). No adjustment of samarium is possible without also measuring the decay precursors of promethium. Care is needed in analyzing measurements reported at discharge to ensure that any short-lived precursors of the measured nuclide are included in the calculations, since these decay contributions cannot be subtracted from the measured concentration. For example, the concentration of ^{239}Pu as reported at discharge includes the contribution from ^{239}Np ($T_{1/2} = 2.35$ days) decay. Therefore, using calculated concentrations at discharge will miss this contribution to the ^{239}Pu inventory. In the present study, a decay time of 500 days was added after irradiation to the calculations to ensure that short-lived precursors were included in the predictions to be consistent with measurements.

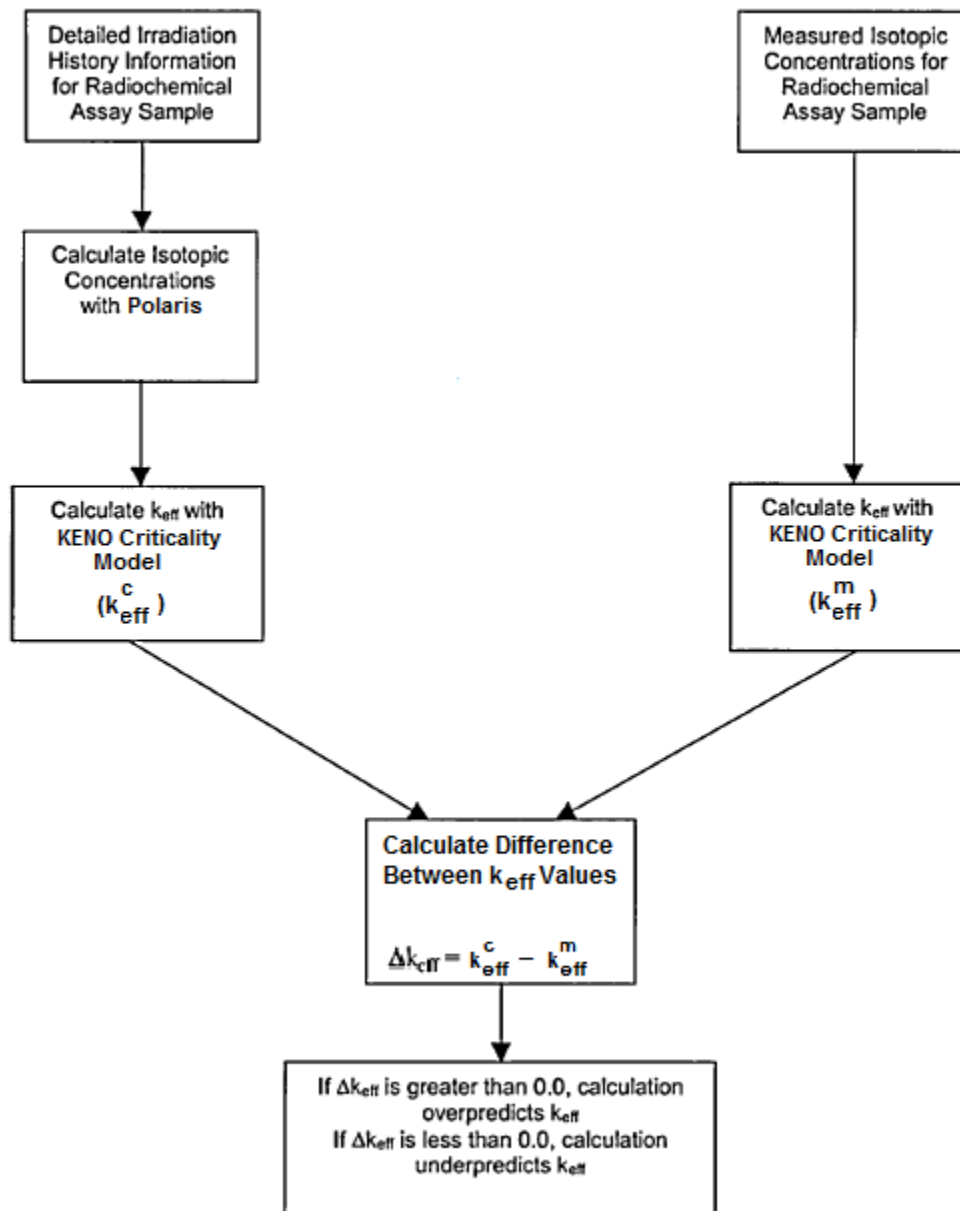


Figure 13 Uncertainty Analysis Methodology for Nuclide Compositions (Adapted from [19])

7.1.3 Partial Isotopic Datasets

The calculation procedure in Figure 13 was applied to all samples using the major actinide-only nuclides and the actinide-plus-fission product datasets. Measurements of all major actinides (Table 1) were available for most samples considered in this report, with the exception of 14 samples that did not measure ^{241}Am . Measurements for minor actinides and fission products (Table 2) were available for a limited number of samples.

To minimize inconsistencies that could arise by comparing k_{eff} values for samples with different sets of nuclides (as available in the measured samples), a common set of minor actinides and fission products (Table 2) were used in all criticality calculations. To account for nuclides not measured in some samples, calculated concentrations were used as a surrogate for measured data. To account for bias in the calculated concentrations, the median bias derived from other samples with measured data was applied. To account for uncertainty in this estimated concentration, the k_{eff} calculation was also performed using surrogate nuclide concentrations adjusted conservatively to maximize k_{eff} and also to minimize the k_{eff} in the cask model. The bounding k_{eff} values were obtained by performing adjustments for uncertainty in the bias-corrected calculated nuclide concentrations using the 10th percentile and the 90th percentile of the distribution (see Sect. 7.2) of deviations obtained between calculated and measured nuclide concentrations. Therefore, in addition to obtaining the k_{eff} bias value for each sample, this approach introduces error bars for each sample due to the application of derived measurement data from the calculations to illustrate the potential impact of adding surrogate data to the k_{eff} calculations.

7.2 Isotopic Bias and Uncertainty

The calculated isotopic concentrations of all nuclides considered in the burnup credit analysis methodology (Table 2) were compared to measured concentrations obtained by destructive radiochemical analysis of the fuel samples. These comparisons were performed at the time of measurement of each isotope (Appendix B).

One sample from the Fukushima Daini-2 assembly 2F2DN23, sample SF99-10, was not included in the analysis due to its very close proximity to the end of the active fuel length. The results for this sample exhibit large biases that are attributed to the spectral change near the ends of the fuel rods which are not accounted for in the 2D models.

The deviations between the Polaris calculations (C) and measurements (M) are expressed as the relative percent difference $(C/M - 1)\%$. The results for each individual sample and nuclide are listed in Appendix B, and a statistical analysis summary is presented in Table 19. The summary includes the total number of measurements available for each isotope, the mean deviation, the standard deviation, the median value, minimum and maximum deviations, the 1st and 3rd quartile (range contains 50% of the data points), and the percentiles for 10% (p10) and 90% (p90) of the data (range contains 80% of the data points).

The statistical analysis presented in Table 19 provides a summary of the isotopic results and illustrates the performance of the Polaris code used in the present study. However, it is important to note that these isotopic results are not essential for the uncertainty methodology used here, since the calculated and measured nuclide concentrations are used directly in the application model without any need to characterize the bias, uncertainty, or statistical distribution of individual nuclides. An exception is for nuclides (minor actinides and fission products) that are not measured in a particular sample. In these cases, surrogate nuclide concentrations are used in lieu of measurements to ensure that all criticality calculations use a consistent set of burnup credit nuclides.

In this study, the surrogate data are nuclide concentrations calculated with Polaris and adjusted to correct for the median bias using deviations observed in other samples. To account for the additional uncertainty in these surrogate data, additional criticality calculations are performed

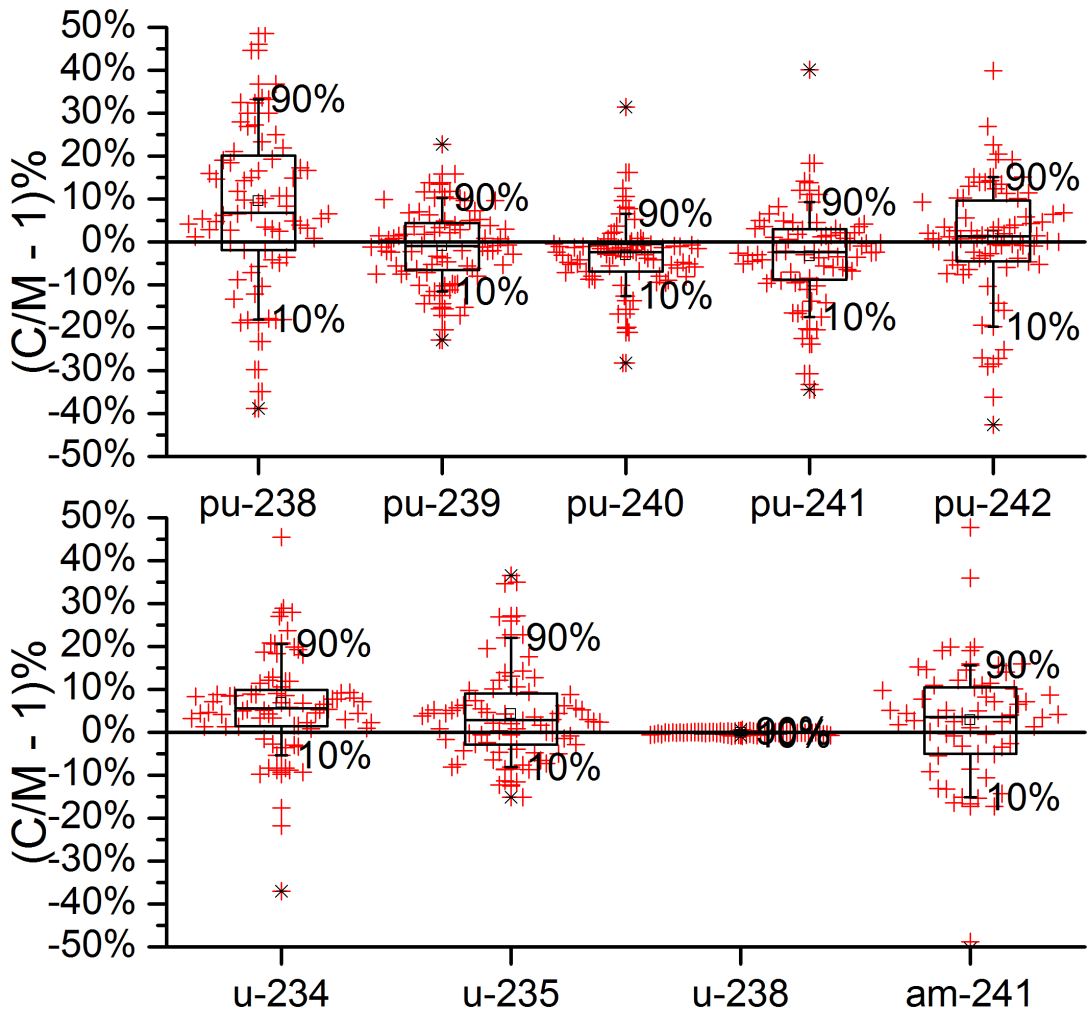
using surrogate data adjusted to the p10 and p90 percentiles to provide a conservative quantitative estimate of the additional uncertainty associated with samples that do not measure all burnup credit isotopes.

The isotopic distributions are presented as box plots in Figures 14, 15, and 16, showing the mean, median, quartiles, and box whiskers that represent the p10 and p90 percentiles and the min/max values in the distributions. The individual values for each sample are also shown. Maximum values in ²³⁴U, ²³⁸Pu, ²⁴²Pu, ²⁴¹Am, ²⁴³Am and ¹⁰⁹Ag percent differences are above 60%, and not shown in the plots in order to display distribution details. These plots are nonparametric and make no assumptions of the statistical isotopic distributions for the samples and are based on the actual observed distributions. An outlier analysis of these distributions can be performed; however, in this study no data were rejected based on outlier analysis.

Table 19 Statistical Analysis of Predicted Isotopic Concentrations (C/M-1) (%)

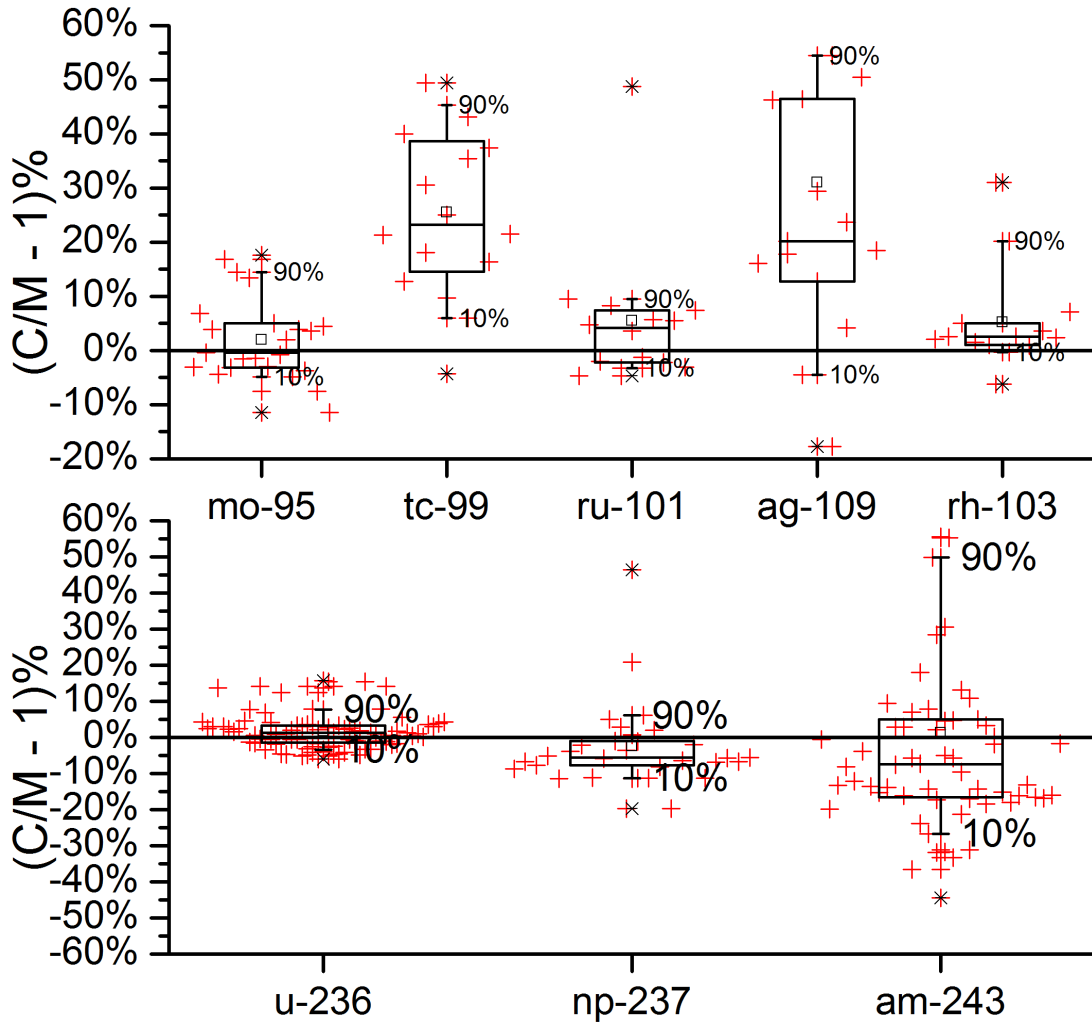
Data	Number of Measurements	Mean	Standard Deviation	Median	Minimum	Maximum	1 st Quartile (Q1)	3 rd Quartile (Q3)	Percentile p10 ^a	Percentile p90 ^a
²³⁴ U	76	6.8%	13.4%	5.5%	-37.0%	66.6%	1.4%	9.9%	-5.4%	20.6%
²³⁵ U	76	4.3%	11.2%	2.8%	-15.1%	36.5%	-2.8%	9.1%	-8.1%	22.0%
²³⁶ U	76	1.6%	4.8%	1.2%	-6.0%	15.7%	-1.5%	3.2%	-3.4%	7.7%
²³⁸ U	76	-0.1%	0.3%	-0.1%	-0.8%	0.5%	-0.2%	0.1%	-0.6%	0.2%
²³⁸ Pu	76	9.5%	21.1%	6.7%	-38.8%	93.6%	-1.9%	20.1%	-18.1%	33.2%
²³⁹ Pu	76	-0.9%	8.7%	-1.0%	-22.8%	22.7%	-6.6%	4.4%	-11.6%	10.2%
²⁴⁰ Pu	76	-3.1%	8.4%	-2.4%	-28.3%	31.4%	-6.9%	-0.5%	-12.6%	6.5%
²⁴¹ Pu	76	-3.3%	11.6%	-2.4%	-34.5%	40.1%	-8.8%	2.9%	-17.6%	9.2%
²⁴² Pu	76	1.2%	17.2%	1.2%	-42.6%	87.9%	-4.5%	9.6%	-19.8%	15.1%
²⁴¹ Am	62	2.8%	17.4%	3.6%	-50.3%	69.1%	-5.0%	10.5%	-15.2%	15.6%
²⁴³ Am	62	1.3%	33.5%	-7.5%	-44.5%	122.8%	-16.6%	4.9%	-26.7%	49.9%
²³⁷ Np	29	-2.4%	11.9%	-5.7%	-19.8%	46.4%	-7.7%	-1.1%	-11.3%	6.1%
¹⁴³ Nd	50	4.5%	4.0%	3.9%	-4.1%	13.1%	2.1%	7.0%	0.0%	10.8%
¹⁴⁵ Nd	50	2.5%	3.2%	1.4%	-2.5%	11.8%	0.7%	3.6%	-0.8%	8.0%
⁹⁵ Mo	23	2.0%	7.7%	-0.4%	-11.5%	17.6%	-3.1%	5.0%	-4.8%	14.5%
⁹⁹ Tc	16	25.5%	15.5%	23.3%	-4.3%	49.5%	14.6%	38.7%	6.0%	45.3%
¹⁰¹ Ru	14	5.5%	13.4%	4.2%	-4.7%	48.8%	-2.2%	7.4%	-3.3%	9.5%
¹⁰⁹ Ag	15	31.0%	38.1%	20.2%	-17.8%	147.2%	12.7%	46.4%	-4.5%	54.5%
¹³³ Cs	16	-3.2%	7.2%	-2.9%	-24.0%	7.7%	-5.0%	1.7%	-11.9%	3.6%
¹⁴⁷ Sm	35	0.2%	8.2%	1.6%	-17.0%	17.0%	-4.8%	6.0%	-10.8%	7.7%
¹⁴⁹ Sm	32	-6.6%	12.2%	-6.7%	-34.0%	20.2%	-16.6%	1.6%	-20.2%	5.6%
¹⁵⁰ Sm	34	2.6%	6.6%	3.3%	-10.4%	15.8%	-4.2%	7.5%	-8.1%	9.6%
¹⁵¹ Sm	35	-0.5%	11.9%	-0.2%	-18.2%	37.9%	-10.0%	4.9%	-12.7%	14.4%
¹⁵² Sm	35	4.7%	6.5%	6.0%	-8.5%	13.6%	0.7%	10.2%	-7.1%	12.2%
¹⁵¹ Eu	15	-9.2%	21.8%	3.2%	-48.4%	11.7%	-32.7%	7.7%	-39.3%	9.3%
¹⁵³ Eu	25	6.3%	3.7%	6.0%	-3.2%	14.0%	4.7%	9.2%	0.6%	10.3%
¹⁵⁵ Gd	25	13.9%	12.8%	10.0%	-8.5%	6.0%	10.0%	19.9%	50.4%	4.0%
¹⁰³ Rh	15	5.2%	9.0%	2.5%	-6.2%	31.1%	1.1%	5.0%	-0.3%	20.2%

^a p10 and p90 are the 10% and 90% percentiles of the distribution of the C/M-1 values.



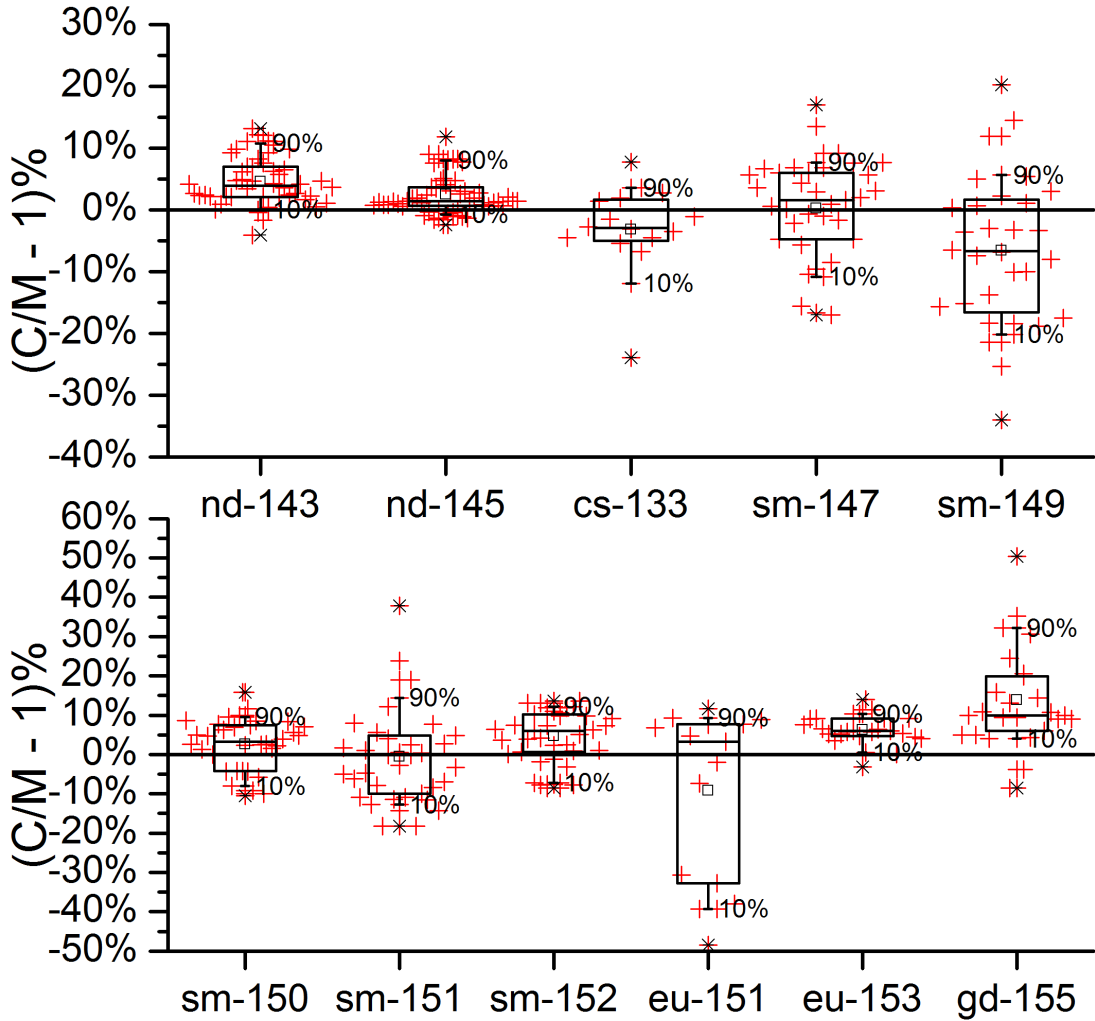
Quartiles (box)
 Median (horizontal line in box)
 10th and 90th percentiles (whiskers)
 Mean (shown as a small square in the box)
 Max/Min data points (x) and individual data points (+) for each sample
 Max data points above 60% are not shown in the plots

Figure 14 Box Plot of the Major Actinide Isotopes



Quartiles (box)
 Median (horizontal line in box)
 10th and 90th percentiles (whiskers)
 Mean (shown as a small square in the box)
 Max/Min data points (x) and individual data points (+) for each sample
 Max data points above 60% are not shown in the plots

Figure 15 Box Plot of the Minor Actinides and Fission Products (Mo, Tc, Ru, Ag, and Rh)



Quartiles (box)
 Median (horizontal line in box)
 10th and 90th percentiles (whiskers)
 Mean (shown as a small square in the box)
 Max/Min data points (x) and individual data points (+) for each sample
 Max data points above 60% are not shown in the plots

Figure 16 Box Plot of the Fission Products (Nd, Cs, Sm, Eu, and Gd)

7.3 Criticality Calculations

The measured isotopic concentrations were applied in the GBC-68 application model, and the k_{eff} values were calculated with KENO V.a using data from the 77 spent fuel sample measurements. As discussed previously, three separate criticality calculations were performed using the measured data for each sample:

1. Measured isotopic data plus calculated surrogate data for isotopes not measured in the sample, with surrogate data calculated based on the median isotopic bias (Table 19)
2. Measured isotopic data with surrogate data calculated based on the p10 percentile bias (Table 19)
3. Measured isotopic data with surrogate data calculated based on the p90 percentile bias (Table 19)

For the application of measurement data to the criticality model, the measured isotopic concentrations in units of mg/gU were converted to atom number densities using a fuel density in the application model of 10.42 g/cm³.

The potential uncertainty introduced by using calculated surrogate data to augment missing measurement data is estimated by analyzing the uncertainties in the surrogate data based on the range of deviations observed in the samples with measurements. In this case, it is important to note that uncertainties are applied such that the calculated concentrations of all surrogate data are simultaneously increased (when the p90 percentile bias was applied) or simultaneously decreased (when the p10 percentile bias was applied), providing a conservative estimate of the uncertainty range. In an earlier study using a similar approach [6], the impact of surrogate data uncertainty was estimated to be small; however, no quantitative analysis of the uncertainty was performed in that study.

The k_{eff} values obtained using measured nuclide concentrations are compared with the values obtained by calculation using the Polaris code for the actinide-only nuclide set (Table 1) and actinides plus fission products (Table 2). Table 20 lists the k_{eff} values and the difference in k_{eff} between the measured and calculated actinide-only isotope set concentrations in absolute units of pcm (1 pcm = 10⁻⁵). Since k_{eff} is calculated by KENO V.a with a stochastic uncertainty of less than 10 pcm, this Monte Carlo sampling uncertainty contribution can be neglected. The uncertainties for the Δk_{eff} values in Table 20 correspond to the uncertainties associated with the use of surrogate data. The plus and minus error bars were not equal due to the non-normal distributions of the nuclide deviations used in developing the p10 and p90 percentile values. However, in most cases the error bars were similar and therefore only the average error bar is listed in Table 20.

Values of the sample burnup and the average void fraction are also listed in Table 20. Sample identifiers are based on the reactor, assembly, fuel rod, and sample name. The reactor names are

- FOR (Forsmark),
- DOD (Dodewaard),
- FD2 (Fukushima Daini),
- LBT (Leibstadt), and
- LIM (Limerick).

Measured uranium and plutonium isotopes were available for all samples. The Forsmark 3 sample F3F6 and samples from Fukushima Daini 1 assemblies 2F1ZN2 and F21ZN3 did not include measurements of major actinide ^{241}Am . Therefore, the k_{eff} values for these samples were calculated using surrogate concentrations for ^{241}Am and include bias and bias uncertainty estimates.

Table 21 provides k_{eff} results for the actinide-plus-fission product isotope dataset with the uncertainties associated with surrogate data for the minor actinides and fission products as estimated using the p10 and p90 percentiles from Table 19.

The k_{eff} bias results are plotted in Figure 17. Each sample is labeled, and the data points are colored to identify the different experimental datasets. In general, the actinide-only results are similar to the actinide-plus-fission product results.

Table 20 Criticality Results for the GBC-68 Cask Model for Major Actinide-Only Compositions

No.	Sample ID	Burnup (GWd/MTU)	Void (%)	Measured k_{eff}^m	Calculated k_{eff}^c	Δk_{eff} (pcm) ^a
1	FD2-2 2F2DN23 SF98 1	4.2	0.0	0.6456	0.6376	-803
2	FD2-2 2F2DN23 SF98 2	26.5	0.0	0.8401	0.8165	-2,358
3	FD2-2 2F2DN23 SF98 3	36.9	3.0	0.7418	0.7474	565
4	FD2-2 2F2DN23 SF98 4	42.4	11.0	0.7151	0.7194	438
5	FD2-2 2F2DN23 SF98 5	44.0	32.0	0.7314	0.7318	42
6	FD2-2 2F2DN23 SF98 6	39.9	54.5	0.7835	0.7787	-482
7	FD2-2 2F2DN23 SF98 7	39.4	68.0	0.7920	0.7986	666
8	FD2-2 2F2DN23 SF98 8	27.2	73.0	0.8452	0.8538	858
9	FD2-2 2F2DN23 SF99 1	7.5	0.0	0.6417	0.6238	-1,790
10	FD2-2 2F2DN23 SF99 2	22.6	1.4	0.8129	0.8210	808
11	FD2-2 2F2DN23 SF99 3	32.4	5.8	0.7543	0.7604	614
12	FD2-2 2F2DN23 SF99 4	35.4	10.8	0.7312	0.7463	1,510
13	FD2-2 2F2DN23 SF99 5	37.4	27.7	0.7510	0.7519	95
14	FD2-2 2F2DN23 SF99 6	32.4	54.7	0.8027	0.8062	355
15	FD2-2 2F2DN23 SF99 7	32.1	66.5	0.8125	0.8214	892
16	FD2-2 2F2DN23 SF99 8	21.8	71.7	0.8493	0.8671	1,776
17	FD2-2 2F2DN23 SF99 9	16.7	72.9	0.8697	0.8845	1,478
18	FD2-2 2F2D1 B3 TU103	10.0	64.0	0.9156	0.9116	-404
19	FD2-2 2F2D1 B3 TU104	9.4	60.2	0.8993	0.9150	1,564
20	FD2-2 2F2D1 B3 TU105	12.3	17.3	0.9030	0.8866	-1,647
21	FD2-2 2F2D1 F6 TU101	14.0	64.3	0.9663	0.9503	-1,606
22	FD2-2 2F2D1 F6 TU102	18.2	12.9	0.9238	0.9160	-779
23	FD2-2 2F2D1 F6 TU106	16.1	59.8	0.9462	0.9381	-808
24	FD2-2 2F2D2 B3 TU203	24.5	63.1	0.8530	0.8387	-1,426
25	FD2-2 2F2D2 B3 TU204	23.5	58.5	0.8385	0.8401	154
26	FD2-2 2F2D2 B3 TU205	22.8	10.4	0.7922	0.8159	2,367
27	FD2-2 2F2D2 F6 TU201	29.1	63.1	0.8935	0.8763	-1,717
28	FD2-2 2F2D2 F6 TU202	32.9	7.0	0.8294	0.8246	-483
29	FD2-2 2F2D3 A4 TU304	37.8	61.0	0.7434	0.7585	1,511
30	FD2-2 2F2D3 A4 TU306	32.3	6.0	0.7011	0.7350	3,393
31	FD2-2 2F2D3 B3 TU308	30.2	63.5	0.7963	0.8114	1,505
32	FD2-2 2F2D3 B3 TU309	34.8	60.5	0.7942	0.7868	-733
33	FD2-2 2F2D3 B3 TU311	33.5	9.1	0.7159	0.7463	3,033
34	FD2-2 2F2D3 H5 TU301	34.6	60.6	0.7490	0.7718	2,285
35	FD2-2 2F2D3 H5 TU302	31.4	5.2	0.7047	0.7406	3,593
36	FD2-2 2F2D8 A4 TU505	59.1	54.9	0.6746	0.6695	-503
37	FD2-2 2F2D8 A4 TU506	57.5	23.0	0.6171	0.6248	775

Table 21 Criticality Results for the GBC-68 Cask Model for Major Actinide-Only Compositions (Con't)

No.	Sample ID	Burnup (GWd/MTU)	Void (%)	Measured k_{eff}^m	Calculated k_{eff}^c	Δk_{eff} (pcm) ^a
38	FD2-2 2F2D8 B3 TU510	53.1	62.2	0.7222	0.7136	-855
39	FD2-2 2F2D8 B3 TU511	48.1	14.0	0.6479	0.6632	1,536
40	FD2-2 2F2D8 H5 TU501	53.2	63.2	0.7004	0.7000	-46
41	FD2-2 2F2D8 H5 TU502	58.9	58.0	0.6661	0.6758	975
42	FD2-2 2F2D8 H5 TU503	55.6	20.6	0.6049	0.6272	2,222
43	FD2-1 2F1ZN2 C2 GdB	35.6	18.4	0.7079	0.7162	734 ± 93
44	FD2-1 2F1ZN2 C2 GdT	27.9	73.7	0.7754	0.7876	890 ± 244
45	FD2-1 2F1ZN2 C3 UB	47.5	18.4	0.7575	0.7623	348 ± 105
46	FD2-1 2F1ZN2 C3 UT	38.2	73.7	0.8268	0.8402	969 ± 272
47	FD2-1 2F1ZN3 A9 UB	61.2	11.4	0.5674	0.5720	312 ± 109
48	FD2-1 2F1ZN3 A9 UM	64.2	38.3	0.5892	0.5731	-1,903 ± 211
49	FD2-1 2F1ZN3 A9 UT	56.3	60.1	0.6276	0.6321	262 ± 144
50	FD2-1 2F1ZN3 C2 GdB	54.6	18.4	0.6147	0.6203	402 ± 131
51	FD2-1 2F1ZN3 C2 GdM	54.5	38.3	0.6329	0.6269	-1,006 ± 293
52	FD2-1 2F1ZN3 C2 GdT	46.3	60.1	0.7120	0.7175	369 ± 136
53	FD2-1 2F1ZN3 C3 UB	68.3	11.4	0.6357	0.6407	329 ± 130
54	FD2-1 2F1ZN3 C3 UM	68.4	38.3	0.6607	0.6549	-876 ± 220
55	FD2-1 2F1ZN3 C3 UT	59.1	60.1	0.7411	0.7542	1,120 ± 134
56	DOD-1 Y013 B2 DU1 ^b	55.0	49.8	0.7050	0.7139	891
57	DOD-1 Y013 B2 DU1 ^c	55.0	49.8	0.6955	0.7033	773
58	FOR-3 14595 F6 F3F6	61.0	58.4	0.6577	0.6463	-1485 ± 274
59	FOR-3 GN592 J8 ENUSA-1	50.4	51.0	0.7257	0.7077	-1,801
60	FOR-3 GN592 J8 ENUSA-2	51.1	51.0	0.7269	0.7077	-1,920
61	FOR-3 GN592 J8 ENUSA-3	51.5	13.3	0.6842	0.6757	-849
62	FOR-3 GN592 J8 ENUSA-4	56.0	60.9	0.7096	0.6824	-2,722
63	FOR-3 GN592 J8 ENUSA-5	43.6	67.0	0.7531	0.7339	-1,916
64	FOR-3 GN592 J8 ENUSA-6	43.1	2.2	0.7058	0.6992	-667
65	FOR-3 GN592 J8 ENUSA-7	47.8	13.3	0.6822	0.6757	-644
66	FOR-3 GN592 J8 ENUSA-8	38.3	66.5	0.7665	0.7628	-371
67	LBT AIA003 KLU1	60.5	8.4	0.6158	0.6261	1,032
68	LBT AIA003 KLU2	62.9	51.2	0.6539	0.6649	1,104
69	LBT AIA003 KLU3	56.5	70.4	0.6729	0.6870	1,407
70	LIM-1 FYJ1433 D8 3D2B	54.8	54.8	0.6972	0.7213	2,412
71	LIM-1 FYJ1433 D8 4G3	37.0	68.8	0.7548	0.7889	3,408
72	LIM-1 FYJ1433 D9 1D2	62.1	12.1	0.6237	0.6255	182
73	LIM-1 FYJ1433 D9 2D2	65.5	44.1	0.6554	0.6581	271
74	LIM-1 FYJ1433 D9 4D4	65.0	65.4	0.6748	0.6709	-391
75	LIM-1 FYJ1433 D9 4G1	56.5	69.1	0.7014	0.7075	607
76	LIM-1 FYJ1433 H5 3A1C	57.9	54.8	0.7175	0.7200	246
77	LIM-1 FYJ1433 H5 3A1G	57.8	57.7	0.7188	0.7200	118

^a $\Delta k_{eff} = k_{eff}^c - k_{eff}^m \pm$ average uncertainty due to use of surrogate nuclide compositions.

^b sample measured by laboratories at SCK•CEN.

^c sample measured by laboratories at PSI.

Table 22 Criticality Results for the GBC-68 Cask Criticality Analysis Model for Actinide and Fission Product Spent Fuel Compositions

No.	Sample ID	Burnup (GWd/MTU)	Void (%)	Measured k_{eff}^m	Calculated k_{eff}^c	Δk_{eff} (pcm) ^a
1	FD2-2 2F2DN23 SF98 1	4.2	0.0	0.6317	0.6238	-785 ± 27
2	FD2-2 2F2DN23 SF98 2	26.5	0.0	0.7881	0.7628	-2532 ± 138
3	FD2-2 2F2DN23 SF98 3	36.9	3.0	0.6744	0.6798	547 ± 176
4	FD2-2 2F2DN23 SF98 4	42.4	11.0	0.6425	0.6463	382 ± 168
5	FD2-2 2F2DN23 SF98 5	44.0	32.0	0.6569	0.6567	-21 ± 181
6	FD2-2 2F2DN23 SF98 6	39.9	54.5	0.7121	0.7071	-502 ± 180
7	FD2-2 2F2DN23 SF98 7	39.4	68.0	0.7212	0.7282	694 ± 172
8	FD2-2 2F2DN23 SF98 8	27.2	73.0	0.7886	0.7993	1070 ± 156
9	FD2-2 2F2DN23 SF99 1	7.5	0.0	0.6205	0.6035	-1697 ± 64
10	FD2-2 2F2DN23 SF99 2	22.6	1.4	0.7631	0.7707	757 ± 292
11	FD2-2 2F2DN23 SF99 3	32.4	5.8	0.6912	0.6970	581 ± 341
12	FD2-2 2F2DN23 SF99 4	35.4	10.8	0.6645	0.6792	1462 ± 349
13	FD2-2 2F2DN23 SF99 5	37.4	27.7	0.6762	0.6758	-38 ± 290
14	FD2-2 2F2DN23 SF99 6	32.4	54.7	0.7399	0.7421	223 ± 335
15	FD2-2 2F2DN23 SF99 7	32.1	66.5	0.7491	0.7574	827 ± 350
16	FD2-2 2F2DN23 SF99 8	21.8	71.7	0.7985	0.8169	1846 ± 315
17	FD2-2 2F2DN23 SF99 9	16.7	72.9	0.8275	0.8430	1546 ± 253
18	FD2-2 2F2D1 B3 TU103	10.0	64.0	0.8757	0.8695	-614 ± 345
19	FD2-2 2F2D1 B3 TU104	9.4	60.2	0.8528	0.8674	1455 ± 405
20	FD2-2 2F2D1 B3 TU105	12.3	17.3	0.8698	0.8510	-1880 ± 278
21	FD2-2 2F2D1 F6 TU101	14.0	64.3	0.9336	0.9153	-1824 ± 263
22	FD2-2 2F2D1 F6 TU102	18.2	12.9	0.8831	0.8742	-888 ± 293
23	FD2-2 2F2D1 F6 TU106	16.1	59.8	0.9095	0.8997	-979 ± 277
24	FD2-2 2F2D2 B3 TU203	24.5	63.1	0.8008	0.7836	-1719 ± 366
25	FD2-2 2F2D2 B3 TU204	23.5	58.5	0.7872	0.7864	-84 ± 370
26	FD2-2 2F2D2 B3 TU205	22.8	10.4	0.7403	0.7632	2286 ± 363
27	FD2-2 2F2D2 F6 TU201	29.1	63.1	0.8384	0.8183	-2010 ± 385
28	FD2-2 2F2D2 F6 TU202	32.9	7.0	0.7687	0.7611	-754 ± 407
29	FD2-2 2F2D3 A4 TU304	37.8	61.0	0.6762	0.6897	1350 ± 471
30	FD2-2 2F2D3 A4 TU306	32.3	6.0	0.6400	0.6735	3345 ± 408
31	FD2-2 2F2D3 B3 TU308	30.2	63.5	0.7353	0.7491	1378 ± 427
32	FD2-2 2F2D3 B3 TU309	34.8	60.5	0.7315	0.7190	-1257 ± 414
33	FD2-2 2F2D3 B3 TU311	33.5	9.1	0.6506	0.6801	2951 ± 442
34	FD2-2 2F2D3 H5 TU301	34.6	60.6	0.6860	0.7071	2111 ± 404
35	FD2-2 2F2D3 H5 TU302	31.4	5.2	0.6445	0.6801	3563 ± 425
36	FD2-2 2F2D8 A4 TU505	59.1	54.9	0.5937	0.5857	-798 ± 488
37	FD2-2 2F2D8 A4 TU506	57.5	23.0	0.5398	0.5448	503 ± 490

Table 23 Criticality Results for the GBC-68 Cask Criticality Analysis Model for Actinide and Fission Product Spent Fuel Compositions (Con't)

No.	Sample ID	Burnup (GWd/MTU)	Void (%)	Measured k_{eff}^m	Calculated k_{eff}^c	Δk_{eff} (pcm) ^a
38	FD2-2 2F2D8 B3 TU510	53.1	62.2	0.6433	0.6311	-1217 ± 519
39	FD2-2 2F2D8 B3 TU511	48.1	14.0	0.5732	0.5863	1,318 ± 473
40	FD2-2 2F2D8 H5 TU501	53.2	63.2	0.6206	0.6199	-69 ± 506
41	FD2-2 2F2D8 H5 TU502	58.9	58.0	0.5831	0.5921	900 ± 524
42	FD2-2 2F2D8 H5 TU503	55.6	20.6	0.5263	0.5484	2,212 ± 472
43	FD2-1 2F1ZN2 C2 GdB	35.6	18.4	0.6427	0.6489	622 ± 548
44	FD2-1 2F1ZN2 C2 GdT	27.9	73.7	0.7164	0.7254	04 ± 265
45	FD2-1 2F1ZN2 C3 UB	47.5	18.4	0.6804	0.6827	230 ± 547
46	FD2-1 2F1ZN2 C3 UT	38.2	73.7	0.7625	0.7699	742 ± 279
47	FD2-1 2F1ZN3 A9 UB	61.2	11.4	0.4936	0.4968	311 ± 659
48	FD2-1 2F1ZN3 A9 UM	64.2	38.3	0.5102	0.4917	-1856± 326
49	FD2-1 2F1ZN3 A9 UT	56.3	60.1	0.5518	0.5536	176 ± 706
50	FD2-1 2F1ZN3 C2 GdB	54.6	18.4	0.5379	0.5408	289 ± 647
51	FD2-1 2F1ZN3 C2 GdM	54.5	38.3	0.5552	0.5447	-1,056± 346
52	FD2-1 2F1ZN3 C2 GdT	46.3	60.1	0.6384	0.6396	119 ± 638
53	FD2-1 2F1ZN3 C3 UB	68.3	11.4	0.5476	0.5490	143 ± 672
54	FD2-1 2F1ZN3 C3 UM	68.4	38.3	0.5702	0.5586	-1,156 ± 315
55	FD2-1 2F1ZN3 C3 UT	59.1	60.1	0.6556	0.6654	985 ± 676
56	DOD-1 Y013 B2 DU1 ^b	55.0	49.8	0.6166	0.6258	925
57	DOD-1 Y013 B2 DU1 ^c	55.0	49.8	0.6108	0.6142	344
58	FOR-3 14595 F6 F3F6	61.0	58.4	0.5774	0.5605	-1688 ± 519
59	FOR-3 GN592 J8 ENUSA-1	50.4	51.0	0.6467	0.6266	-2,011 ± 473
60	FOR-3 GN592 J8 ENUSA-2	51.1	51.0	0.6462	0.6266	-1,964 ± 506
61	FOR-3 GN592 J8 ENUSA-3	51.5	13.3	0.6075	0.5964	-1,111 ± 524
62	FOR-3 GN592 J8 ENUSA-4	56.0	60.9	0.6301	0.6007	-2,935 ± 472
63	FOR-3 GN592 J8 ENUSA-5	43.6	67.0	0.6795	0.6589	-2,057 ± 548
64	FOR-3 GN592 J8 ENUSA-6	43.1	2.2	0.6331	0.6245	-861 ± 265
65	FOR-3 GN592 J8 ENUSA-7	47.8	13.3	0.6067	0.5964	-1,033 ± 547
66	FOR-3 GN592 J8 ENUSA-8	38.3	66.5	0.6979	0.6933	-464 ± 279
67	LBT AIA003 KLU1	60.5	8.4	0.5316	0.5408	918 ± 659
68	LBT AIA003 KLU2	62.9	51.2	0.5672	0.5749	766 ± 326
69	LBT AIA003 KLU3	56.5	70.4	0.5880	0.5999	1,193 ± 706
70	LIM-1 FYJ1433 D8 3D2B	54.8	54.8	0.6121	0.6347	2,259 ± 647
71	LIM-1 FYJ1433 D8 4G3	37.0	68.8	0.6817	0.7184	3,672 ± 346
72	LIM-1 FYJ1433 D9 1D2	62.1	12.1	0.5395	0.5380	-153 ± 638
73	LIM-1 FYJ1433 D9 2D2	65.5	44.1	0.5671	0.5664	-71 ± 672
74	LIM-1 FYJ1433 D9 4D4	65.0	65.4	0.5862	0.5792	-699 ± 315
75	LIM-1 FYJ1433 D9 4G1	56.5	69.1	0.6164	0.6203	391 ± 676
76	LIM-1 FYJ1433 H5 3A1C	57.9	54.8	0.6331	0.6325	-58 ± 519
77	LIM-1 FYJ1433 H5 3A1G	57.8	57.7	0.6345	0.6325	-203 ± 473

^a $\Delta k_{eff} = k_{eff}^c - k_{eff}^m \pm$ average uncertainty due to use of surrogate nuclide compositions.

^b sample measured by laboratories at SCK•CEN.

^c sample measured by laboratories at PSI.

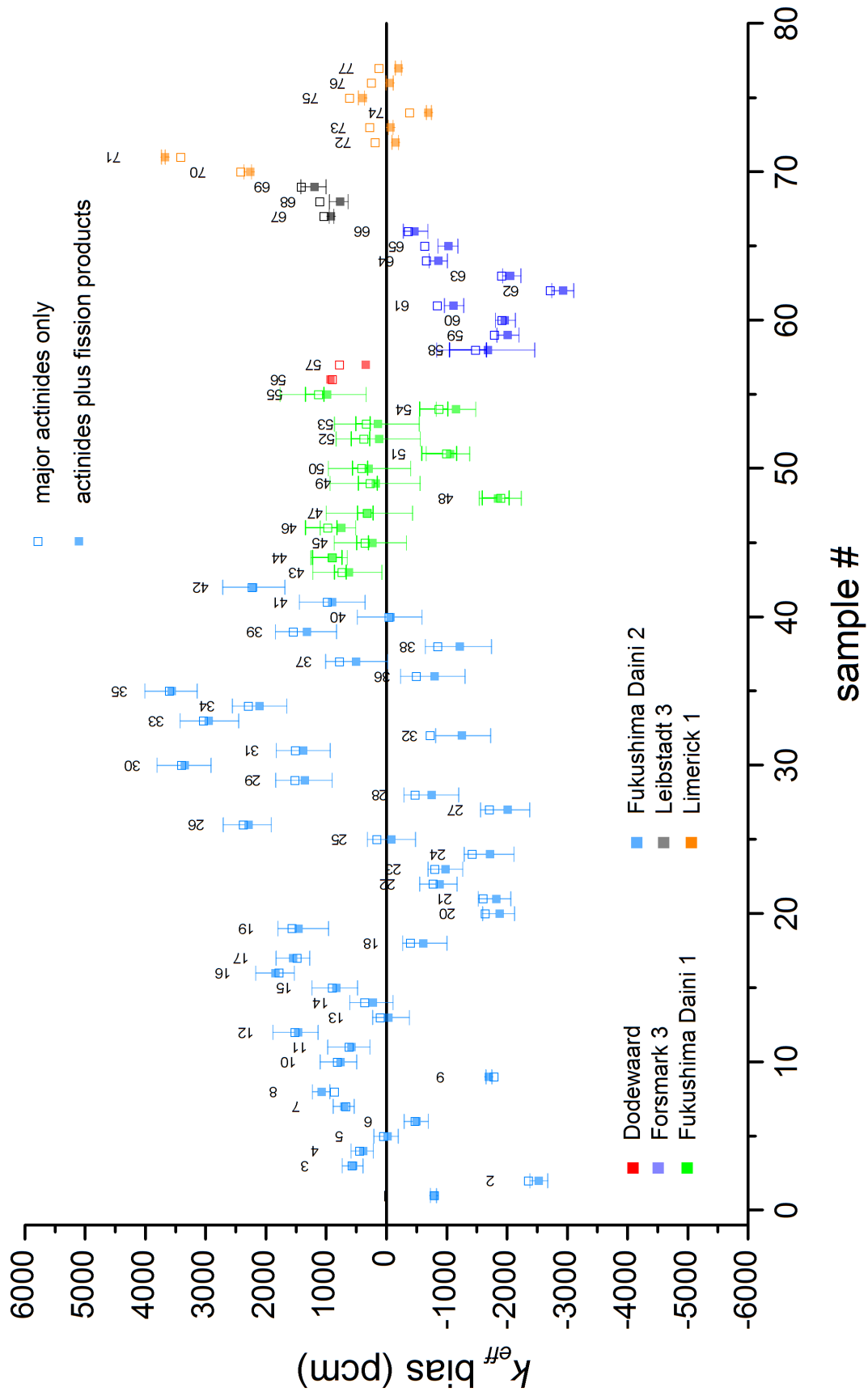


Figure 17 k_{eff} Bias for Actinide-Only and Actinide-Plus-Fission Products Results

7.4 Experimental Correlations

Correlations are inherent in both the measurements and calculations. Correlations in spent fuel isotopic measurements by laboratory may occur due to biases associated with using a common measurement technique, instrument, or reference standard to calibrate the measurements. Similarly, correlations in the simulations can occur for samples obtained from the same fuel rod, assembly, or reactor due to common variations in the design data or estimated operating parameters and void fraction. Also, any error in the sample burnup will impact biases in the calculated nuclide compositions for the sample in a highly correlated way.

The approach used in this study inherently accounts for isotope correlations within the same sample since the measured and calculated nuclide concentrations are used directly in the criticality model without the need to address the bias and uncertainty of each individual nuclide. However, this approach also assumes that each sample is independent.

Sobes et al. [64] implemented modifications to the USLSTATS statistical analysis code, used to predict the upper subcritical limit (USL) for critical experiments, to account for potential correlations in critical experiments. However, the degree of correlation for samples within the same rod or samples in the same assembly is not known, and for this analysis, all samples are assumed to be independent and uncorrelated.

7.5 Isotopic Model Uncertainties

7.5.1 Measurements

Measurement uncertainties are reported by the laboratories for all isotopic concentration values used in this study. The uncertainty depends to a large extent on the measurement method, the type of instrument used for mass spectrometry, the use and accuracy of reference standards, and the isotopic concentration of the isotope in the fuel. The reported uncertainties can vary significantly by laboratory and depend on the uncertainty analysis methods and rigor, reliance on past experience, and which components of the measurement uncertainty have been included in the process (i.e., reproducibility of a measurement or analysis of all steps starting with cutting and dissolution of fuel samples). Due to the inconsistency of current uncertainty estimates, measurement uncertainties were not used to weight the individual sample results in this study.

One sample from the Dodewaard reactor, DU1, was measured at independent laboratories at SCK•CEN and PSI. A comparison of the k_{eff} results using these two measurement sets shows a difference of about 550 pcm attributed to the measurements alone.

7.5.2 Void

Void fraction information is calculated by the operator with time steps shorter than the cycle length. The uncertainty in the void fraction has been estimated by comparison of calculated to measured average void fractions. Measurements analyzed by Morooka [65] suggest a relative standard deviation of 5.3% and 6.3% for the predictive codes COBRA/BWR and THERMIT. These values apply to average void fraction within an axial segment of an assembly (node).

The void distribution within the assembly flow channel is not uniform, and the uncertainty in local void in the vicinity of any single fuel rod can be much larger than the uncertainty in the average node void level. Studies suggest that the void fraction distribution in regions near the channel or

corner and water rods [66] can be 25% less than the average void fraction for some conditions. However, this radial variability can depend significantly on the axial location within the assembly.

The impact of the void fraction during depletion on the k_{inf} of the fuel in out-of-reactor conditions was previously evaluated by Wagner [67]. For core average void fractions of typically 40%, a 10% uncertainty in the void fraction was shown to have a corresponding uncertainty in k_{inf} of about ± 300 pcm. Further studies performed in this work investigated void fraction uncertainties for fuel rod C3 of Fukushima Daini 1 assembly 2F1ZN3. Three samples, UB (bottom), UM (middle), and UT (top) were irradiated with void fractions of nominally 10%, 40%, and 70%. Reanalysis of these samples using a $\pm 10\%$ change on void fraction uncertainty resulted in a k_{eff} uncertainty up to ± 30 , ± 600 , and ± 300 pcm at the respective axial locations, with the largest sensitivity to void uncertainty observed for the middle sample (40% void).

The variability in the k_{eff} results (Figure 17) is larger than that expected on the basis of a 5–6% uncertainty in the void fraction alone, as determined from previous studies for node average values. Large deviations observed for some samples may be attributed to larger void uncertainties in local void fraction values that have been estimated to be as large as 25%. In such a case, errors in the calculated k_{eff} of up to 1,500 pcm would be expected. Two of the largest deviations are observed for Limerick 1 samples from rod D8. This rod contained Gd_2O_3 and had a lower average power and therefore may have experienced a lower void fraction compared to other rods in the assembly. The calculations significantly overestimate the k_{eff} for these samples, consistent with an overestimate of the local void conditions for this rod.

7.5.3 Fuel Temperature

The fuel temperature is generally reported with the operating history data as obtained by core code calculations. The uncertainty in these values has been estimated to be $\pm 50^\circ C$ when data are provided by the operator and $\pm 100^\circ C$ when values are estimated from other sources of information [68]. An analysis of Forsmark 3 GE14 assembly GN592 samples was performed by increasing the average fuel temperature from 792 K to 950 K during the depletion analysis. The impact for all axial sample positions was nominally 2 pcm/ $^\circ C$ in the application model. Therefore, even assuming large uncertainties of $100^\circ C$ in the fuel temperature, the uncertainty in k_{eff} is no greater than 200 pcm. This indicates that while fuel temperature is important, the impact is likely to be less than that due to many other sources of uncertainty present in BWR depletion models.

7.5.4 Sample Burnup

The reported burnup of each sample is derived from measurements of ^{148}Nd [69], ^{148}Nd plus other fission products [70], and also using uranium and plutonium in limited cases [52]. Consequently, the burnup is not known precisely due to uncertainties in the isotopic measurements, the derivation methods and nuclear data in the burnup derivation. Uncertainty in the burnup, an input parameter in the depletion calculations, can affect the nuclide concentrations and the k_{eff} of the application model.

The impact of burnup uncertainty on k_{eff} was estimated using a sample UM (mid-axial height) from rod C3 of Fukushima Daini 1 assembly 2F1ZN3 with an average void of 38%. The uncertainty was evaluated at the end of each cycle of irradiation, for five cycles, to cover a range of sample burnups. An uncertainty in fuel burnup of nominally 2% was found to have a 200 pcm effect at low burnup, and up to 600 pcm at high burnup, for the GBC-68 application model.

In the case of the Fukushima Daini 2 data, where uncertainties in the sample burnup values of up to 6.5% were reported, the potential impact of k_{eff} can be as large as 2,000 pcm. These samples (Figure 17) exhibit some of the larger variations in the analyzed data.

7.5.5 Summary of Model Uncertainties

Uncertainties in both the measurements and the calculations contribute to the total uncertainty in the criticality model. Calculation uncertainties were assessed in this study for the input parameters of void fraction, fuel temperature, and burnup of the measured sample using models for several samples. The impact of the uncertainty parameters on the calculated k_{eff} of the cask model are summarized in Table 22. The different parameter values reflect the typical uncertainty and the maximum uncertainty values. The range of k_{eff} uncertainty values for some parameters reflects different sample burnup and void values. These uncertainties, when combined (assuming they are independent) result in a total uncertainty in the application model from about 600 to 1,900 pcm. The measurements represent a large source of the overall uncertainty both in terms of the nuclide concentration values and the estimation of the sample burnup that is also derived from the measurements.

Table 24 Summary of Uncertainties

Parameter	Parameter uncertainty	k_{eff} uncertainty (pcm)
RCA measurements	1%–5%	550
Fuel temperature	50 K 100 K	100 200
Void fraction	6 % 25 %	10–90 50–375
Sample burnup	2 % 6 %	200–600 600–1,800
Combined		600–1,900

7.6 Trending Analysis

The k_{eff} results presented in Section 7.3 were further analyzed by trending on parameters that have the largest impact on the isotopic concentrations. This analysis included trending on sample burnup and moderator void fraction. Trending was also performed on the k_{eff} of the application model. This parameter includes a measure of both the fuel burnup and initial enrichment that is not reflected by trending on fuel burnup alone.

Trending analysis was performed using linear regression analysis of the Δk_{eff} results in Tables 20 and 21. Sample uncertainties associated with the use of surrogate data described in Section 7.2 were analyzed to illustrate the impact of surrogate data and provide a potential means of weighting different samples using these uncertainties. However, other uncertainties associated with each sample including the measurement uncertainties and the sample burnup uncertainties (usually based on the measured ^{148}Nd) are not included in the error bars. Because there is usually insufficient information reported on the how measurement uncertainties are estimated by different laboratories, and inconsistent approaches are frequently applied for uncertainty analysis, no weighting was applied to avoid potential incorrect weighting of the samples and biasing the results.

A statistical analysis of the trending data was performed to estimate the lower one-sided 95% tolerance limit (LTL) of the population at the 95% confidence level. An analysis of the residuals of the linear regression fit was performed using the Shapiro-Wilk test to verify normality of the distributions. The data were determined at the 0.05 level to be significantly drawn from a normally distributed population for all trending parameters.

7.6.1 Trends with Fuel Burnup

The k_{eff} bias associated with the isotopic predictions as a function of fuel sample burnup is shown in Figure 18 for the case of major actinides and actinides plus fission products, with the linear regression fit and the 95% LTL shown in the graph. The LTL uses the same statistical methods as are used in the calculation of the Upper Subcritical Limit (USL) for critical systems for which no statistically significant trend is present. The regression analysis indicates that the slope of the trend is not statistically significant, and the slope was therefore set to zero for the fit.

The mean bias corresponds to the k_{eff} bias term, β_i , in Eq. (1). The LTL can be used to estimate the k_{eff} bias uncertainty, Δk_i , associated with the depletion code. In this report, the reported total margin for uncertainty associated with the depletion code includes both the bias and the bias uncertainty terms ($\beta_i + \Delta k_i$). Positive bias is not credited, consistent with common criticality safety practice. In the case that positive biases were to be credited, any positive bias would be subtracted from the reported total uncertainty values.

For the actinide-only calculations, there is a positive bias, β_i , of 253 pcm. The LTL band is relatively constant, ranging from a maximum value of -2,150 to -2,074 pcm. For actinide plus fission products, the mean bias is 161 pcm, with an LTL band of -2,368 to -2,288 pcm over the range of all fuel burnups. The maximum total margin for uncertainty, not crediting the positive bias, is 2,403 pcm for major actinide only burnup credit, and 2,529 pcm for actinide plus fission product credit.

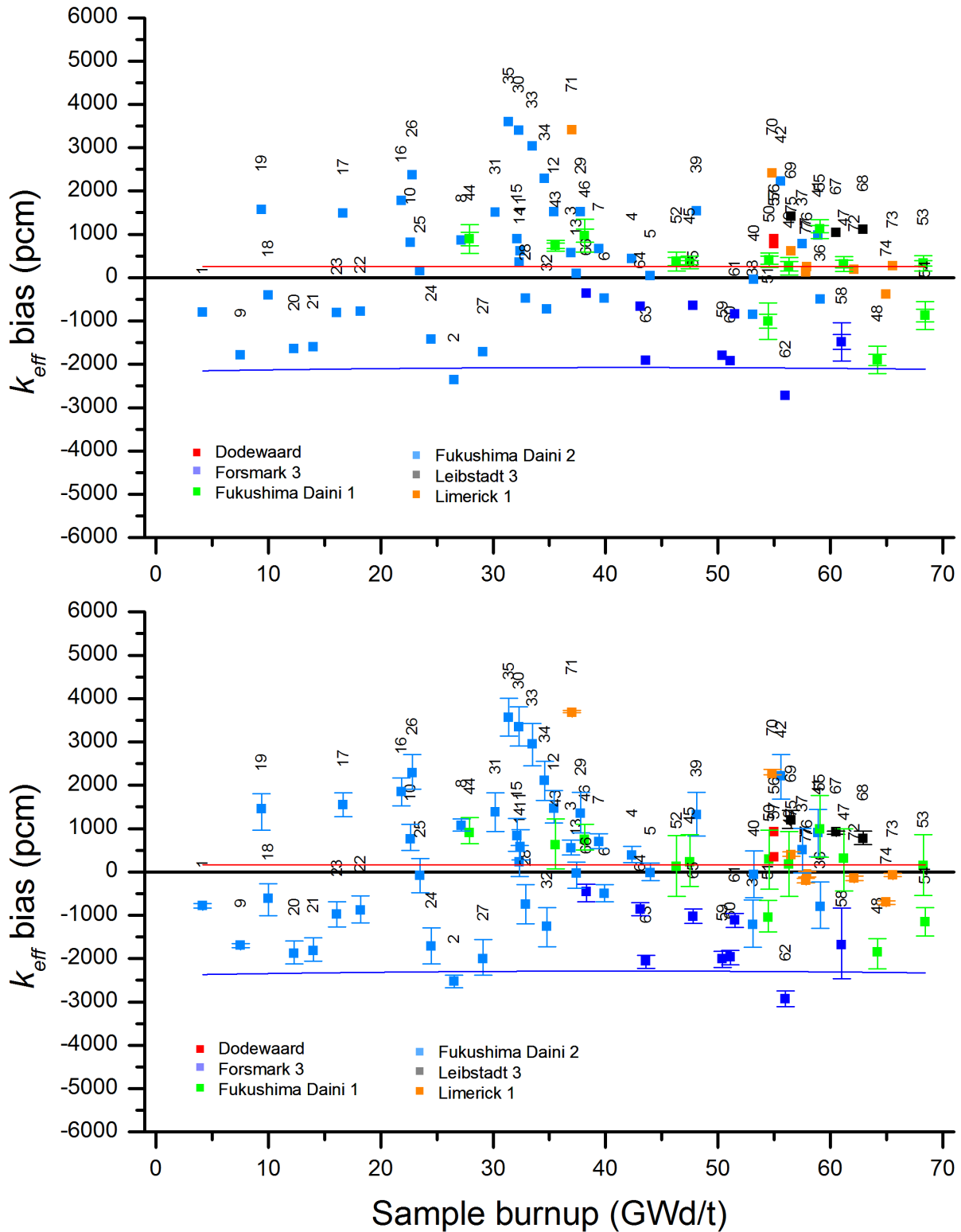


Figure 18 k_{eff} Bias for Actinide-Only (top) and Actinide-Plus-Fission Products (bottom) Results as a Function of fuel Burnup Showing Mean (red) and 95% LTL Band (blue)

7.6.2 Trends with Moderator Void

The k_{eff} bias as a function of average moderator void fraction is shown in Figure 19 for the case of major actinides and actinides plus fission products, with the linear regression fit and the 95% LTL shown in the graph. Again, the slope of the linear regression fit is not statistically significant and is set to zero.

The major actinide-only results show a positive bias of 253 pcm and an LTL band range from -2,114 to -2,074 pcm. For actinides plus fission products, the mean bias is 161 pcm with an LTL band from -2,330 to -2,288 pcm. The maximum total margin for uncertainty, not crediting the positive bias, is 2,367 pcm for major actinide only burnup credit, and 2,491 pcm for actinide plus fission product credit.

7.6.3 Trends with Fuel Reactivity

Trending with the k_{eff} bias was also investigated as a function of the k_{eff} of the GBC-68 application model to assess both the burnup and the initial enrichment of the samples. The k_{eff} bias with reactivity is shown in Figure 20 for the case of major actinides and actinides plus fission products. Again, the slope of the linear regression fit is not statistically significant and is set to zero.

The linear regression fit for the major actinide results shows a positive bias of 253 pcm and LTL band range from -2,166 to -2,074 pcm. For actinides plus fission products, the mean bias is 161 pcm with an LTL band from -2,288 to -2,390 pcm. The maximum total margin for uncertainty, not crediting the positive bias, is 2,419 pcm for major actinide only burnup credit, and 2,551 pcm for actinide plus fission product credit.

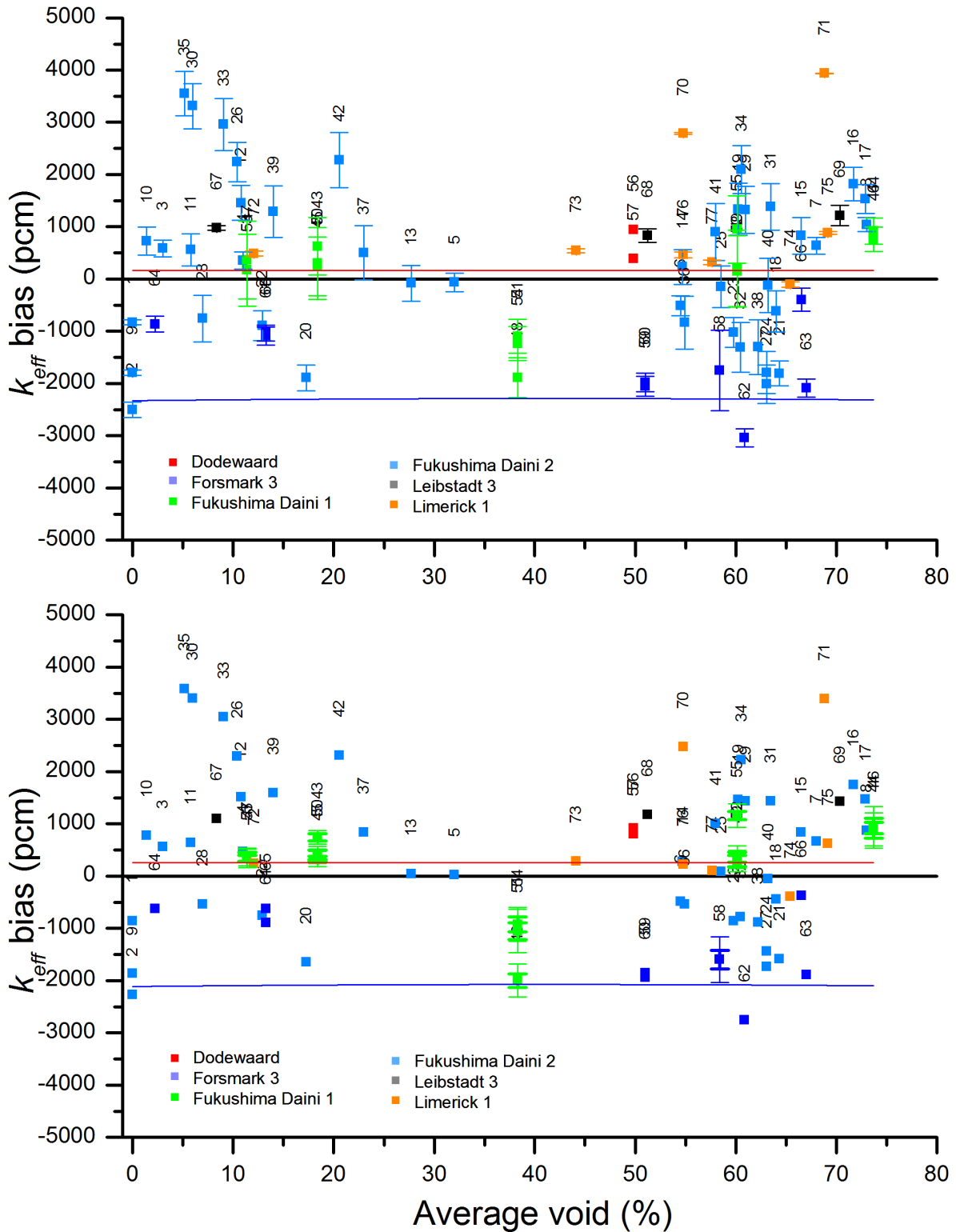


Figure 19 k_{eff} Bias for Actinide-Only (bottom) and Actinide-Plus-Fission Products (top) Results as a Function of Moderator Void Showing Mean (red) and 95% LTL Band (blue)

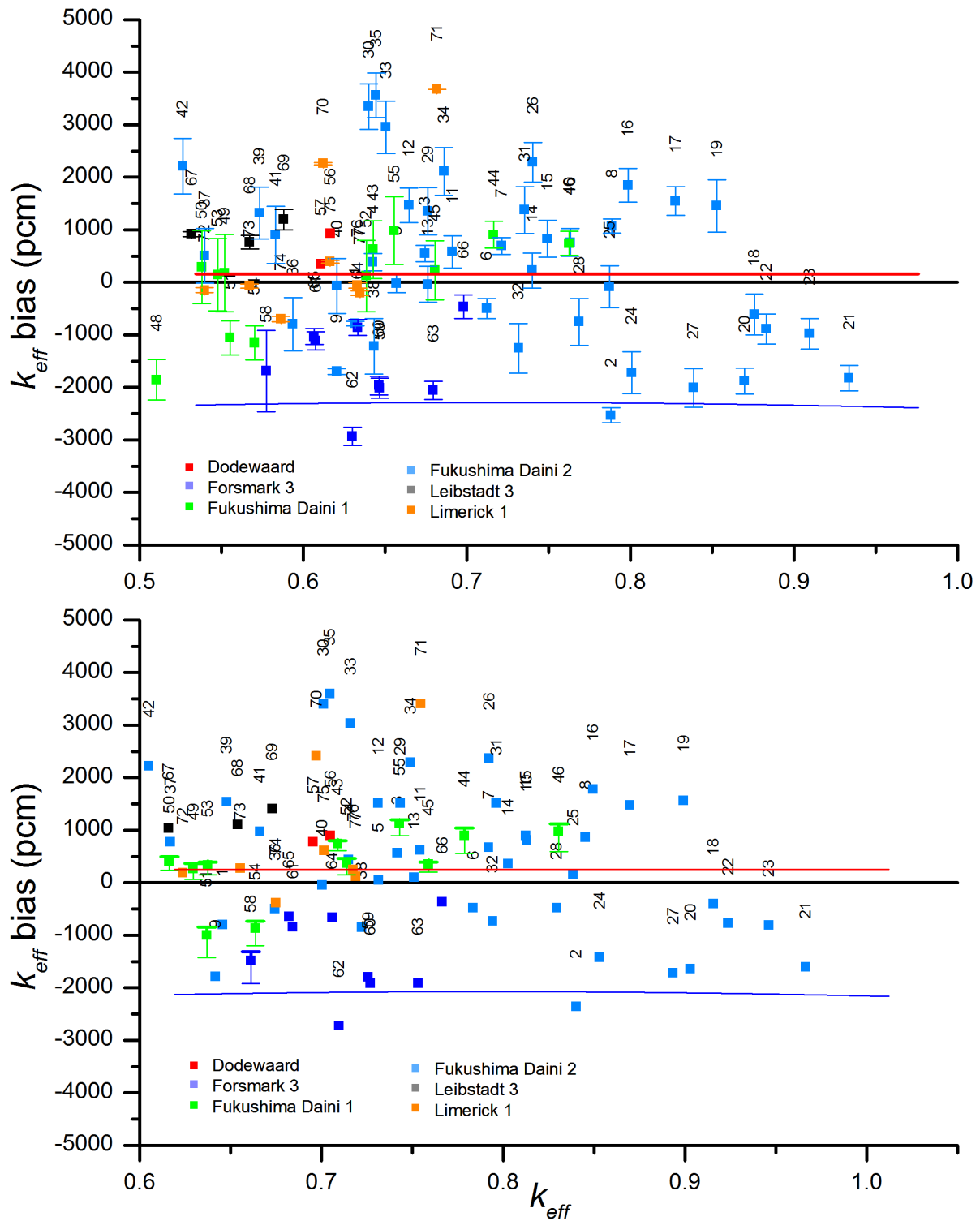


Figure 20 k_{eff} Bias for Actinide-Only (bottom) and Actinide-Plus-Fission Products (top) Results as a Function of Application k_{eff} Showing Mean (red) and 95% LTL Band (blue)

7.7 Margins for Isotopic Uncertainty

Margins for uncertainty in k_{eff} calculations due to the predicted nuclide concentrations are developed from the trending analysis and the lower one-sided 95% LTL for the distribution. Analysis of the trending parameters shows that the slope of the mean bias is not statistically significant. Therefore, a constant bias is appropriate. The average bias, the maximum 95% LTL values, and the total margins for uncertainty are listed in Table 22. The bias and minimum LTL values are seen to be the same for all trending parameters because there is no significant slope in the fit of the data. The maximum LTL band value is only weakly dependent on the trending parameter. The LTL values do not include the bias component. Consistent with past criticality safety practice, positive bias is added to the LTL value and negative bias is set to zero.

The KENO V.a criticality calculations in this study were performed using axially and radially uniform fuel compositions. In practice, burnup credit criticality analyses are usually performed using models with axially varying burnup and fuel compositions. In these cases, the region with the peak fission densities and therefore the region dominant in the k_{eff} calculation is near the top end of the BWR fuel assembly. This region has a higher fissile material content a greater reactivity than the assembly average due to the lower burnup and higher void fractions during irradiation. To ensure an appropriate margin for isotopic uncertainty, the margin for uncertainty corresponding to the maximum over the range of fuel parameters for the assembly should be used. The LTL is observed to be only weakly correlated to the trending parameters, and the margin for uncertainty is relatively constant over the parameter ranges.

Table 25 Summary of Bias and Uncertainties for Trending Parameters

Isotope set	Trending parameter	Mean bias (pcm)	LTL min. (pcm)	Total margin for uncertainty (pcm)
Major actinides only	Fuel burnup	253	-2,150	2,403
	Void fraction	253	-2,114	2,367
	System k_{eff}	253	-2,166	2,419
Actinides plus fission products	Fuel burnup	161	-2,368	2,529
	Void fraction	161	-2,330	2,491
	System k_{eff}	161	-2,390	2,551

8 SUMMARY AND CONCLUSIONS

Experimental data from the destructive assay of 77 BWR spent fuel samples have been evaluated in this report to calculate margins for uncertainty in the predictions of isotopic inventories as applied to burnup credit criticality calculations. Measurements cover a wide range of modern assemblies including 8 × 8-2, 8 × 8-4, 9 × 9-7, GE11 9 × 9, 9 × 9-9, GE14 10 × 10, SVEA-96, and SVEA-100 10 × 10 fuel assembly designs. The data cover a range of void conditions up to 74% and a burnup range from 7 to 68 GWd/MTU. Most of the measurement data used in this report are obtained from public references and additional information compiled and documented as part of the OECD/NEA SFCOMPO spent nuclear fuel measurement database. Several datasets used in this study are from proprietary programs. These data may be made available to support licensing applications through nondisclosure agreements.

The uncertainty analysis methodology used in this study is independent of the application model or the computational methods. The methodology is based on the validation of separate components of the criticality calculation. The margins for isotopic uncertainty are developed by the direct application of measurement and calculated nuclide concentrations to the application model and statistical analysis of the results. This procedure, as applied to the major actinide-only calculations, requires only minimal analysis of the isotopic distributions of individual nuclides since most samples include measurements for all major actinide isotopes. For minor actinide and fission product credit, analysis of individual isotopic bias and uncertainty was used to develop surrogate isotope concentration data with uncertainties for isotopes not measured in a fuel sample.

This uncertainty analysis approach is demonstrated in this report using SCALE 6.2.2. with ENDF/B-VII.1 cross section data. Specifically, depletion calculations were performed using the Polaris code and criticality calculations were performed using KENO V.a Margins for uncertainty associated with the predicted nuclide compositions are developed for a GBC-68 dry storage cask model. Therefore, the results presented in this report are specific to this code system and application model but are expected to be similar for other dry storage and transportation cask designs, when using same computer codes and cross section data.

The use of measured isotopic concentrations to develop margins for uncertainty is expected to be conservative. Significant uncertainties in the measured isotopic concentrations can be introduced due to the complexity of the radiochemical analysis procedures. Biases of more than 500 pcm were observed using measurements performed by two different laboratories for the same sample. Measurements are also used to estimate the sample burnup, used in the depletion calculations for the sample, adding to uncertainty. Moreover, the input data associated with the operating history obtained for core operating and fuel management calculations can also have large uncertainties. In particular, the void conditions for an assembly are obtained from core thermal-hydraulic calculations for the axial node of an assembly, with uncertainties of 5–6% for average void conditions and larger uncertainties for local void conditions within the assembly. These uncertainties in the input data contribute to uncertainty in k_{eff} of more than 1,000 pcm. These uncertainties are not associated with the accuracy of the code calculations themselves but nevertheless contribute to the estimated margins for code uncertainty since these sources of error are not easily separated from other sources.

A margin for uncertainty is developed from the bias and 95% one-sided lower tolerance limit for the population of measurement data, and trending analysis was performed for sample burnup, average void, and k_{eff} of the application model. For the Polaris calculations and the GBC-68 application model used in the present study, the k_{eff} bias for actinide-only calculations is 253 pcm with a conservative margin for isotopic uncertainty of 2,419 pcm for the range of fuel samples

included in the current analysis. This margin is observed to be largely independent of fuel burnup or void fraction based on the analysis of available experimental data. For actinide-plus-fission product calculations, the k_{eff} bias is 161 pcm and the most conservative margin for isotopic uncertainty is 2,551 pcm. These values do not credit the positive bias observed for all calculations performed in this study.

These results are similar to those shown in previous studies for PWR burnup credit [6], where average biases for a dry storage cask of 320 to 720 pcm and uncertainties of 1,430 to 2,050 pcm were reported for fuel with burnup less than 50 GWd/MTU. The larger uncertainties seen in the present study are likely attributed to the increased complexity of the BWR fuel and reactor modeling.

9 REFERENCES

- [1] Interim Staff Guidance 8, Revision 3, *Burnup Credit in the Criticality Safety Analyses of PWR Spent Fuel in Transportation and Storage Casks*. US Nuclear Regulatory Commission, September 2012. < <https://www.nrc.gov/docs/ML1226/ML12261A186.pdf> >
- [2] J. Hu, J. L. Peterson, I. C. Gauld, and S. M. Bowman, *U.S. Commercial Spent Nuclear Fuel Assembly Characteristics – 1968–2013*, US Nuclear Regulatory Commission report NUREG/CR-7227, September 2016. < <https://doi.org/10.2172/1330516> >
- [3] B. J. Marshall et al., *Validation of k_{eff} Calculations for Extended BWR Burnup Credit*, NUREG/CR-7252, prepared for the US Nuclear Regulatory Commission by Oak Ridge National Laboratory, Oak Ridge, Tennessee, 2018.
- [4] O. W. Hermann and M. D. DeHart, *Validation of Scale (SAS2H) Isotopic Predictions for BWR Spent Fuel*, Oak Ridge National Laboratory report ORNL/TM-13315, September 1998. < <https://doi.org/10.2172/814258> >
- [5] U. Merturek, M. W. Francis, and I. C. Gauld, *SCALE 5 Analysis of BWR Spent Nuclear Fuel Isotopic Compositions for Safety Studies*, Oak Ridge National Laboratory report ORNL/TM-2010/286, December 2010. < <https://doi.org/10.2172/1081684> >
- [6] G. Radulescu, I. C. Gauld, G. Ilas, and J. C. Wagner, *An Approach for Validating Actinide and Fission Product Burnup Credit Criticality Safety Analyses—Isotopic Composition Predictions*, NUREG/CR-7108, prepared for the US Nuclear Regulatory Commission by Oak Ridge National Laboratory, Oak Ridge, Tennessee, 2012.
- [7] L. Wimmer, *Isotopic Generation and Confirmation of the BWR Application Model*, AREVA Framatome ANP, Document 32-5035847-01 Yucca Mountain Site Characterization Office, 2004, DOC 20040630.0007.
- [8] Y. Nakahara, K. Suyama, J. Inagawa, R. Nagaiishi, S. Kurosawa, N. Kohno, M. Onuki, and H. Mochizuki, “Nuclide Composition Benchmark Data Set for Verifying Burnup Codes on Spent Light Water Reactor Fuels,” *Nuclear Technology* **137**, pp. 111–126 (2002). <<https://doi.org/10.13182/NT02-2>>
- [9] OECD/NEA Working Party on Nuclear Criticality Safety, Expert Group on Assay Data for Spent Nuclear Fuel. < <https://www.oecd-nea.org/science/wpncs/ADSNF/index.html> >
- [10] F. Michel-Sendis, I. Gauld, J. S. Martinez, et al., “SFCOMPO-2.0: An OECD/NEA Database of Spent Nuclear Fuel Isotopic Assays, Reactor Design Specifications, and Operating Data,” *Annals of Nuclear Energy* **110**, pp. 779–788 (2017). <<https://doi.org/10.1016/j.anucene.2017.07.022>>
- [11] J. Conde, C. Alejano, and J. M. Rey, “Nuclear Fuel Research Activities of the Consejo De Seguridad Nuclear,” *Transactions of the 2006 International Meeting on LWR Fuel Performance*, TopFuel 2006, Salamanca, Spain, 22–26 October 2006.
- [12] D. Boulanger, M. Lippens, L. Mertens, J. Basselier, and B. Lance, “High Burnup PWR and BWR MOX Fuel Performance: A Review of Belgonucleaire Recent Experimental Programs,” *Proceedings of the 2004 International Topical meeting on LWR Fuel Performance*, September 19–22, 2004, American Nuclear Society, 2004.
- [13] H. R. Radulescu, *Limerick Unit 1 Radiochemical Assay Comparisons to SAS2H Calculations*, CAL-DSU-NU-000002 Rev 00A, Office of Civilian Radioactive Waste Management, August 2003.

- [14] M. A. Jessee, W. A. Wieselquist, et al., "Polaris: A New Two-Dimensional Lattice Physics Analysis Capability for the SCALE Code System," *Proceedings of the International Conference on Physics of Reactors*, PHYSOR 2014, Kyoto, Japan, 2014.
- [15] B. T. Rearden and M. A. Jessee, Eds., *SCALE Code System*, ORNL/TM-2005/39, Version 6.2.2, Oak Ridge National Laboratory, Oak Ridge, Tennessee, 2017. Available from Radiation Safety Information Computational Center as CCC-834.
- [16] M. B. Chadwick, M. Herman, and P. Obložinský et al., "ENDF/B-VII.1 Nuclear Data for Science and Technology: Cross Sections, Covariances, Fission Product Yields and Decay Data," *Nuclear Data Sheets* **112**:12, pp. 2887–2996 (2011). < <https://doi.org/10.1016/j.nds.2011.11.002>>
- [17] *Code of Federal Regulations*, Title 10, "Energy," 2011.
- [18] *Burnup Credit for LWR Fuel*, ANSI/ANS-8.27-2015, American Nuclear Society, La Grange Park, IL, 2015.
- [19] A. H. Wells, *Isotopic Model for Commercial SNF Burnup Credit*, US Department of Energy, Office of Civilian Radioactive Waste Management report CAL-DSU-NU-000007 REV 00B, November 2004. < <https://doi.org/10.2172/862151> >
- [20] I. C. Gauld, *Strategies for Application of Isotopic Uncertainties in Burnup Credit*, NUREG/CR-6811, prepared for the US Nuclear Regulatory Commission by Oak Ridge National Laboratory, Oak Ridge, Tennessee, 2003.
- [21] C. V. Parks, M. D. DeHart, and J. C. Wagner, *Review and Prioritization of Technical Issues Related to Burnup Credit for LWR Fuel*, NUREG/CR-6665, prepared for the US Nuclear Regulatory Commission by Oak Ridge National Laboratory, Oak Ridge, Tennessee, 2000.
- [22] J. Rhodes, K. Smith, and D. Lee, *CASMO-5/CASMO-5M, A Fuel Assembly Burnup Program, User's Manual*, SSP-07/431 Rev. 0, Studsvik Scandpower, Inc., 2007.
- [23] M. Ouisloumen et al., "PARAGON: The New Westinghouse Assembly Lattice Code," in *Proceedings of the ANS International Meeting on Mathematical Methods for Nuclear Applications*, Salt Lake City, Utah, USA, 2001.
- [24] *MCNP—Monte Carlo N-Particle Transport Code System*, Version 5, Vol. 1: LA-UR-03-1987, Vol. 2: LA-CP-03-0245, and Vol. 3: LA-CP-03-0284, Los Alamos National Laboratory, 2003. Available from Radiation Safety Information Computational Center at Oak Ridge National Laboratory as CCC-740.
- [25] M. L. Williams and K.-S. Kim, "The Embedded Self-Shielding Method," in *PHYSOR 2012: Advances in Reactor Physics*, Knoxville, TN, 2012.
- [26] U. Mertzyurek, B. R. Betzler, M. A. Jessee, and S. M. Bowman, "SCALE 6.2 Lattice Physics Code Accuracy Assessment for Light Water Reactor Fuel," *Proceedings of the International Conference on Physics of Reactors*, PHYSOR 2018, Cancun, Mexico, 2018.
- [27] J-Ch. Sublet, A. J. Koning, R. A. Forrest, and J. Kopecky, "The JEFF-3.0/A Neutron Activation File—EAF-2003 into ENDF-6 Format," JEFDOC-982, Commissariat à l'Energie Atomique, France, November 2003.
- [28] T. R. England and B. F. Rider, *Evaluation and Compilation of Fission Product Yields 1993*, LA-UR-94-3106 (ENDF-349), Los Alamos National Laboratory, 1994.

- [29] M. T. Pigni, M. W. Francis, and I. C. Gauld, "Investigation of Inconsistent ENDF/B-VII.1 Independent and Cumulative Fission Product Yields with Proposed Revisions," *Nuclear Data Sheets* **123**, pp. 231–236 (2015).
- [30] R. J. Guenther, D.E. Blahnik, T. K. Campbell, U. P. Jenquin, J. E. Mendel, L. E. Thomas, and C.K. Thornhill, *Characterization of Spent Fuel Approved Testing Material-ATM-105*, PNL-5109-105/UC-802, December 1991. < <https://doi.org/10.2172/138325> >
- [31] P. Barbero et al., "Post Irradiation Analysis of the Gundremmingen BWR Spent Fuel," EUR 6301en, Joint Research Center Ispra and Karlsruhe Establishments, 1978.
- [32] H. Natsume et al., "Gamma-Ray Spectrometry and Chemical Analysis Data of JPDR-I Spent Fuel," *Journal of Nuclear Science and Technology* **14**(10), pp. 745–761 (1977).
- [33] T. Suzuki et al., "Non-Destructive and Destructive Measurements on Burnup Characteristics of Japan Power Demonstration Reactor-I Full-Core Fuel Assemblies," *Journal of Nuclear Science and Technology* **23**(1), pp. 53–72 (1986).
- [34] R. T. Primm III, *ARIANE International Programme Final Report*, Oak Ridge National Laboratory report ORNL/SUB/97-XSV750-1, April 2002.
- [35] P. Ortego and A. Rodríguez, *Evaluation of Dodewaard DU1 Sample*, report prepared for the OECD/NEA Expert Group on Assay Data for Spent Nuclear Fuel.
- [36] G. Rowlands, "Resonance absorption and non-uniform temperature distributions," *Journal of Nuclear Energy Parts A/B Reactor Science and Technology* **16**, pp. 235–236 (1964).
- [37] D. J. Kelly, "Depletion of a BWR lattice using the RACER continuous energy Monte Carlo code," *Proc. Int. Natl. Conf. on Mathematics and Computations, Reactor Physics, and Environmental Analyses*, Portland, Vol. II, p. 1011, 1995.
- [38] H.-U. Zwicky, *Isotopic Data of Sample F3F6 from a Rod Irradiated in the Swedish Boiling Water Reactor FORSMARK 3*, ZC-08/001, September 2008. < <https://www.oecd-nea.org/science/wpncs/ADSNF/reports/Forsmark3/F3F6.pdf> >
- [39] F. Lindström, *Forsmark 3 – Characteristic Data of Fuel Rod J8 in Bundle GN592*, VNF-1002152744/02, Vattenfall Nuclear Fuel AB report, 2011.
- [40] H.-U. Zwicky, J. Low, and M. Granfors, *Fuel Pellet Isotopic Analyses of Samples from a GE14 Fuel Rod Irradiated in Forsmark 3— Final Report*, STUDSVIK/N-10/007, Studsvik Nuclear AB report, 2010.
- [41] D. E. Mueller, J. M. Scaglione, J. C. Wagner, and S. M. Bowman, *Computational Benchmark for Estimated Reactivity Margin from Fission Products and Minor Actinides in BWR Burnup Credit*, NUREG/CR-7157, prepared for the US Nuclear Regulatory Commission by Oak Ridge National Laboratory, Oak Ridge, Tenn., February 2013).
- [42] T. Yamamoto and Y. Kanayama, "Lattice Physics Analysis of Burnups and Isotope Inventories of U, Pu, and Nd of Irradiated BWR 9×9-9 UO₂ Fuel Assemblies," *Journal of Nuclear Science and Technology*, **45**:6, pp. 547–566 (2008). <<https://doi.org/10.1080/18811248.2008.9711879> >
- [43] M. Suzuki, T. Yamamoto, H. Fukaya, K. Suyama, and G. Uchiyama, "Lattice physics analysis of measured isotopic compositions of irradiated BWR 9 × 9 UO₂ fuel," *Journal of Nuclear Science and Technology*, **50**:12, pp. 1161–1176 (2013), DOI: 10.1080/00223131.2013.837845.
- [44] T. Yamamoto, *Irradiation Report of Fuel Samples of BWR 9 × 9-9 Fuel*, report prepared for the OECD NEA Data Bank contribution to SFCOMPO, February 2014.

- [45] International Atomic Energy Agency, *In-core fuel management code package validation for BWRs*, IAEA-TECDOC-849, 1995.
- [46] Y. Nakahara, K. Suyama, and T. Suzaki, *Technical Development on Burn-Up Credit for Spent LWR Fuels*, JAERI-Tech 2000-071, Japan Atomic Energy Research Institute, 2000 (in Japanese). English translation published as report ORNL/TR-2001/01, 2002).
- [47] T. Yamamoto and M. Yamamoto, "Nuclear Analysis of PIE Data of Irradiated BWR 8×8-2 and 8×8-4 UO₂ Fuel Assemblies," *Journal of Nuclear Science and Technology*, **45**:11, pp. 1193–1214 (2008), DOI: 10.1080/18811248.2008.9711908.
- [48] T. Yamamoto, *Compilation of Measurement and Analysis Results of Isotopic Inventories of Spent BWR Fuels*, report contributed to the OECD/NEA and included as part of the SFCOMPO spent fuel database, February 2012.
- [49] MALIBU Program, *Final Report on the Extension Scope*, SCK•CEN report MA 2015/20, November 2015.
- [50] MALIBU Program, *Irradiation Data Report of the MALIBU Extension Program*, SCK•CEN report MA 2010/05, March 2010.
- [51] "Fuel design data," Nuclear Engineering International, September 2004.
- [52] R. Reager, *BWR Spent Fuel Isotopic Characterization*, NEDO-33094, Revision 0, GE Nuclear Energy, February 2003, MOL.20030528.0184.2003.
- [53] C. W. Mays, *Code to Code Comparison of One- and Two-Dimensional Methods*, AREVA document 32-5048840-00, 2004, DOC.20041015.0003.
- [54] R. Gauntt et al., *Fukushima Daiichi Accident Study*, SAND2012-6173, Sandia National Laboratories, 2012.
- [55] R. S. Moore, *Physical Characteristics of GE Fuel Assemblies*, ORNL/TM-10902, Oak Ridge National Laboratory, April 1989.
- [56] R. D. Reager and R. B. Adamson, *TRW Yucca Mountain Project: Test Report Phase I*, Reference no. A09112CC8A, 1999.
- [57] R. D. Reager and R.B. Adamson, *TRW Yucca Mountain Project: Test Report Phase II*, Reference no. A09112CC8A, 1999.
- [58] S. F. Wolf, D. L. Bowers and J. C. Cunnane, *Analysis of Spent Nuclear Fuel Samples from Three Mile Island and Quad Cities Reactors: Final Report*, Argonne National Laboratory report (November 2000).
- [59] *Quad Cities Updated Final Safety Analysis Report*, Revision 11, October 2011.
- [60] D. E. Mueller, S. M. Bowman, W. J. Marshall, and J. M. Scaglione, *Review and Prioritization of Technical Issues Related to Burnup Credit for BWR Fuel*, NUREG/CR-7158, prepared for the US Nuclear Regulatory Commission by Oak Ridge National Laboratory, Oak Ridge, Tenn., February 2013.
- [61] W. J. Marshall, B. J. Ade, S. Bowman, and J. S. Martinez-Gonzalez, *Axial Moderator Density Distributions, Control Blade Usage, and Axial Burnup Distributions for Extended BWR Burnup Credit*, NUREG/CR-7224 (ORNL/TM-2015/544), prepared for the US Nuclear Regulatory Commission by Oak Ridge National Laboratory, Oak Ridge, Tenn., August 2016.

- [62] M. D. DeHart, *Sensitivity and Parametric Evaluations of Significant Aspects of Burnup Credit for PWR Spent Fuel Packages*, ORNL/TM-12973, Oak Ridge National Laboratory, May 1996.
- [63] M. D. DeHart, *A Stochastic Method for Estimating the Effect of Isotopic Uncertainties in Spent Nuclear Fuel*, ORNL/TM-2001/83, Oak Ridge National Laboratory, September 2001.
- [64] V. Sobes, B. T. Rearden, D. E. Mueller, W.J. Marshall, J. M. Scaglione, and M. Dunn, "Upper Subcritical Calculations Based on Correlated Data," International Conference on Nuclear Criticality Safety, ICNC 2015, 2015.
- [65] S. Morooka, T. Ishizuka, M. Iizuka, and K. Yoshimura, "Experimental Study on Void Fraction in a Simulated BWR Fuel Assembly (Evaluation of Cross-Sectional Averaged Void Fraction)," *Nuclear Engineering and Design* **114**, pp. 91–98 (1989).
- [66] A. Inoue, T. Kurosu, T. Aoki, M. Yagi, T. Mitsutake, and S. Morooka, "Void Fraction Distribution in BWR Fuel Assembly and Evaluation of Subchannel Code," *Journal of Nuclear Science and Technology* **32**(7), pp. 629–640 (July 1995).
- [67] J. C. Wagner, M. D. DeHart, and B. L. Broadhead, *Investigation of Burnup Credit Modeling Issues Associated with BWR Fuel*, ORNL/TM-1999/193, Oak Ridge National Laboratory.
- [68] OECD Nuclear Energy Agency, *Evaluation Guide for the Evaluated Spent Nuclear Fuel Assay Database (SFCOMPO)*, NEA/NSC/R 2015, 8, February 2016.
- [69] "Standard Test Method for Atom Percent Fission in Uranium and Plutonium Fuel (Neodymium-148 Method)," ASTM Standard, ASTM E321 – 96, 2012.
- [70] C. Devida, M. Betti, P. Peerani, E. H. Toscano, and W. Goll, "A Quantitative Burn-up Determination: A Comparison of Different Experimental Methods, pp. 106–113 in *HOTLAB: European Hot Laboratories Research Capacities and Needs*, "HOTLAB" Plenary Meeting, Norway, September 6–8, 2004.

**APPENDIX A MEASURED NUCLIDE CONCENTRATIONS IN SPENT
FUEL SAMPLES**

APPENDIX A MEASURED NUCLIDE CONCENTRATIONS IN SPENT FUEL SAMPLES

Table A.1 Measured Nuclide Concentrations in Spent Fuel Samples (mg/g uranium initial)

Nuclide	FDN-2															
	2F2DN23 SF98 1 ^a	2F2DN23 SF98 2 ^a	2F2DN23 SF98 3 ^a	2F2DN23 SF98 4 ^a	2F2DN23 SF98 5 ^a	2F2DN23 SF98 6 ^a	2F2DN23 SF98 7 ^a	2F2DN23 SF98 8 ^a	2F2DN23 SF98 1 ^a	2F2DN23 SF98 2 ^a	2F2DN23 SF98 3 ^a	2F2DN23 SF98 4 ^a	2F2DN23 SF98 5 ^a	2F2DN23 SF98 6 ^a	2F2DN23 SF98 7 ^a	2F2DN23 SF98 8 ^a
U-234	4.880E-02	2.680E-01	2.180E-01	1.980E-01	1.900E-01	1.860E-01	1.960E-01	2.350E-01	4.880E-02	2.680E-01	2.180E-01	1.980E-01	1.900E-01	1.860E-01	1.960E-01	2.350E-01
U-235	4.13E+00	1.74E+01	8.14E+00	5.97E+00	6.32E+00	9.06E+00	9.36E+00	1.55E+01	4.13E+00	1.74E+01	8.14E+00	5.97E+00	6.32E+00	9.06E+00	9.36E+00	1.55E+01
U-236	4.86E-01	3.55E+00	4.99E+00	5.28E+00	5.31E+00	5.14E+00	5.14E+00	4.29E+00	4.86E-01	3.55E+00	4.99E+00	5.28E+00	5.31E+00	5.14E+00	5.14E+00	4.29E+00
U-238	9.88E+02	9.46E+02	9.41E+02	9.36E+02	9.33E+02	9.33E+02	9.33E+02	9.43E+02	9.88E+02	9.46E+02	9.41E+02	9.36E+02	9.33E+02	9.33E+02	9.33E+02	9.43E+02
Np-237	2.38E-02	1.48E-01	3.35E-01	4.32E-01	3.86E-01	5.16E-01	4.57E-01	2.92E-01	2.38E-02	1.48E-01	3.35E-01	4.32E-01	3.86E-01	5.16E-01	4.57E-01	2.92E-01
Pu-238	3.13E-03	2.83E-02	1.17E-01	1.68E-01	1.94E-01	1.69E-01	2.08E-01	9.54E-02	3.13E-03	2.83E-02	1.17E-01	1.68E-01	1.94E-01	1.69E-01	2.08E-01	9.54E-02
Pu-239	2.30E+00	3.37E+00	3.69E+00	3.79E+00	4.26E+00	5.30E+00	5.63E+00	5.34E+00	2.30E+00	3.37E+00	3.69E+00	3.79E+00	4.26E+00	5.30E+00	5.63E+00	5.34E+00
Pu-240	5.47E-01	1.12E+00	2.14E+00	2.46E+00	2.61E+00	2.63E+00	2.67E+00	1.82E+00	5.47E-01	1.12E+00	2.14E+00	2.46E+00	2.61E+00	2.63E+00	2.67E+00	1.82E+00
Pu-241	1.33E-01	4.31E-01	8.95E-01	1.03E+00	1.17E+00	1.29E+00	1.36E+00	9.08E-01	1.33E-01	4.31E-01	8.95E-01	1.03E+00	1.17E+00	1.29E+00	1.36E+00	9.08E-01
Pu-242	1.69E-02	9.29E-02	4.62E-01	6.62E-01	6.94E-01	5.43E-01	5.44E-01	2.22E-01	1.69E-02	9.29E-02	4.62E-01	6.62E-01	6.94E-01	5.43E-01	5.44E-01	2.22E-01
Am-241	1.03E-02	2.30E-02	3.27E-02	3.42E-02	3.73E-02	4.09E-02	4.39E-02	3.30E-02	1.03E-02	2.30E-02	3.27E-02	3.42E-02	3.73E-02	4.09E-02	4.39E-02	3.30E-02
Am-243	5.84E-04	6.99E-03	6.68E-02	1.14E-01	1.27E-01	1.12E-01	1.09E-01	3.26E-02	5.84E-04	6.99E-03	6.68E-02	1.14E-01	1.27E-01	1.12E-01	1.09E-01	3.26E-02
Mo-95	N/A															
Tc-99	N/A															
Ru-101	N/A															
Rh-103	N/A															
Ag-109	N/A															
Cs-133	N/A															
Nd-143	1.21E-01	7.57E-01	8.23E-01	8.49E-01	9.04E-01	9.20E-01	9.18E-01	7.36E-01	1.21E-01	7.57E-01	8.23E-01	8.49E-01	9.04E-01	9.20E-01	9.18E-01	7.36E-01
Nd-145	9.19E-02	5.97E-01	7.65E-01	8.42E-01	8.67E-01	7.95E-01	7.85E-01	5.77E-01	9.19E-02	5.97E-01	7.65E-01	8.42E-01	8.67E-01	7.95E-01	7.85E-01	5.77E-01
Sm-147	4.78E-02	2.30E-01	3.09E-01	3.21E-01	3.02E-01	2.89E-01	2.80E-01	2.45E-01	4.78E-02	2.30E-01	3.09E-01	3.21E-01	3.02E-01	2.89E-01	2.80E-01	2.45E-01
Sm-149	6.37E-04	2.20E-03	2.55E-03	2.50E-03	3.70E-03	3.37E-03	4.20E-03	4.08E-03	6.37E-04	2.20E-03	2.55E-03	2.50E-03	3.70E-03	3.37E-03	4.20E-03	4.08E-03
Sm-150	3.34E-02	1.79E-01	3.31E-01	3.87E-01	3.81E-01	N/A	3.51E-01	2.41E-01	3.34E-02	1.79E-01	3.31E-01	3.87E-01	3.81E-01	N/A	3.51E-01	2.41E-01
Sm-151	2.55E-03	8.20E-03	9.19E-03	9.74E-03	1.04E-02	1.27E-02	1.31E-02	1.24E-02	2.55E-03	8.20E-03	9.19E-03	9.74E-03	1.04E-02	1.27E-02	1.31E-02	1.24E-02
Sm-152	2.23E-02	9.02E-02	1.42E-01	1.56E-01	1.43E-01	1.23E-01	1.22E-01	9.77E-02	2.23E-02	9.02E-02	1.42E-01	1.56E-01	1.43E-01	1.23E-01	1.22E-01	9.77E-02
Eu-151	N/A															
Eu-153	N/A															
Gd-155	N/A															

^a Measurements reported at the time of discharge from the reactor (no cooling time), on 11/14/1992, except for samarium isotopes that are reported at the time of measurement on 5/10/1998.

Table A.1 Measured Nuclide Concentrations in Spent Fuel Samples (mg/g uranium initial) (con't)

Nuclide	FDN-2 2F2DN23 SF99 10 ^b	FDN-2 2F2DN23 SF99 1 ^b	FDN-2 2F2DN23 SF99 2 ^b	FDN-2 2F2DN23 SF99 3 ^b	FDN-2 2F2DN23 SF99 4 ^b	FDN-2 2F2DN23 SF99 5 ^b	FDN-2 2F2DN23 SF99 6 ^b	FDN-2 2F2DN23 SF99 7 ^b
U-234	4.090E-02	3.900E-02	2.010E-01	1.780E-01	1.670E-01	1.600E-01	1.650E-01	1.640E-01
U-235	3.04E+00	2.91E+00	1.40E+01	8.66E+00	6.98E+00	7.38E+00	1.05E+01	1.09E+01
U-236	6.74E-01	6.87E-01	3.47E+00	4.25E+00	4.48E+00	4.52E+00	4.30E+00	4.25E+00
U-238	9.84E+02	9.84E+02	9.52E+02	9.45E+02	9.43E+02	9.39E+02	9.41E+02	9.40E+02
Np-237	5.49E-02	5.67E-02	2.18E-01	3.63E-01	3.67E-01	4.62E-01	4.15E-01	4.46E-01
Pu-238	1.10E-02	1.13E-02	3.96E-02	9.70E-02	1.15E-01	1.23E-01	1.37E-01	1.38E-01
Pu-239	3.01E+00	3.01E+00	3.91E+00	3.98E+00	3.86E+00	4.55E+00	5.63E+00	6.04E+00
Pu-240	1.05E+00	1.06E+00	1.52E+00	2.13E+00	2.29E+00	2.53E+00	2.45E+00	2.49E+00
Pu-241	3.36E-01	3.60E-01	6.76E-01	9.45E-01	1.01E+00	1.20E+00	1.26E+00	1.31E+00
Pu-242	7.33E-02	8.24E-02	1.90E-01	4.37E-01	5.57E-01	6.07E-01	4.33E-01	4.21E-01
Am-241	1.61E-02	2.70E-02	2.11E-02	3.95E-02	3.41E-02	4.36E-02	4.56E-02	4.85E-02
Am-243	5.62E-03	5.79E-03	1.89E-02	6.50E-02	9.04E-02	1.13E-01	8.51E-02	8.45E-02
Mo-95	N/A	N/A	N/A	N/A	N/A	N/A	N/A	N/A
Tc-99	N/A	N/A	N/A	N/A	N/A	N/A	N/A	N/A
Ru-101	N/A	N/A	N/A	N/A	N/A	N/A	N/A	N/A
Rh-103	N/A	N/A	N/A	N/A	N/A	N/A	N/A	N/A
Ag-109	N/A	N/A	N/A	N/A	N/A	N/A	N/A	N/A
Cs-133	N/A	N/A	N/A	N/A	N/A	N/A	N/A	N/A
Nd-143	1.89E-01	1.95E-01	6.14E-01	7.63E-01	7.81E-01	N/A	7.98E-01	8.09E-01
Nd-145	1.52E-01	1.58E-01	4.92E-01	6.73E-01	7.20E-01	N/A	6.52E-01	6.51E-01
Sm-147	N/A	7.78E-02	N/A	N/A	N/A	2.77E-01	N/A	N/A
Sm-149	N/A	8.84E-04	N/A	N/A	N/A	2.72E-03	N/A	N/A
Sm-150	N/A	6.17E-02	N/A	N/A	N/A	3.25E-01	N/A	N/A
Sm-151	N/A	3.41E-03	N/A	N/A	N/A	1.03E-02	N/A	N/A
Sm-152	N/A	3.95E-02	N/A	N/A	N/A	1.27E-01	N/A	N/A
Eu-151	N/A	N/A	N/A	N/A	N/A	N/A	N/A	N/A
Eu-153	N/A	N/A	N/A	N/A	N/A	N/A	N/A	N/A
Gd-155	N/A	N/A	N/A	N/A	N/A	N/A	N/A	N/A

^b Measurements reported at the time of discharge from the reactor (no cooling time), on 11/14/1992, except for Sm isotopes that are reported at the date of analysis of 5/21/1999.

Table A.1 Measured Nuclide Concentrations in Spent Fuel Samples (mg/g uranium initial) (con't)

Nuclide	FDN-2 2F2DN23 SF99j8 ^b	FDN-2 2F2DN23 SF99j9 ^b	FDN-2 2F2DN23 SF99j9 ^b	LIM-1 FYJ1433 D8 3D2B ^c	LIM-1 FYJ1433 D8 4G3 ^c	LIM-1 FYJ1433 D9 1D2 ^c	LIM-1 FYJ1433 D9 2D2 ^c	LIM-1 FYJ1433 D9 4D4 ^c	LIM-1 FYJ1433 D9 4G1 ^c
U-234	1.960E-01	2.180E-01	1.490E-01	1.820E-01	1.53E-01	1.50E-01	1.50E-01	1.51E-01	1.71E-01
U-235	1.58E+01	1.91E+01	3.94E+00	8.18E+00	1.57E+00	2.01E+00	2.01E+00	2.47E+00	3.98E+00
U-236	3.46E+00	2.83E+00	5.29E+00	4.86E+00	5.54E+00	5.52E+00	5.52E+00	5.55E+00	5.55E+00
U-238	9.49E+02	9.54E+02	N/A	N/A	N/A	N/A	N/A	N/A	N/A
Np-237	2.76E-01	1.98E-01	7.33E-01	5.06E-01	7.08E-01	8.26E-01	8.26E-01	8.13E-01	7.60E-01
Pu-238	6.48E-02	3.43E-02	4.06E-01	2.39E-01	3.69E-01	4.66E-01	4.66E-01	4.98E-01	4.11E-01
Pu-239	5.45E+00	4.73E+00	5.05E+00	5.18E+00	3.64E+00	4.38E+00	4.38E+00	4.86E+00	5.03E+00
Pu-240	1.65E+00	1.18E+00	3.43E+00	2.72E+00	2.88E+00	3.21E+00	3.21E+00	3.31E+00	3.10E+00
Pu-241	8.33E-01	5.37E-01	1.28E+00	1.07E+00	9.79E-01	1.20E+00	1.20E+00	1.31E+00	1.28E+00
Pu-242	1.72E-01	8.33E-02	1.10E+00	5.94E-01	1.42E+00	1.49E+00	1.49E+00	1.43E+00	1.14E+00
Am-241	3.62E-02	2.88E-02	3.60E-01	2.97E-01	2.61E-01	2.99E-01	2.99E-01	3.50E-01	3.41E-01
Am-243	2.57E-02	9.26E-03	2.81E-01	1.22E-01	3.34E-01	3.60E-01	3.60E-01	3.84E-01	2.78E-01
Mo-95	N/A	N/A	1.18E+00	9.32E-01	1.32E+00	1.30E+00	1.30E+00	1.26E+00	1.17E+00
Tc-99	N/A	N/A	1.18E+00	9.37E-01	1.28E+00	1.25E+00	1.25E+00	1.28E+00	1.07E+00
Ru-101	N/A	N/A	1.19E+00	8.97E-01	1.38E+00	1.39E+00	1.39E+00	1.35E+00	1.23E+00
Rh-103	N/A	N/A	6.90E-01	5.69E-01	6.67E-01	6.97E-01	6.97E-01	7.34E-01	6.85E-01
Ag-109	N/A	N/A	1.49E-01	1.03E-01	1.35E-01	1.40E-01	1.40E-01	1.42E-01	1.12E-01
Cs-133	N/A	N/A	N/A	N/A	N/A	N/A	N/A	N/A	N/A
Nd-143	6.14E-01	5.01E-01	9.44E-01	8.62E-01	7.87E-01	9.04E-01	9.04E-01	9.54E-01	9.61E-01
Nd-145	4.67E-01	3.71E-01	9.35E-01	7.49E-01	1.04E+00	1.04E+00	1.04E+00	1.06E+00	9.79E-01
Sm-147	N/A	N/A	2.67E-01	2.42E-01	2.72E-01	2.72E-01	2.72E-01	2.66E-01	2.76E-01
Sm-149	N/A	N/A	2.49E-03	2.73E-03	1.54E-03	2.16E-03	2.16E-03	2.58E-03	2.85E-03
Sm-150	N/A	N/A	4.45E-01	3.13E-01	4.60E-01	5.06E-01	5.06E-01	4.98E-01	4.53E-01
Sm-151	N/A	N/A	1.25E-02	1.15E-02	9.32E-03	1.14E-02	1.14E-02	1.24E-02	1.25E-02
Sm-152	N/A	N/A	1.41E-01	1.13E-01	1.65E-01	1.62E-01	1.62E-01	1.52E-01	1.46E-01
Eu-151	N/A	N/A	4.42E-04	4.05E-04	3.16E-04	3.71E-04	3.71E-04	4.02E-04	4.18E-04
Eu-153	N/A	N/A	1.80E-01	1.32E-01	1.93E-01	2.03E-01	2.03E-01	1.97E-01	1.86E-01
Gd-155	N/A	N/A	1.10E-02	9.08E-03	7.20E-03	8.06E-03	8.06E-03	8.42E-03	7.20E-03

^b Measurements reported at the time of discharge from the reactor (no cooling time), on 11/14/1992, except for Sm that is reported at a date of analysis of 5/21/1999.

^c Date of analysis: 7/15/2002.

Table A.1 Measured Nuclide Concentrations in Spent Fuel Samples (mg/g uranium initial) (con't)

Nuclide	DOD-1 Y013 B2 DU1 ^d	DOD-1 Y013 B2 DU1 ^e	FOR-3 GN592 J8 ENUSA-1 ^f	FOR-3 GN592 J8 ENUSA-2 ^f	FOR-3 GN592 J8 ENUSA-3 ^f	FOR-3 GN592 J8 ENUSA-4 ^f	FOR-3 GN592 J8 ENUSA-5 ^f	FOR-3 GN592 J8 ENUSA-6 ^f
U-234	1.49E-01	1.41E-01	1.80E-01	1.83E-01	1.89E-01	1.75E-01	2.00E-01	2.05E-01
U-235	6.13E+00	5.76E+00	5.72E+00	5.79E+00	4.56E+00	4.97E+00	8.02E+00	6.06E+00
U-236	7.18E+00	7.11E+00	6.08E+00	5.96E+00	5.97E+00	4.98E+00	5.63E+00	5.66E+00
U-238	9.21E+02	9.14E+02	9.31E+02	9.31E+02	9.36E+02	9.29E+02	9.34E+02	9.40E+02
Np-237	6.75E-01	7.08E-01	N/A	N/A	N/A	N/A	N/A	N/A
Pu-238	2.69E-01	3.05E-01	3.55E-01	3.37E-01	2.86E-01	3.73E-01	2.67E-01	1.97E-01
Pu-239	3.74E+00	3.88E+00	5.14E+00	5.16E+00	4.02E+00	4.83E+00	5.05E+00	3.98E+00
Pu-240	2.56E+00	2.71E+00	2.97E+00	2.99E+00	2.67E+00	2.99E+00	2.67E+00	2.43E+00
Pu-241	7.99E-01	9.84E-01	1.25E+00	1.26E+00	9.70E-01	1.22E+00	1.12E+00	8.73E-01
Pu-242	7.99E-01	8.54E-01	9.77E-01	9.64E-01	9.34E-01	1.06E+00	7.07E-01	6.96E-01
Am-241	3.68E-01	2.05E-01	3.40E-01	3.46E-01	2.64E-01	3.28E-01	2.91E-01	2.40E-01
Am-243	1.80E-01	1.72E-01	2.12E-01	2.31E-01	1.81E-01	2.46E-01	1.29E-01	1.30E-01
Mo-95	1.09E+00	1.36E+00	1.14E+00	1.10E+00	1.12E+00	1.01E+00	1.03E+00	8.84E-01
Tc-99	9.82E-01	1.29E+00	N/A	N/A	N/A	N/A	N/A	N/A
Ru-101	8.65E-01	1.13E+00	N/A	N/A	N/A	N/A	N/A	N/A
Rh-103	5.20E-01	5.73E-01	N/A	N/A	N/A	N/A	N/A	N/A
Ag-109	4.50E-02	5.31E-02	N/A	N/A	N/A	N/A	N/A	N/A
Cs-133	1.72E+00	1.70E+00	1.89E+00	2.19E+00	1.72E+00	1.76E+00	1.56E+00	1.61E+00
Nd-143	9.81E-01	1.05E+00	9.27E-01	9.53E-01	8.64E-01	9.37E-01	8.98E-01	8.35E-01
Nd-145	1.08E+00	1.09E+00	9.33E-01	9.47E-01	9.39E-01	9.59E-01	8.49E-01	8.92E-01
Sm-147	3.57E-01	3.10E-01	2.66E-01	2.64E-01	2.63E-01	2.45E-01	3.29E-01	3.36E-01
Sm-149	2.44E-03	3.01E-03	2.30E-03	2.50E-03	1.80E-03	2.50E-03	2.50E-03	1.70E-03
Sm-150	4.55E-01	4.42E-01	4.18E-01	4.17E-01	3.84E-01	4.09E-01	3.41E-01	3.28E-01
Sm-151	1.08E-02	1.08E-02	1.20E-02	1.30E-02	9.00E-03	1.10E-02	9.00E-03	7.00E-03
Sm-152	1.67E-01	1.61E-01	1.47E-01	1.50E-01	1.58E-01	1.49E-01	1.33E-01	1.44E-01
Eu-151	6.19E-04	6.85E-04	N/A	N/A	N/A	N/A	N/A	N/A
Eu-153	1.70E-01	1.76E-01	1.61E-01	1.57E-01	1.55E-01	1.67E-01	1.51E-01	1.35E-01
Gd-155	8.11E-03	5.65E-03	5.40E-03	5.20E-03	5.20E-03	6.00E-03	4.00E-03	4.10E-03

^dMeasurements performed by PSI. Date of analysis: 4/22/1999 (U), 4/12/1999 (Pu), 9/15/1999 (Np), 12/11/1999 (Am), 5/28/1999 (Nd), 8/13/1999 (Sm), Eu, Gd), 9/6/1999 (Cs), 1/11/2000 (Mo, Ru, Ag), 12/13/1999 (Rh), 1/20/2000 (Tc).

^eMeasurements performed by SCK•CEN. Date of analysis: 5/6/1996 (U, Np), 4/12/1996 (Pu), 6/18/1996 (Am), 10/16/1996 (Nd), 11/27/1996 (Sm), 11/28/1996 (Eu), 6/24/1996 (Gd), 10/1/1996 (Cs), 4/10/2000 (Mo, Tc, Ru, Rh, Ag).

^f Date of analysis: 6/15/2009 (U), 6/16/2009 (Pu, Am), 7/1/2009 (Nd, Sm, Eu, Gd), 8/31/2009 (Cs), 10/28/2009 (Mo).

T Table A.1 Measured Nuclide Concentrations in Spent Fuel Samples (mg/g uranium initial) (cont't)

Nuclide	FOR-3 GN592 J8 ENUSA-7 ^f	FOR-3 GN592 J8 ENUSA-8 ^f	FOR-3 14595 F6 F3F6 ^g	LIM-1 FYJ1433 H5 3A1C ^c	LIM-1 FYJ1433 H5 3A1G ^c	LBT AIA003 KLU1 ^h	LBT AIA003 KLU2 ^h	LBT AIA003 KLU3 ^h
U-234	1.84E-01	2.07E-01	1.50E-01	1.66E-01	1.66E-01	1.51E-01	1.49E-01	1.58E-01
U-235	4.44E+00	9.43E+00	3.16E+00	4.42E+00	4.50E+00	1.91E+00	2.76E+00	3.69E+00
U-236	5.80E+00	5.24E+00	5.66E+00	5.72E+00	5.72E+00	5.99E+00	6.06E+00	5.94E+00
U-238	9.37E+02	9.39E+02	9.17E+02	N/A	N/A	9.21E+02	9.15E+02	9.19E+02
Np-237	N/A	N/A	N/A	7.92E-01	7.97E-01	6.58E-01	7.52E-01	7.11E-01
Pu-238	2.57E-01	2.05E-01	3.88E-01	4.67E-01	4.68E-01	3.31E-01	4.04E-01	3.88E-01
Pu-239	3.98E+00	4.90E+00	4.62E+00	5.66E+00	5.69E+00	3.32E+00	4.06E+00	4.17E+00
Pu-240	2.65E+00	2.41E+00	3.05E+00	3.46E+00	3.47E+00	2.75E+00	3.18E+00	2.97E+00
Pu-241	9.62E-01	9.89E-01	8.90E-01	1.38E+00	1.38E+00	8.63E-01	1.09E+00	1.08E+00
Pu-242	9.11E-01	5.41E-01	1.26E+00	1.07E+00	1.05E+00	1.31E+00	1.31E+00	1.17E+00
Am-241	2.61E-01	2.71E-01	N/A	3.76E-01	3.81E-01	3.01E-01	3.89E-01	3.81E-01
Am-243	1.78E-01	1.19E-01	N/A	2.73E-01	2.74E-01	2.98E-01	3.50E-01	2.83E-01
Mo-95	1.06E+00	9.11E-01	N/A	1.18E+00	1.18E+00	1.09E+00	N/A	N/A
Tc-99	N/A	N/A	N/A	1.12E+00	1.09E+00	1.10E+00	1.11E+00	N/A
Ru-101	N/A	N/A	N/A	1.22E+00	1.25E+00	N/A	N/A	N/A
Rh-103	N/A	N/A	N/A	6.95E-01	7.22E-01	5.79E-01	N/A	N/A
Ag-109	N/A	N/A	N/A	1.23E-01	1.39E-01	1.15E-01	N/A	N/A
Cs-133	1.70E+00	1.42E+00	N/A	N/A	N/A	1.83E+00	2.03E+00	1.91E+00
Nd-143	8.24E-01	8.61E-01	9.69E-01	1.02E+00	1.02E+00	8.77E-01	1.07E+00	1.07E+00
Nd-145	8.97E-01	7.64E-01	1.02E+00	9.86E-01	9.86E-01	1.11E+00	1.16E+00	1.11E+00
Sm-147	2.53E-01	3.14E-01	N/A	2.71E-01	2.72E-01	3.05E-01	2.94E-01	3.00E-01
Sm-149	1.90E-03	N/A	N/A	2.71E-03	2.72E-03	1.58E-03	N/A	N/A
Sm-150	3.76E-01	2.98E-01	N/A	4.67E-01	4.64E-01	4.74E-01	4.80E-01	4.38E-01
Sm-151	7.60E-03	1.00E-02	N/A	1.42E-02	1.41E-02	9.63E-03	8.83E-03	1.03E-02
Sm-152	1.53E-01	1.24E-01	N/A	1.37E-01	1.36E-01	1.77E-01	1.60E-01	1.50E-01
Eu-151	N/A	N/A	N/A	4.78E-04	4.85E-04	5.49E-04	N/A	N/A
Eu-153	1.55E-01	1.19E-01	N/A	1.81E-01	1.81E-01	2.00E-01	1.97E-01	1.74E-01
Gd-155	4.50E-03	3.80E-03	N/A	7.92E-03	7.45E-03	7.59E-03	6.16E-03	6.17E-03

^g Date of analysis 12/14/2006.

^h Date of analysis 12/31/2009.

Table A.1 Measured Nuclide Concentrations in Spent Fuel Samples (mg/g uranium initial) (con't)

Nuclide	FDN-2		FD2-2									
	2F2D1	F6 TU101 ⁱ	2F2D1	F6 TU102 ^j	2F2D1	B3 TU103 ^k	2F2D1	B3 TU104 ^k	2F2D1	B3 TU105 ^k	2F2D1	F6 TU106 ^k
U-234	3.33E-01	3.41E-01	2.46E-01	2.56E-01	2.55E-01	2.56E-01	2.56E-01	2.56E-01	2.55E-01	2.55E-01	3.12E-01	3.12E-01
U-235	3.33E+01	2.76E+01	2.51E+01	2.76E+01	2.40E+01	2.33E+01	2.33E+01	2.33E+01	2.40E+01	2.40E+01	2.93E+01	2.93E+01
U-236	2.57E+00	2.96E+00	1.77E+00	2.96E+00	2.00E+00	2.00E+00	2.00E+00	2.00E+00	2.00E+00	2.00E+00	3.06E+00	3.06E+00
U-238	9.43E+02	9.45E+02	9.57E+02	9.45E+02	9.55E+02	9.57E+02	9.59E+02	9.59E+02	9.55E+02	9.55E+02	9.43E+02	9.43E+02
Np-237	N/A	N/A										
Pu-238	1.96E-02	1.95E-02	9.84E-03	1.95E-02	9.81E-03	9.84E-03	1.97E-02	1.97E-02	9.81E-03	9.81E-03	2.93E-02	2.93E-02
Pu-239	4.76E+00	4.04E+00	4.73E+00	4.04E+00	4.55E+00	4.73E+00	4.54E+00	4.54E+00	4.55E+00	4.55E+00	5.63E+00	5.63E+00
Pu-240	7.15E-01	8.78E-01	7.18E-01	8.78E-01	9.42E-01	7.18E-01	8.17E-01	8.17E-01	9.42E-01	9.42E-01	1.02E+00	1.02E+00
Pu-241	2.74E-01	3.03E-01	2.66E-01	3.03E-01	3.73E-01	2.66E-01	3.25E-01	3.25E-01	3.73E-01	3.73E-01	4.59E-01	4.59E-01
Pu-242	2.94E-02	3.90E-02	1.97E-02	3.90E-02	3.93E-02	1.97E-02	3.94E-02	3.94E-02	3.93E-02	3.93E-02	5.86E-02	5.86E-02
Am-241	5.82E-02	6.82E-02	5.74E-02	6.82E-02	6.82E-02	5.74E-02	6.97E-02	6.97E-02	6.82E-02	6.82E-02	9.95E-02	9.95E-02
Am-243	1.70E-03	1.59E-03	1.51E-03	1.59E-03	1.50E-03	1.51E-03	1.84E-03	1.84E-03	1.50E-03	1.50E-03	1.78E-03	1.78E-03
Mo-95	N/A	N/A										
Tc-99	N/A	N/A										
Ru-101	N/A	N/A										
Rh-103	N/A	N/A										
Ag-109	N/A	N/A										
Cs-133	N/A	N/A										
Nd-143	N/A	N/A										
Nd-145	N/A	N/A										
Sm-147	N/A	N/A										
Sm-149	N/A	N/A										
Sm-150	N/A	N/A										
Sm-151	N/A	N/A										
Sm-152	N/A	N/A										
Eu-151	N/A	N/A										
Eu-153	N/A	N/A										
Gd-155	N/A	N/A										

ⁱ Date of analysis 9/5/1994.

^j Date of analysis 8/31/1994.

^k Date of analysis 10/31/1994.

Table A.1 Measured Nuclide Concentrations in Spent Fuel Samples (mg/g uranium initial) (con't)

Nuclide	FD2-2 2F2D2 F6 TU202 ^k	FD2-2 2F2D2 B3 TU203/	FD2-2 2F2D2 B3 TU204 ^k	FD2-2 2F2D2 B3 TU205 ^k	FD2-2 2F2D3 H5 TU301 ^l	FD2-2 2F2D3 H5 TU302 ^l	FD2-2 2F2D3 A4 TU304 ^l	FD2-2 2F2D3 A4 TU306 ^l
U-234	2.68E-01	1.93E-01	2.03E-01	2.03E-01	1.62E-01	1.63E-01	1.61E-01	1.82E-01
U-235	1.56E+01	1.55E+01	1.43E+01	1.24E+01	6.46E+00	6.29E+00	6.21E+00	5.96E+00
U-236	4.83E+00	3.44E+00	3.42E+00	3.57E+00	4.61E+00	4.47E+00	4.53E+00	4.46E+00
U-238	9.37E+02	9.45E+02	9.48E+02	9.53E+02	9.42E+02	9.49E+02	9.39E+02	9.48E+02
Np-237	N/A	N/A	N/A	N/A	N/A	N/A	N/A	N/A
Pu-238	8.62E-02	8.68E-02	9.66E-02	6.78E-02	2.67E-01	1.25E-01	2.56E-01	1.34E-01
Pu-239	4.47E+00	6.49E+00	6.30E+00	4.19E+00	5.59E+00	3.52E+00	5.34E+00	3.60E+00
Pu-240	1.90E+00	2.00E+00	2.08E+00	1.80E+00	2.84E+00	2.11E+00	2.71E+00	2.17E+00
Pu-241	8.14E-01	1.00E+00	9.85E-01	7.07E-01	1.33E+00	7.68E-01	1.27E+00	7.96E-01
Pu-242	2.68E-01	2.22E-01	2.61E-01	2.52E-01	7.53E-01	4.99E-01	7.31E-01	5.37E-01
Am-241	1.37E-01	1.55E-01	1.73E-01	1.25E-01	2.37E-01	1.36E-01	2.09E-01	1.47E-01
Am-243	1.84E-02	1.96E-02	3.40E-02	2.28E-02	1.41E-01	5.28E-02	1.41E-01	7.19E-02
Mo-95	N/A	N/A	N/A	N/A	N/A	N/A	N/A	N/A
Tc-99	N/A	N/A	N/A	N/A	N/A	N/A	N/A	N/A
Ru-101	N/A	N/A	N/A	N/A	N/A	N/A	N/A	N/A
Rh-103	N/A	N/A	N/A	N/A	N/A	N/A	N/A	N/A
Ag-109	N/A	N/A	N/A	N/A	N/A	N/A	N/A	N/A
Cs-133	N/A	N/A	N/A	N/A	N/A	N/A	N/A	N/A
Nd-143	N/A	N/A	N/A	N/A	N/A	N/A	N/A	N/A
Nd-145	N/A	N/A	N/A	N/A	N/A	N/A	N/A	N/A
Sm-147	N/A	N/A	N/A	N/A	N/A	N/A	N/A	N/A
Sm-149	N/A	N/A	N/A	N/A	N/A	N/A	N/A	N/A
Sm-150	N/A	N/A	N/A	N/A	N/A	N/A	N/A	N/A
Sm-151	N/A	N/A	N/A	N/A	N/A	N/A	N/A	N/A
Sm-152	N/A	N/A	N/A	N/A	N/A	N/A	N/A	N/A
Eu-151	N/A	N/A	N/A	N/A	N/A	N/A	N/A	N/A
Eu-153	N/A	N/A	N/A	N/A	N/A	N/A	N/A	N/A
Gd-155	N/A	N/A	N/A	N/A	N/A	N/A	N/A	N/A

^l Date of analysis 8/1/1995.

Table A.1 Measured Nuclide Concentrations in Spent Fuel Samples (mg/g uranium initial) (con't)

Nuclide	FD2-2 2F2D3 B3 TU308/	FD2-2 2F2D3 B3 TU309/	FD2-2 2F2D3 B3 TU311/	FDN-2 2F2D8 H5 TU501 ^m	FDN-2 2F2D8 H5 TU502 ^m	FDN-2 2F2D8 H5 TU503 ^m	FDN-2 2F2D8 A4 TU505 ⁿ	FD2-2 2F2D8 A4 TU506 ⁿ
U-234	2.11E-01	2.00E-01	2.11E-01	1.40E-01	1.39E-01	1.21E-01	1.39E-01	1.30E-01
U-235	1.07E+01	8.86E+00	6.84E+00	3.71E+00	2.32E+00	1.40E+00	2.27E+00	1.51E+00
U-236	4.22E+00	4.51E+00	4.58E+00	4.89E+00	4.90E+00	4.86E+00	4.85E+00	4.69E+00
U-238	9.43E+02	9.37E+02	9.46E+02	9.25E+02	9.20E+02	9.27E+02	9.19E+02	9.24E+02
Np-237	N/A	N/A	N/A	N/A	N/A	N/A	N/A	N/A
Pu-238	1.63E-01	2.76E-01	1.34E-01	4.48E-01	4.73E-01	3.18E-01	5.28E-01	3.44E-01
Pu-239	5.82E+00	7.22E+00	3.75E+00	4.75E+00	4.20E+00	2.97E+00	4.81E+00	3.42E+00
Pu-240	2.43E+00	3.44E+00	2.30E+00	3.02E+00	3.01E+00	2.44E+00	3.49E+00	2.90E+00
Pu-241	1.04E+00	1.49E+00	8.33E-01	1.32E+00	1.33E+00	8.68E-01	1.39E+00	9.68E-01
Pu-242	3.93E-01	7.13E-01	5.46E-01	1.03E+00	1.26E+00	1.16E+00	1.49E+00	1.33E+00
Am-241	1.90E-01	2.57E-01	1.49E-01	1.83E-01	2.42E-01	1.41E-01	2.60E-01	2.22E-01
Am-243	6.90E-02	1.02E-01	6.03E-02	2.08E-01	3.05E-01	2.50E-01	3.55E-01	2.51E-01
Mo-95	N/A	N/A	N/A	N/A	N/A	N/A	N/A	N/A
Tc-99	N/A	N/A	N/A	N/A	N/A	N/A	N/A	N/A
Ru-101	N/A	N/A	N/A	N/A	N/A	N/A	N/A	N/A
Rh-103	N/A	N/A	N/A	N/A	N/A	N/A	N/A	N/A
Ag-109	N/A	N/A	N/A	N/A	N/A	N/A	N/A	N/A
Cs-133	N/A	N/A	N/A	N/A	N/A	N/A	N/A	N/A
Nd-143	N/A	N/A	N/A	N/A	N/A	N/A	N/A	N/A
Nd-145	N/A	N/A	N/A	N/A	N/A	N/A	N/A	N/A
Sm-147	N/A	N/A	N/A	N/A	N/A	N/A	N/A	N/A
Sm-149	N/A	N/A	N/A	N/A	N/A	N/A	N/A	N/A
Sm-150	N/A	N/A	N/A	N/A	N/A	N/A	N/A	N/A
Sm-151	N/A	N/A	N/A	N/A	N/A	N/A	N/A	N/A
Sm-152	N/A	N/A	N/A	N/A	N/A	N/A	N/A	N/A
Eu-151	N/A	N/A	N/A	N/A	N/A	N/A	N/A	N/A
Eu-153	N/A	N/A	N/A	N/A	N/A	N/A	N/A	N/A
Gd-155	N/A	N/A	N/A	N/A	N/A	N/A	N/A	N/A

^m Date of analysis 7/6/1999.

ⁿ Date of analysis 7/8/1999.

Table A.1 Measured Nuclide Concentrations in Spent Fuel Samples (mg/g uranium initial) (con't)

Nuclide	FD2-2 2F2D8 B3 TU510 ^o	FD2-2 2F2D8 B3 TU511 ^p	FD2-1 2F1ZN2 C2 GdB ^q	FD2-1 2F1ZN2 C2 GdT ^r	FD2-1 2F1ZN2 C3 UB ^s	FD2-1 2F1ZN2 C3 UT ^s	FD2-1 2F1ZN3 A9 UM ^u	FD2-1 2F1ZN3 A9 UM ^u
U-234	1.40E-01	1.50E-01	1.88E-01	1.61E-01	2.78E-01	3.08E-01	9.14E-02	6.24E-02
U-235	4.50E+00	2.94E+00	5.85E+00	1.07E+01	9.59E+00	1.64E+01	9.18E-02	2.10E-01
U-236	5.09E+00	5.12E+00	4.07E+00	3.63E+00	6.55E+00	5.92E+00	2.67E+00	2.67E+00
U-238	9.22E+02	9.32E+02	9.45E+02	9.48E+02	9.26E+02	9.29E+02	9.26E+02	9.21E+02
Np-237	N/A	N/A	N/A	N/A	N/A	N/A	N/A	N/A
Pu-238	5.03E-01	3.10E-01	1.56E-01	1.24E-01	2.07E-01	1.72E-01	2.73E-01	3.70E-01
Pu-239	5.74E+00	3.64E+00	4.01E+00	5.63E+00	4.05E+00	5.83E+00	2.91E+00	3.77E+00
Pu-240	3.86E+00	2.94E+00	2.47E+00	2.26E+00	2.43E+00	2.29E+00	2.50E+00	3.05E+00
Pu-241	1.51E+00	9.69E-01	9.55E-01	7.23E-01	9.57E-01	6.70E-01	8.64E-01	9.47E-01
Pu-242	1.15E+00	1.14E+00	6.21E-01	3.44E-01	5.99E-01	3.63E-01	1.97E+00	2.20E+00
Am-241	2.78E-01	2.26E-01	N/A	N/A	N/A	N/A	N/A	N/A
Am-243	2.47E-01	2.10E-01	N/A	N/A	N/A	N/A	N/A	N/A
Mo-95	N/A	N/A	N/A	6.80E-01	N/A	9.33E-01	N/A	1.22E+00
Tc-99	N/A	N/A	N/A	4.96E-01	N/A	6.59E-01	N/A	8.82E-01
Ru-101	N/A	N/A	N/A	6.73E-01	N/A	8.93E-01	N/A	1.51E+00
Rh-103	N/A	N/A	N/A	4.32E-01	N/A	5.19E-01	N/A	6.84E-01
Ag-109	N/A	N/A	N/A	4.51E-02	N/A	4.47E-02	N/A	1.61E-01
Cs-133	N/A	N/A	N/A	N/A	N/A	1.30E+00	N/A	1.78E+00
Nd-143	N/A	N/A	7.61E-01	7.08E-01	1.05E+00	9.88E-01	5.15E-01	6.33E-01
Nd-145	N/A	N/A	7.08E-01	5.67E-01	9.70E-01	7.91E-01	9.41E-01	9.92E-01
Sm-147	N/A	N/A	N/A	2.38E-01	N/A	3.17E-01	N/A	2.62E-01
Sm-149	N/A	N/A	N/A	3.07E-03	N/A	3.65E-03	N/A	2.03E-03
Sm-150	N/A	N/A	N/A	2.30E-01	N/A	3.04E-01	N/A	4.79E-01
Sm-151	N/A	N/A	N/A	1.09E-02	N/A	1.34E-02	N/A	9.46E-03
Sm-152	N/A	N/A	N/A	8.94E-02	N/A	1.09E-01	N/A	1.68E-01
Eu-151	N/A	N/A	N/A	1.41E-03	N/A	1.28E-03	N/A	8.97E-04
Eu-153	N/A	N/A	N/A	9.58E-02	N/A	1.13E-01	N/A	2.08E-01
Gd-155	N/A	N/A	N/A	1.27E-02	N/A	6.35E-03	N/A	1.15E-02

^o Date of analysis: 8/2/1999; ^p Date of analysis: 8/4/1999; ^q Date of analysis: 9/10/2002.

^r Date of analysis: 1/12/2010 (U, Pu, Nd, Gd), 1/9/2011 (Sm, Eu, Cs), 12/29/2011 (Tc, Mo, Ru, Rh, Ag).

^s Date of analysis: 7/20/2012 (U, Pu, Nd), 10/28/2010 (Eu, Sm, Gd), 12/29/2011 (Cs), 12/29/2011 (Tc, Mo, Ru, Rh, Ag).

^t Date of analysis: 3/10/2005.

^u Date of analysis: 1/11/2010 (U, Pu, Nd), 12/20/2010 (Sm, Eu, Gd), 12/31/2011 (Cs, Tc, Mo, Ru, Rh, Ag).

Table A.1 Measured Nuclide Concentrations in Spent Fuel Samples (mg/g uranium initial) (con't)

Nuclide	FD2-1 2F1ZN3 A9 UT ^t	FD2-1 2F1ZN3 C2 GdB ^v	FD2-1 2F1ZN3 C2 GdM ^w	FD2-1 2F1ZN3 C2 GdT ^v	FD2-1 2F1ZN3 C3 UB ^v	FD2-1 2F1ZN3 C3 UM ^u	FD2-1 2F1ZN3 C3 UT ^v
U-234	9.17E-02	9.20E-02	1.29E-01	9.25E-02	1.81E-01	2.11E-01	1.83E-01
U-235	6.45E-01	1.29E+00	2.14E+00	4.18E+00	2.18E+00	3.35E+00	6.69E+00
U-236	2.87E+00	4.36E+00	4.44E+00	4.39E+00	7.12E+00	7.19E+00	7.09E+00
U-238	9.29E+02	9.30E+02	9.27E+02	9.33E+02	9.11E+02	9.08E+02	9.14E+02
Np-237	N/A	N/A	N/A	N/A	N/A	N/A	N/A
Pu-238	3.81E-01	3.33E-01	3.60E-01	3.81E-01	4.44E-01	5.29E-01	4.86E-01
Pu-239	4.07E+00	3.44E+00	4.43E+00	5.42E+00	3.52E+00	4.32E+00	5.21E+00
Pu-240	2.94E+00	2.85E+00	3.37E+00	3.44E+00	2.94E+00	3.32E+00	3.27E+00
Pu-241	1.24E+00	1.01E+00	9.40E-01	1.43E+00	1.04E+00	1.04E+00	1.37E+00
Pu-242	1.66E+00	1.41E+00	1.41E+00	1.02E+00	1.43E+00	1.39E+00	9.68E-01
Am-241	N/A	N/A	N/A	N/A	N/A	N/A	N/A
Am-243	N/A	N/A	N/A	N/A	N/A	N/A	N/A
Mo-95	N/A	N/A	1.18E+00	N/A	N/A	1.53E+00	N/A
Tc-99	N/A	N/A	8.44E-01	N/A	N/A	1.08E+00	N/A
Ru-101	N/A	N/A	1.27E+00	N/A	N/A	1.60E+00	N/A
Rh-103	N/A	N/A	6.55E-01	N/A	N/A	7.48E-01	N/A
Ag-109	N/A	N/A	9.82E-02	N/A	N/A	1.06E-01	N/A
Cs-133	N/A	N/A	1.74E+00	N/A	N/A	2.09E+00	N/A
Nd-143	7.34E-01	7.36E-01	8.53E-01	8.95E-01	9.31E-01	1.08E+00	1.16E+00
Nd-145	9.21E-01	9.54E-01	9.56E-01	8.52E-01	1.23E+00	1.23E+00	1.11E+00
Sm-147	N/A	N/A	3.13E-01	N/A	N/A	3.76E-01	N/A
Sm-149	N/A	N/A	2.02E-03	N/A	N/A	2.19E-03	N/A
Sm-150	N/A	N/A	4.44E-01	N/A	N/A	5.30E-01	N/A
Sm-151	N/A	N/A	1.04E-02	N/A	N/A	1.17E-02	N/A
Sm-152	N/A	N/A	1.48E-01	N/A	N/A	1.69E-01	N/A
Eu-151	N/A	N/A	1.21E-03	N/A	N/A	1.15E-03	N/A
Eu-153	N/A	N/A	1.85E-01	N/A	N/A	2.09E-01	N/A
Gd-155	N/A	N/A	1.42E-02	N/A	N/A	1.16E-02	N/A

^v Date of analysis: 8/25/2005.

^w Date of analysis: 7/19/2012 (U, Pu, Nd), 10/11/2011 (Eu, Sm, Gd), 12/31/2011 (Cs, Tc, Mo, Ru, Rh, Ag).

**APPENDIX B COMPARISON OF POLARIS-CALCULATED NUCLIDE
COMPOSITIONS WITH MEASUREMENTS**

APPENDIX B COMPARISON OF POLARIS-CALCULATED NUCLIDE COMPOSITIONS WITH MEASUREMENTS

Table B.1 Comparisons of Polaris Calculations and Measurements for Burnup Credit Isotopes (C/M – 1)(%)

Nuclide	FD2-2 2F2DN23 SF98 1	FD2-2 2F2DN23 SF98 2	FD2-2 2F2DN23 SF98 3	FD2-2 2F2DN23 SF98 4	FD2-2 2F2DN23 SF98 5	FD2-2 2F2DN23 SF98 6	FD2-2 2F2DN23 SF98 7	FD2-2 2F2DN23 SF98 8	FD2-2 2F2DN23 SF99 1	FD2-2 2F2DN23 SF99 2
U-234	-9.3%	11.4%	18.0%	18.7%	19.2%	28.0%	20.8%	19.9%	3.0%	9.2%
U-235	-1.7%	-15.1%	5.2%	5.6%	0.8%	-0.9%	5.2%	4.4%	-8.1%	6.1%
U-236	-2.1%	13.6%	-1.3%	-1.0%	-0.5%	-1.2%	-1.6%	-3.4%	0.0%	0.9%
U-238	0.0%	0.1%	0.0%	0.1%	0.1%	0.2%	0.1%	0.0%	0.1%	0.0%
Np-237	-11.4%	46.4%	2.0%	-3.9%	20.8%	-11.3%	5.0%	6.1%	-19.8%	-6.5%
Pu-238	-13.3%	93.6%	6.5%	5.4%	10.7%	19.1%	4.2%	1.1%	0.8%	36.8%
Pu-239	-7.6%	9.6%	0.4%	-0.9%	-1.2%	-5.4%	0.8%	3.8%	-10.1%	1.4%
Pu-240	-5.1%	31.4%	-3.1%	-4.8%	-4.8%	-8.1%	-7.1%	-5.3%	0.2%	-1.1%
Pu-241	-16.5%	40.1%	-2.6%	-3.1%	-2.5%	-5.1%	-2.4%	-0.4%	-14.2%	-4.6%
Pu-242	-16.0%	87.9%	-5.3%	-5.4%	-1.0%	0.0%	-4.4%	-4.6%	-6.5%	-7.7%
Am-241	-50.3%	3.4%	-14.3%	-17.3%	-13.1%	-2.7%	1.7%	10.9%	-48.9%	35.9%
Am-243	-36.6%	122.8%	-16.0%	-16.6%	-8.2%	-16.9%	-13.3%	-12.2%	-31.2%	-16.2%
Mo-95										
Tc-99										
Ru-101										
Rh-103										
Ag-109										
Cs-133										
Nd-143	-0.1%	-4.1%	3.7%	4.6%	2.3%	1.1%	2.6%	2.4%	0.1%	2.2%
Nd-145	-0.3%	-1.3%	1.4%	2.1%	1.2%	1.4%	0.7%	0.8%	1.3%	0.7%
Sm-147	-8.5%	2.0%	-10.4%	-10.8%	-4.8%	-4.8%	-5.7%	-9.6%	-2.2%	
Sm-149	-10.0%	5.4%	1.1%	11.9%	-17.5%	-3.2%	-15.7%	-21.4%	-20.2%	
Sm-150	-8.1%	15.8%	-9.9%	-10.4%	-4.2%	-4.2%	-5.8%	-9.2%	-4.2%	
Sm-151	-14.3%	-3.2%	-10.9%	-11.5%	-7.0%	-12.7%	-4.9%	-6.2%	-18.2%	
Sm-152	-7.1%	12.0%	-7.8%	-8.5%	-1.8%	1.1%	-3.1%	-7.6%	-1.2%	
Eu-151										
Eu-153										
Gd-155										

Table B.1 Comparisons of Polaris Calculations and Measurements for Burnup Credit Isotopes (C/M – 1)(%) (con't)

Nuclide	FD2-2 2F2DN23 SF99 3	FD2-2 2F2DN23 SF99 4	FD2-2 2F2DN23 SF99 5	FD2-2 2F2DN23 SF99 6	FD2-2 2F2DN23 SF99 7	FD2-2 2F2DN23 SF99 8	FD2-2 2F2DN23 SF99 9	FD2-2 F2D1 F6 TU101	FD2-2 2F2D1 F6 TU102
U-234	7.1%	8.8%	9.1%	12.1%	11.9%	7.9%	4.6%	0.8%	-3.6%
U-235	5.7%	12.7%	2.9%	4.4%	6.3%	8.8%	5.1%	-6.6%	-2.8%
U-236	2.3%	1.2%	2.4%	0.4%	1.5%	0.2%	2.9%	12.3%	15.3%
U-238	0.0%	0.0%	0.1%	0.1%	0.0%	-0.1%	-0.2%	0.3%	0.1%
Np-237	-11.2%	-1.1%	-11.3%	-6.0%	-8.2%	-2.1%	-2.2%		
Pu-238	24.9%	30.0%	48.6%	18.5%	26.9%	28.0%	32.5%	-12.1%	4.7%
Pu-239	0.8%	5.2%	-2.1%	-2.2%	1.7%	10.1%	13.7%	-10.0%	-5.6%
Pu-240	-1.3%	-1.0%	-4.2%	-6.1%	-5.1%	0.9%	2.0%	-4.2%	-0.9%
Pu-241	-1.0%	1.0%	-3.6%	-3.0%	0.0%	6.5%	12.1%	-9.0%	-3.5%
Pu-242	-0.9%	-3.9%	0.1%	0.6%	0.3%	2.1%	6.4%	-3.2%	26.9%
Am-241	-13.2%	2.8%	-10.6%	4.3%	7.1%	14.0%	1.3%	12.1%	11.4%
Am-243	-13.6%	-15.1%	-13.9%	-18.1%	-15.3%	-13.1%	-3.9%	7.8%	92.7%
Mo-95									
Tc-99									
Ru-101									
Rh-103									
Ag-109									
Cs-133									
Nd-143	2.2%	4.1%		1.7%	0.9%	0.5%	-0.5%		
Nd-145	0.8%	1.1%		1.3%	0.0%	-1.1%	-1.6%		
Sm-147			-1.7%						
Sm-149			5.0%						
Sm-150			-4.4%						
Sm-151			-8.3%						
Sm-152			0.2%						
Eu-151									
Eu-153									
Gd-155									

Table B.1 Comparisons of Polaris Calculations and Measurements for Burnup Credit Isotopes (C/M – 1)(%) (con't)

Nuclide	FD2-2 2F2D1 B3 TU103	FD2-2 2F2D1 B3 TU104	FD2-2 2F2D1 B3 TU105	FD2-2 2F2D1 F6 TU106	FD2-2 2F2D2 F6 TU201	FD2-2 2F2D2 F6 TU202	FD2-2 2F2D2 B3 TU203	FD2-2 2F2D2 B3 TU204	FD2-2 2F2D2 B3 TU205	FD2-2 2F2D3 H5 TU301
U-234	1.3%	-1.6%	-3.0%	5.3%	5.2%	5.0%	7.7%	4.2%	7.7%	12.9%
U-235	0.1%	10.1%	-5.1%	-0.3%	-4.3%	-0.1%	-1.5%	9.7%	19.5%	36.5%
U-236	14.1%	-4.6%	14.1%	4.1%	7.8%	6.8%	7.7%	5.5%	-0.6%	-4.7%
U-238	0.0%	-0.1%	0.2%	0.2%	0.2%	0.1%	0.2%	0.0%	-0.2%	0.0%
Np-237										
Pu-238	44.6%	-38.8%	46.1%	-23.2%	-4.9%	3.9%	3.2%	-18.1%	-18.8%	-34.9%
Pu-239	-7.5%	-8.0%	-17.2%	-20.5%	-12.5%	-6.8%	-14.4%	-15.2%	-2.4%	-6.2%
Pu-240	-1.3%	-21.1%	-12.6%	-20.2%	-8.0%	-8.0%	-9.0%	-16.8%	-13.7%	-19.9%
Pu-241	-8.6%	-34.5%	-30.8%	-33.2%	-20.5%	-16.1%	-17.6%	-22.5%	-16.7%	-20.2%
Pu-242	40.0%	-42.6%	3.4%	-28.5%	20.5%	-3.8%	4.6%	-19.4%	-25.2%	-36.2%
Am-241	15.6%	-16.5%	3.3%	-16.6%	7.2%	-0.4%	4.0%	-9.2%	-3.4%	-15.4%
Am-243	10.8%	-31.8%	49.9%	68.6%	120.6%	55.5%	55.3%	-23.9%	-21.3%	-44.5%
Mo-95										
Tc-99										
Ru-101										
Rh-103										
Ag-109										
Cs-133										
Nd-143										
Nd-145										
Sm-147										
Sm-149										
Sm-150										
Sm-151										
Sm-152										
Eu-151										
Eu-153										
Gd-155										

Table B.1 Comparisons of Polaris Calculations and Measurements for Burnup Credit Isotopes (C/M – 1)(%) (con't)

Nuclide	FD2-2 2F2D3 H5 TU302	FD2-2 2F2D3 A4 TU304	FD2-2 2F2D3 A4 TU306	FD2-2 2F2D3 B3 TU308	FD2-2 2F2D3 B3 TU309	FD2-2 2F2D3 B3 TU311	FD2-2 2F2D8 H5 TU501	FD2-2 2F2D8 H5 TU502	FD2-2 2F2D8 H5 TU503	FD2-2 2F2D8 A4 TU505
U-234	20.6%	8.5%	6.5%	-8.3%	-8.8%	-9.8%	4.4%	-2.7%	11.9%	-3.3%
U-235	34.7%	22.0%	34.9%	14.3%	12.2%	27.1%	-11.3%	-7.3%	7.4%	-11.5%
U-236	-5.0%	0.5%	-3.3%	-0.8%	-0.6%	-3.3%	1.0%	0.8%	1.2%	1.7%
U-238	-0.2%	0.0%	-0.2%	-0.1%	0.3%	-0.2%	0.0%	0.0%	-0.1%	0.2%
Np-237										
Pu-238	-17.9%	-18.3%	-18.2%	-8.9%	-29.8%	-0.3%	11.8%	19.2%	33.2%	5.3%
Pu-239	6.9%	-1.2%	4.9%	-2.3%	-22.8%	6.7%	9.6%	15.7%	22.7%	-2.1%
Pu-240	-8.9%	-9.6%	-8.8%	-9.4%	-28.3%	-5.4%	2.2%	5.2%	16.1%	-10.2%
Pu-241	-5.9%	-9.7%	-6.5%	-2.4%	-23.9%	0.8%	4.9%	3.0%	18.3%	-4.2%
Pu-242	-27.1%	-19.8%	-27.0%	-6.0%	-29.1%	-14.3%	15.1%	13.9%	19.2%	-2.4%
Am-241	-0.5%	2.4%	-5.2%	5.1%	-15.2%	6.6%	69.1%	19.8%	47.7%	7.7%
Am-243	-18.4%	-26.7%	-33.3%	-16.2%	-14.3%	4.9%	30.5%	13.1%	18.0%	-1.9%
Mo-95										
Tc-99										
Ru-101										
Rh-103										
Ag-109										
Cs-133										
Nd-143										
Nd-145										
Sm-147										
Sm-149										
Sm-150										
Sm-151										
Sm-152										
Eu-151										
Eu-153										
Gd-155										

Table B.1 Comparisons of Polaris Calculations and Measurements for Burnup Credit Isotopes (C/M – 1)(%) (con't)

Nuclide	FD2-2 2F2D8 A4 TU506	FD2-2 2F2D8 B3 TU510	FD2-2 2F2D8 B3 TU511	FD2-1 2F1ZN2 C2 GdB	FD2-1 2F1ZN2 C2 GdT	FD2-1 2F1ZN2 C3 UB	FD2-1 2F1ZN2 C3 UT	FD2-1 2F1ZN3 C2 GdB	FD2-1 2F1ZN3 C2 GdM	FD2-1 2F1ZN3 C2 GdT
U-234	1.3%	8.4%	5.3%	-17.7%	8.9%	-5.4%	-3.6%	27.0%	10.5%	45.4%
U-235	-12.3%	-7.5%	17.6%	5.4%	3.5%	1.6%	4.6%	13.0%	2.7%	9.4%
U-236	4.5%	0.6%	-1.8%	1.0%	1.7%	1.8%	2.0%	3.2%	2.6%	2.3%
U-238	0.0%	0.3%	0.1%	-0.1%	-0.2%	-0.1%	-0.2%	-0.1%	-0.1%	-0.2%
Np-237										
Pu-238	30.0%	2.8%	10.7%	6.2%	8.3%	4.8%	2.8%	14.3%	16.6%	2.9%
Pu-239	7.3%	-5.6%	3.5%	2.9%	6.3%	1.8%	3.9%	2.1%	-7.1%	-2.0%
Pu-240	-1.1%	-15.7%	-6.9%	-0.6%	-0.1%	-1.6%	-3.8%	3.7%	-3.1%	-5.6%
Pu-241	8.2%	-6.8%	2.1%	1.5%	4.5%	0.6%	1.4%	1.2%	-7.1%	-2.2%
Pu-242	10.1%	-0.6%	-10.3%	1.2%	4.2%	1.4%	-0.8%	5.6%	2.6%	0.7%
Am-241	-5.5%	19.0%	0.1%							
Am-243	28.4%	7.0%	-7.7%							
Mo-95										
Tc-99					-7.6%		-4.4%		-4.8%	
Ru-101					37.4%		39.9%		45.3%	
Rh-103					-3.1%		-2.1%		-1.3%	
Ag-109					0.9%		1.5%		5.0%	
Cs-133					46.3%		50.5%		54.5%	
Nd-143				2.6%	2.1%	2.1%	2.4%	6.2%	4.2%	4.9%
Nd-145				0.6%	0.5%	0.9%	0.8%	1.9%	2.4%	1.8%
Sm-147					-0.7%		-1.0%		0.1%	
Sm-149					5.6%		14.5%		-7.4%	
Sm-150					1.4%		3.9%		0.1%	
Sm-151					2.5%		4.0%		-7.9%	
Sm-152					6.3%		7.4%		10.6%	
Eu-151					-30.7%		-7.4%		-48.4%	
Eu-153					11.4%		5.4%		3.5%	
Gd-155					-8.5%		10.9%		-3.8%	

Table B.1 Comparisons of Polaris Calculations and Measurements for Burnup Credit Isotopes (C/M – 1)(%) (con't)

Nuclide	FD2-1 2F1ZN3 A9 UB	FD2-1 2F1ZN3 A9 UM	FD2-1 2F1ZN3 A9 UT	FD2-1 2F1ZN3 C3 UB	FD2-1 2F1ZN3 C3 UM	FD2-1 2F1ZN3 C3 UT	DOD Y013 U0004 DU1 ^a	DOD Y013 U0004 DU1 ^b	FOR-3 14595 F6 F3F6	FOR-3 GN592 J8 ENUSA-1
U-234	-37.0%	18.3%	-21.9%	8.7%	2.3%	23.7%	66.6%		28.9%	5.0%
U-235	26.0%	-4.7%	2.2%	13.9%	-0.7%	10.6%	0.4%		-2.4%	-7.6%
U-236	3.2%	3.5%	1.3%	2.9%	3.2%	2.6%	-0.7%		2.1%	-6.0%
U-238	-0.2%	-0.1%	-0.2%	-0.1%	-0.2%	-0.2%	-0.3%		0.5%	-0.6%
Np-237							-3.6%			
Pu-238	27.2%	10.0%	15.0%	9.7%	6.5%	2.5%	23.3%		-4.2%	-1.9%
Pu-239	4.8%	-9.8%	3.3%	-0.8%	-6.3%	2.2%	10.2%		-9.8%	-11.2%
Pu-240	12.5%	0.1%	6.5%	-0.8%	-3.0%	-2.9%	7.7%		-6.9%	-2.0%
Pu-241	4.5%	-10.3%	2.9%	-2.2%	-5.9%	1.8%	9.2%		-11.1%	-9.3%
Pu-242	13.9%	3.8%	11.2%	0.0%	5.8%	2.6%	13.4%		-2.8%	1.9%
Am-241							8.2%			-3.3%
Am-243							-5.7%			-9.6%
Mo-95		-3.1%			-3.8%		16.8%			-1.5%
Tc-99		49.5%			43.2%		35.4%			
Ru-101		-3.3%			-2.2%		48.8%			
Rh-103		1.1%			2.5%		31.1%			
Ag-109		20.2%			46.4%		147.2%			
Cs-133		1.9%			2.7%		7.7%			-11.9%
Nd-143	5.7%	1.9%	3.4%	6.5%	3.5%	4.7%	12.2%		-1.7%	9.2%
Nd-145	3.0%	1.5%	1.2%	1.9%	2.8%	1.4%	2.6%		3.6%	5.0%
Sm-147		1.6%			0.6%		0.9%			6.0%
Sm-149		-15.2%			0.7%		2.2%			-18.9%
Sm-150		2.2%			4.7%		1.6%			2.4%
Sm-151		-10.0%			-4.7%		-0.1%			-11.4%
Sm-152		9.8%			13.1%		0.7%			6.0%
Eu-151		-39.3%			-38.0%		-1.9%			
Eu-153		0.1%			5.3%		6.1%			6.5%
Gd-155		4.4%			10.7%		15.9%			19.9%

Table B.1 Comparisons of Polaris Calculations and Measurements for Burnup Credit Isotopes (C/M – 1)(%) (con't)

Nuclide	FOR-3 GN592 J8 ENUSA-2	FOR-3 GN592 J8 ENUSA-3	FOR-3 GN592 J8 ENUSA-4	FOR-3 GN592 J8 ENUSA-5	FOR-3 GN592 J8 ENUSA-6	FOR-3 GN592 J8 ENUSA-7	FOR-3 GN592 J8 ENUSA-8	LBT AIA003 KLU1	LBT AIA003 KLU3	LBT AIA003 KLU2
U-234	3.3%	1.5%	5.8%	3.3%	1.5%	4.3%	6.7%	6.9%	9.0%	8.6%
U-235	-8.7%	-6.5%	-12.5%	-8.7%	-4.7%	-4.0%	0.8%	2.0%	4.3%	-0.6%
U-236	-4.2%	-5.2%	15.7%	-2.6%	-3.2%	-2.5%	-0.5%	-4.1%	-1.8%	-2.7%
U-238	-0.5%	-0.7%	-0.4%	-0.2%	-0.6%	-0.8%	-0.3%	-0.3%	-0.2%	-0.4%
Np-237								-1.1%	0.6%	2.9%
Pu-238	3.4%	-1.9%	-7.2%	-5.7%	6.9%	9.2%	-10.4%	33.6%	32.4%	50.3%
Pu-239	-11.6%	-4.6%	-15.6%	-10.3%	-3.4%	-3.8%	-5.3%	10.5%	13.4%	11.8%
Pu-240	-2.4%	-1.5%	-3.5%	-1.9%	-1.4%	-0.5%	-1.9%	8.1%	10.5%	9.6%
Pu-241	-9.6%	-3.8%	-13.9%	-8.5%	-2.2%	-3.0%	-5.6%	9.3%	13.7%	14.1%
Pu-242	3.3%	0.9%	1.3%	2.7%	1.5%	3.4%	-0.6%	12.3%	14.2%	22.6%
Am-241	-5.0%	2.5%	-8.6%	1.1%	5.0%	3.7%	-0.9%	10.5%	14.5%	10.9%
Am-243	-17.1%	-7.4%	-17.3%	-5.0%	-14.3%	-5.8%	-31.8%	4.6%	2.1%	4.7%
Mo-95	1.9%	-0.8%	13.4%	-3.0%	14.5%	5.0%	-1.5%	17.6%		30.5%
Tc-99								25.0%		
Ru-101										
Rh-103								20.2%		
Ag-109								29.4%		
Cs-133	-24.0%	-4.5%	-2.8%	-4.5%	-6.7%	-3.5%	-5.4%	3.6%	-3.1%	-1.5%
Nd-143	6.2%	6.9%	4.6%	7.6%	8.2%	12.1%	7.0%	2.2%	0.0%	0.4%
Nd-145	3.5%	3.1%	4.7%	4.1%	0.0%	7.9%	4.7%	-0.6%	-2.5%	-0.4%
Sm-147	6.8%	9.1%	17.0%	-16.7%	-15.6%	13.5%	-17.0%	2.9%	4.4%	6.8%
Sm-149	-25.4%	-13.8%	-34.0%	-18.5%	-6.9%	-18.3%		-10.1%		
Sm-150	2.7%	6.3%	7.0%	7.5%	9.6%	8.5%	7.7%	2.3%	10.0%	11.7%
Sm-151	-18.2%	0.5%	-10.9%	12.1%	23.8%	19.0%	-0.2%	-2.7%	14.4%	37.9%
Sm-152	3.9%	0.9%	9.8%	7.3%	2.5%	4.2%	5.1%	2.3%	11.0%	11.9%
Eu-151								-32.7%		
Eu-153	9.2%	5.7%	4.7%	-3.2%	6.0%	5.7%	5.2%	0.6%	14.0%	10.3%
Gd-155	24.5%	13.1%	9.4%	32.2%	20.6%	30.7%	14.4%	9.4%	35.3%	50.4%

Table B.1 Comparisons of Polaris Calculations and Measurements for Burnup Credit Isotopes (C/M – 1)(%) (con't)

Nuclide	LIM-1 FYJ1433 D9 1D2	LIM-1 FYJ1433 D9 4G1	LIM-1 FYJ1433 D9 4D4	LIM-1 FYJ1433 D9 2D2	LIM-1 FYJ1433 H5 3A1C	LIM-1 FYJ1433 H5 3A1G	LIM-1 FYJ1433 D8 4G3	LIM-1 FYJ1433 D8 3D2B
U-234	1.3%	0.9%	3.2%	2.3%	4.3%	4.3%	7.2%	8.3%
U-235	3.0%	3.8%	-2.9%	2.4%	4.3%	2.5%	26.9%	22.7%
U-236	3.5%	3.9%	4.2%	4.3%	3.0%	3.0%	-1.8%	2.4%
U-238	-0.6%	-0.6%	-0.7%	-0.7%	-0.5%	-0.5%	-0.2%	-0.5%
Np-237	-6.9%	-6.8%	-5.7%	-8.7%	-5.2%	-5.8%	-7.7%	-6.8%
Pu-238	21.9%	16.0%	16.6%	21.1%	14.9%	14.6%	-3.6%	17.3%
Pu-239	0.7%	3.0%	-2.9%	1.4%	-0.7%	-1.3%	11.6%	9.9%
Pu-240	0.6%	0.2%	-1.6%	-0.5%	-0.8%	-1.1%	-5.9%	-2.4%
Pu-241	2.2%	4.2%	-0.2%	3.0%	3.5%	3.5%	5.0%	11.1%
Pu-242	9.2%	6.7%	11.4%	10.2%	12.9%	15.1%	-7.5%	10.2%
Am-241	5.1%	9.8%	4.2%	15.2%	10.1%	8.6%	14.6%	16.0%
Am-243	2.8%	-0.7%	0.1%	9.4%	3.2%	2.8%	-19.8%	-1.7%
Mo-95	-0.4%	3.6%	6.9%	4.4%	3.8%	3.8%	-11.5%	-3.1%
Tc-99	9.7%	21.5%	12.8%	16.4%	18.1%	21.3%	-4.3%	6.0%
Ru-101	3.6%	5.5%	9.5%	7.4%	8.3%	5.7%	-4.7%	4.8%
Rh-103	5.0%	2.3%	2.1%	7.1%	3.6%	-0.3%	-6.2%	2.6%
Ag-109	12.7%	23.7%	16.1%	18.5%	17.8%	4.2%	-17.8%	-4.5%
Cs-133								
Nd-143	11.1%	10.5%	9.2%	11.0%	9.8%	9.8%	4.2%	13.1%
Nd-145	8.1%	7.7%	9.0%	11.8%	8.2%	8.2%	-0.9%	7.6%
Sm-147	7.6%	3.1%	7.7%	5.6%	6.0%	5.6%	3.6%	6.6%
Sm-149	20.2%	-6.6%	-8.0%	3.0%	-3.0%	-3.4%	-3.6%	0.3%
Sm-150	8.3%	4.8%	8.7%	7.0%	5.0%	5.6%	-4.3%	2.6%
Sm-151	5.7%	2.8%	1.7%	4.9%	0.4%	1.1%	7.7%	8.0%
Sm-152	10.2%	6.4%	13.6%	9.2%	12.2%	13.0%	3.6%	7.3%
Eu-151	7.6%	6.8%	8.9%	11.7%	4.8%	3.2%	9.3%	7.7%
Eu-153	6.5%	4.1%	10.3%	7.6%	9.2%	9.2%	4.5%	9.1%
Gd-155	10.2%	8.7%	5.3%	9.2%	3.9%	10.4%	5.8%	4.6%

^a Sample measured by PSI

^b Sample measured by SCK•CEN

APPENDIX C POLARIS MODEL INPUT FILES

APPENDIX C POLARIS MODEL INPUT FILES

Table C.1 Polaris Input File for the Dodeward Assembly Y013 (6 × 6)

```
=polaris
title "Dodeward DU1 model "
lib "xn56v7.1"
sys BWR
geom FuelNode : ASSM 6 1.793
channel COOL
hGAP 0.476 0.872 : MOD.1 MOD.1

box hspan=5.505 rad=0.9652 thick=0.17

opt KEFF UpscatterSuperGroup=1

shield ALL=N FUEL=P GAD=R
basis ALL=no FUEL.100=yes
deplete FUEL=yes GAD=yes

%A
mat FUEL.1 : uo2_A temp=900 dens=10.412
  comp uo2_A : UOX 3.2

%X
mat FUEL.100 : uo2_du1 temp=900 dens=10.462306
  comp uo2_du1 : UOX 4.941

%B
mat GAD.1 : uo2gd_B temp=900 dens=10.412
  comp uox_B : UOX 3.2
  comp uo2gd_B : WT GD203=2.653 uox_B=-100

%C
mat FUEL.2 : uo2_C temp=900 dens=10.412
  comp uo2_C : UOX 2.6

%D
mat FUEL.3 : uo2_D temp=900 dens=10.412
  comp uo2_D : UOX 1.8

%mat FUEL.3 : uo2_A temp=900 dens=10.412
%  comp uo2_E : UOX 3.2

mat FUEL.4 : mox_M temp=900 dens=10.34003664
  comp uvec : WT scale=PCT
    U234=0.003
    U235=0.239
    U235=0.001
    U238=-100
  comp puvec : WT scale=PCT
    PU238=1.405
    PU239=61.844
    PU240=23.380
    PU241=8.826
    PU242=4.545
  comp uo2_mox : FORM uvec=1 O=2
  comp puo2_mox : FORM puvec=1 O=2
  comp mox_M : WT scale=PCT
    uo2_mox = 93.50514401
    puo2_mox = 6.426611176
    am241 = 0.068244814

mat GAP.1 : he_GAP temp=564
  comp he_GAP : CONC
    2003=1.50456E-11
```

```

2004=1.50456E-05
mat COOL.1 : H2O temp=564
% void=32
mat MOD.1 : H2O temp=564
% void=0

```

```

pin X : 0.5176 0.5275 0.6135 : FUEL.100 GAP.1 CLAD.1
pin A : 0.574 0.5855 0.6745 : FUEL.1 GAP.1 CLAD.1
pin B : 0.574 0.5855 0.6745 : GAD.1 GAP.1 CLAD.1
pin C : 0.574 0.5855 0.6745 : FUEL.2 GAP.1 CLAD.1
pin D : 0.574 0.5855 0.6745 : FUEL.3 GAP.1 CLAD.1
pin E : 0.574 0.5855 0.6745 : FUEL.1 GAP.1 CLAD.1
pin M : 0.5178 0.5275 0.6135 : FUEL.4 GAP.1 CLAD.1

pin G : 0.5855 0.6745 : MOD.1 CAN.1

```

```

pinmap D C E E A C
      C X B A A A
      E B A A B E
      E A A G M E
      A A B M B A
      C A E E A A

```

```

mesh COOL : nx=9 ny=9 ns=16 nr=2
%<specialfield2>
mesh MOD : nf=4 nd=5 nx=10 ny=10 ns=16 nr=4
mesh FUEL : nr=3 ns=16
mesh GAD : nr=7 ns=16
%mesh CLAD : ns=16
mesh TUBE : ns=16

```

```

state
  ALL : temp=564
  FUEL : temp=900
  MOD : void=0 temp=564
  COOL : void=32 temp=564

```

```

read history
%power is reduced by 1.02 void is reduced by 1.0
%cycle 19
STATE COOL : void = 53.1 52.4 52.1 51.9 52.7 52.7 52.3 52.0 52.8 53.3 53.8 52.9 53.6 53.8 53.5
53.4 53.5 53.5 54.1 53.5 52.7 52.1 52.1
  FUEL : temp = 924.7 955.3 963.3 988.6 975.6 979.8 1011.7 1016.8 1019.0 1024.1 1026.8 1057.3
1065.9 1080.8 1101.9 1107.6 1115.6 1110.2 1094.6 1069.6 1050.2 1011.9 1011.9
  GAD : temp = 924.7 955.3 963.3 988.6 975.6 979.8 1011.7 1016.8 1019.0 1024.1 1026.8 1057.3
1065.9 1080.8 1101.9 1107.6 1115.6 1110.2 1094.6 1069.6 1050.2 1011.9 1011.9
power 28.336 29.845 30.07 31.324 30.325 30.335 32.518 20.706 39.29 33.007 33.181 35.404 36.057
37.046 38.546 38.964 39.464 39.148 37.913 35.751 33.701 32.426 0.0
dt 6.3 12.03 21.54 20.87 7.3 15.67 11.48 7.29 13.55 14.09 9.9 17.89 17.71 20.9 23.47 22.07
20.03 20.74 10.6 16.89 6.75 11.04 73.0
%cycle 20
STATE COOL : void = 23.9 88.0 53.15 53.19 52.80 52.00 51.37 50.55 50.55
  FUEL : temp = 1016.8 1080.8 1051.78 1046.44 1052.33 1066.48 1077.01 1037.75 1037.75
  GAD : temp = 1016.8 1080.8 1051.78 1046.44 1052.33 1066.48 1077.01 1037.75 1037.75
power 29.876 36.873 33.446 33.007 34.058 35.873 37.322 33.028 0.0
dt 4.26 13.32 64.65 48.6 27.1 29.8 55.64 44.63 50.0
%cycle 21
STATE COOL : void = 48.83 58.09 57.03 55.41 54.64 53.30 50.07 50.36 52.70 52.70

```

```

    FUEL : temp = 1051.39 1128.78 1090.98 1053.75 1027.34 1043.67 1064.28 1091.97 1027.44
1027.44
    GAD : temp = 1051.39 1128.78 1090.98 1053.75 1027.34 1043.67 1064.28 1091.97 1027.44
1027.44
power 31.232 42.707 40.361 37.556 34.966 37.108 39.148 41.412 36.128 0.0
dt    8.1 32.84 68.82 41.91 28.97 19.9 63.14 27.14 25.07 54.0
%cycle 22
STATE COOL : void = 48.78 55.20 50.79 45.15 39.90 46.43 47.23 48.58 48.58
    FUEL : temp = 1099.88 1114.99 1145.96 1132.02 1075.93 1131.26 1065.71 972.45 972.45
    GAD : temp = 1099.88 1114.99 1145.96 1132.02 1075.93 1131.26 1065.71 972.45 972.45
power 36.995 42.799 44.431 43.432 38.383 41.116 37.189 30.733 0.0
dt    20.43 19.64 45.71 53.76 47.67 64.08 33.87 32.13 39.0
%cycle 23
STATE COOL : void = 48.67 45.94 39.59 36.64 36.13 38.36 42.98 46.51
    FUEL : temp = 976.53 992.19 977.68 931.56 922.97 938.25 909.21 814.07
    GAD : temp = 976.53 992.19 977.68 931.56 922.97 938.25 909.21 814.07
power 30.253 31.079 29.876 27.234 26.571 27.173 25.469 23.093
dt    48.95 57.93 64.76 48.5 36.85 31.23 24.42 11.35

STATE COOL : void = 46.51
power 0 0 0 0 0 0 0 0 0 0
dt    2295 25 11 77 24 9 4 19 54 12 10 19 9

    end history

end

```

Table C.2 Polaris Input File for the Forsmark 3 Assembly 14595 (SVEA100)

```

=polaris
title "SVEA-96 Optima2"
lib "xn56v7.1"

sys BWR
geom FuelNode : ASSM 10 1.24
channel COOL
hgap 0.6775 0.7775 : MOD.1 MOD.1

box hspan=6.867 rad=1.01 thick=0.14

shield ALL=N FUEL=P GAD=R

mat CAN.1 : ZIRC2 temp=560

mat CLAD.1 : ZIRC2 temp=560

mat FUEL.9 : uo2_f9 10.62 temp=800
  comp uo2_f9 : UOX 4.0
mat FUEL.10 : uo2_f10 10.62 temp=800
  comp uo2_f10 : UOX 3.6
mat FUEL.11 : uo2_f11 10.62 temp=800
  comp uo2_f11 : UOX 3.6
mat FUEL.12 : uo2_f12 10.62 temp=800
  comp uo2_f12 : UOX 1.98
mat FUEL.13 : uo2_f13 10.62 temp=800
  comp uo2_f13 : UOX 2.22
mat FUEL.14 : uo2_f14 10.62 temp=800
  comp uo2_f14 : UOX 2.81
mat FUEL.15 : uo2_f15 10.62 temp=800
  comp uo2_f15 : UOX 3.17
mat FUEL.16 : uo2_f16 10.62 temp=800
  comp uo2_f16 : UOX 3.6
mat FUEL.17 : uo2_f17 10.62 temp=800
  comp uo2_f17 : UOX 4.0
mat FUEL.100 : uo2_f17 10.62 temp=800
mat GAD.18 : uo2gd_f315 temp=800 dens=10.37
  comp uox317 : UOX 3.17
  comp uo2gd_f315 : WT GD203=3.15 uox317=-100

mat gap.1 : he_gap temp=560
  comp he_gap : CONC
    2003=1.50456E-11
    2004=1.50456E-05
mat COOL.1 : H2O void=20 temp=560

mat MOD.1 : H2O void=0 temp=560

mat COOL.2 : H2O void=20 temp=560

pin W1 : 0.65 : COOL.1 : SQR
pin 9 : 0.4095 0.418 0.481 : FUEL.9 gap.1 clad.1
pin 10 : 0.4095 0.418 0.481 : FUEL.10 gap.1 clad.1
pin 11 : 0.4095 0.418 0.481 : FUEL.11 gap.1 clad.1
pin 12 : 0.4095 0.418 0.481 : FUEL.12 gap.1 clad.1
pin 13 : 0.4095 0.418 0.481 : FUEL.13 gap.1 clad.1
pin 14 : 0.4095 0.418 0.481 : FUEL.14 gap.1 clad.1
pin 15 : 0.4095 0.418 0.481 : FUEL.15 gap.1 clad.1

```

```

pin 16 : 0.4095 0.418 0.481 : FUEL.16 gap.1 clad.1
pin 17 : 0.4095 0.418 0.481 : FUEL.17 gap.1 clad.1
pin 18 : 0.4095 0.418 0.481 : GAD.18 gap.1 clad.1
pin A : 0.4095 0.418 0.481 : FUEL.100 gap.1 clad.1

```

```

pinmap
12
13 14
14 18 10
14 11 17 17
14 16 17 17 A
14 16 17 17 17
14 11 17 17 17 17
14 16 9 17 17 17 9
14 18 16 11 16 16 11 16 18
13 14 15 15 15 15 15 14 13

```

```
%0.242 0.689 0.931 4.077 4.505 5.185 5.711 6.192
```

```

cross 0.456 0.08 : 0 0.242 0.689 0.931 4.077 4.505 5.185 5.711 5.883 6.273 6.403 6.87
              7.337 7.467 7.857 8.029 8.555 9.235 9.663 12.809 13.051 13.498 13.74

```

```

: 0.78 0.00 0.00 0.2 0.2 0.2 0.2 0.2 0.2 0.3 0.4 0.912
  0.4 0.3 0.2 0.2 0.2 0.2 0.2 0.2 0.2 0.00 0.00 0.78
: -0.0 -0.0 -0.0 -0.0 -0.0 -0.0 -0.0 -0.0 -0.0 -0.0 -0.0 -0.0 -0.0
  -0.0 -0.0 -0.0 -0.0 -0.0 -0.0 -0.0 -0.0 -0.0 -0.0 -0.0 -0.0

```

```

: 1 1 1 8 2 2 2 1 2 1 2
  2 1 2 1 2 2 2 8 1 1 1

```

```

dymap
-0.0
0.0 -0.0
0.0 0.0 0.0
0.0 0.0 0.0 0.0
0.0 0.0 0.0 0.0 0
-0.0 -0.0 -0.0 -0.0 0 0
-0.0 -0.0 -0.0 -0.0 0 0 -0.0
-0.0 -0.0 -0.0 -0.0 0 0 -0.0 -0.0
-0.0 -0.0 -0.0 -0.0 0 0 -0.0 -0.0 -0.0
0.0 0.0 0.0 0.0 0 0 0.0 0.0 0.0 0.00

```

```

dxmap
-0.0
0.0 -0.0
0.0 0.0 0.0
0.0 0.0 0.0 0.0
0.0 0.0 0.0 0.0 0
-0.0 -0.0 -0.0 -0.0 0 0
-0.0 -0.0 -0.0 -0.0 0 0 -0.0
-0.0 -0.0 -0.0 -0.0 0 0 -0.0 -0.0
-0.0 -0.0 -0.0 -0.0 0 0 -0.0 -0.0 -0.0
0.0 0.0 0.0 0.0 0 0 0.0 0.0 0.0 0.00

```

```

mesh COOL : nx=9 ny=9 ns=16 nr=2
mesh COOL.2 : nx=9 ny=9 ns=16 nr=4
mesh MOD : nf=4 nd=5 nx=10 ny=10 ns=16 nr=4
mesh MOD.2 : ns=4 nr=1
mesh FUEL : nr=3 ns=16
mesh GAD : nr=7 ns=16

```

mesh TUBE : ns=16

DEplete FUEL=yes GAD=yes
BASIS ALL=no FUEL.100=yes
read history

STATE COOL : VOID= 67.27 69.24 68.81 73.21 68.97 69.16 69.36 69.46 69.25 70.22 71.36 64.81 60.05
38.34

FUEL : TEMP= 852.30 835.90 838.63 745.35 852.24 856.41 858.87 846.00 865.16 887.47 878.10
862.32 828.09 734.56

GAD : TEMP= 852.30 835.90 838.63 745.35 852.24 856.41 858.87 846.00 865.16 887.47 878.10
862.32 828.09 734.56

power 34.60 32.53 32.65 21.41 33.88 34.18 34.30 32.77 34.98 37.68 36.59 34.92 31.04 20.36

dt 5.25 8.13 23.72 37.92 26.56 25.76 27.38 6.91 26.72 27.28 27.69 27.46 27.47 79.75

power 0.00

dt 21.00

STATE COOL : VOID= 65.78 64.20 66.85 67.52 65.38 63.62 65.19 62.07 64.85 66.90 64.98 57.40

FUEL : TEMP= 818.30 852.05 880.64 879.15 880.96 905.63 882.96 899.29 889.04 834.89 814.62
703.20

GAD : TEMP= 818.30 852.05 880.64 879.15 880.96 905.63 882.96 899.29 889.04 834.89 814.62
703.20

power 30.26 34.22 37.26 37.13 37.42 40.35 37.73 39.80 38.53 32.16 29.84 16.92

dt 6.85 8.35 28.02 22.19 18.59 8.15 32.38 12.13 24.49 39.12 29.07 50.65

power 0.00

dt 28.00

STATE COOL : VOID= 62.23 62.72 62.14 61.46 61.03 59.13 58.42 57.66 57.34 58.12 51.44 59.07 52.19

FUEL : TEMP= 864.39 865.90 864.45 861.75 856.24 847.26 830.67 770.58 790.46 678.03 779.96
805.88 667.08

GAD : TEMP= 864.39 865.90 864.45 861.75 856.24 847.26 830.67 770.58 790.46 678.03 779.96
805.88 667.08

power 36.92 37.09 36.90 36.57 35.90 34.82 32.82 25.49 27.95 14.12 26.75 29.53 12.88

dt 38.96 25.85 30.16 28.43 24.95 35.79 28.54 36.22 12.32 36.29 18.57 31.61 23.32

power 0.00

dt 18.00

STATE COOL : VOID= 59.07 59.45 59.89 59.24 59.22 60.02 58.99 57.81 58.01 58.74 58.19 54.57 51.22
46.62 40.41 36.92

FUEL : TEMP= 757.10 827.04 839.57 832.60 826.96 829.23 835.94 847.86 847.96 835.43 832.85
801.70 752.00 739.79 720.79 711.09

GAD : TEMP= 757.10 827.04 839.57 832.60 826.96 829.23 835.94 847.86 847.96 835.43 832.85
801.70 752.00 739.79 720.79 711.09

power 24.01 32.39 33.93 33.12 32.44 32.68 33.58 35.16 35.21 33.66 33.35 29.62 23.53 22.04 19.70

18.53

dt 7.16 27.00 27.22 26.07 26.88 22.33 29.19 27.13 21.17 28.15 5.72 29.56 31.37 32.35 22.91 16.78

power 0.00

dt 18.00

STATE COOL : VOID= 56.88 59.31 59.24 58.21 57.49 56.71 55.88 55.31 54.52 56.19 52.00

FUEL : TEMP= 831.33 815.79 808.05 803.02 800.52 799.59 799.49 812.47 814.44 821.55 746.62
GAD : TEMP= 831.33 815.79 808.05 803.02 800.52 799.59 799.49 812.47 814.44 821.55 746.62

power 33.14 31.22 30.31 29.67 29.28 29.08 28.94 30.34 30.54 31.13 22.38

dt 10.05 14.96 19.43 26.51 26.68 26.58 31.41 16.28 6.31 25.04 50.74

power 0.00

dt 34.00

STATE COOL : VOID= 45.64 46.01 48.17 46.18 44.72 44.74 44.48 43.54 41.76 40.07 40.67 35.75 31.01

FUEL : TEMP= 719.84 691.84 665.55 704.55 712.11 710.45 707.85 705.35 706.64 719.87 714.22
677.15 693.47

GAD : TEMP= 719.84 691.84 665.55 704.55 712.11 710.45 707.85 705.35 706.64 719.87 714.22
677.15 693.47

power 18.60 15.37 12.34 16.75 17.56 17.32 16.98 16.66 16.76 18.17 17.48 13.45 15.22

dt 6.42 31.17 26.89 19.04 29.03 28.81 29.73 29.53 30.12 30.28 29.88 35.00 27.11

power 0.00

dt 3775.00

```
power 0.00  
dt 12.00  
power 0.00  
dt 15.00  
end history
```

```
end
```

Table C.3 Polaris Input File for Forsmark 3 Assembly GN592 (GE14 Dominant Lattice)

```
=polaris
  title "FORSMARK N3 DOM"

lib "xn56v7.1"

sys BWR
geom FuelNode : ASSM 10 [      ]
channel COOL
hgap [      ] : MOD.1 MOD.1

box [      ]

mat CAN.1 : ZIRC2 temp=560
mat CLAD.1 : ZIRC2 temp=560

[
```

```

]
mat GAP.1 : FILLGAS temp=560

mat COOL.1 : H2O temp=560
mat COOL.2 : H2O temp=560

% comp h2o_mod : CONC
%      1001=3.06145E-02
%      8016=1.53073E-02
mat MOD.1 : H2O temp=560
% comp h2o_mod1 : CONC
%      1001=4.93677E-02
%      8016=2.46838E-02

pin 1 :    0.43815    0.44704    0.51308
        :    FUEL.1    GAP.1    CLAD.1

pin 2 :    0.43815    0.44704    0.51308
        :    FUEL.2    GAP.1    CLAD.1

pin 3 :    0.43815    0.44704    0.51308
        :    FUEL.3    GAP.1    CLAD.1

pin 4 :    0.43815    0.44704    0.51308
        :    FUEL.4    GAP.1    CLAD.1

pin 5 :    0.43815    0.44704    0.51308
        :    FUEL.5    GAP.1    CLAD.1

pin 6 :    0.43815    0.44704    0.51308
        :    FUEL.6    GAP.1    CLAD.1

pin 7 :    0.43815    0.44704    0.51308
        :    FUEL.7    GAP.1    CLAD.1

```

```

pin 8 : 0.43815 0.44704 0.51308
        : FUEL.8 GAP.1 CLAD.1

pin 9 : 0.43815 0.44704 0.51308
        : FUEL.9 GAP.1 CLAD.1

pin A : 0.43815 0.44704 0.51308
        : FUEL.100 GAP.1 CLAD.1

pin 10 : 0.43815 0.44704 0.51308
         : GAD.10 GAP.1 CLAD.1

pin 11 : 0.43815 0.44704 0.51308
         : GAD.11 GAP.1 CLAD.1

pin V : 0.51308 : COOL.1

pin W1 size=2 :[ ]
              : MOD.1 CAN.1

```

```

deplete FUEL=yes GAD=yes
basis ALL=no FUEL.100=yes
shield ALL=N FUEL=P GAD=R
opt KEFF UpscatterSuperGroup=1

```

```

pinmap
1
2 V
3 6 10
4 V 7 7
4 10 7 7 V
4 6 7 W1 W1 V
4 V 7 W1 W1 7 7
4 11 7 7 7 7 7
3 V 11 V 7 7 V 10 V
2 3 6 6 7 7 7 A 4 5

```

```

mesh COOL.1 nr=2 ns=16
mesh COOL.2 nr=3 ns=16
mesh MOD : nf=3 nd=4 nx=6 ny=6 ns=16 nr=4
mesh FUEL nr=3 ns=16
mesh GAD nr=7 ns=16

```

```

state ALL : temp=560
        FUEL : temp=792
        GAD : temp=792
        MOD : void=0
        COOL : void=40

```

```

%-----%
% operating history provided by RCA benchmark
%-----%

```

```

read history

```

```

%power is reduced by 0.91 void is reduced by 1.0
%-----%

```

```

% cycle 16
%-----%

```

```

STATE COOL : void = 72.3 71.0 71.9 72.2 72.5 73.0 72.8 72.0 71.4 69.5 67.4 65.3 61.5 55.2

```

```
power 4.45 32.778 38.62 42.515 38.029 40.832 43.453 42.752 46.064 44.19 45.8 38.73 35.263
35.617
dt 24.24 19.76 22.36 25.4 28.39 34.38 24.84 27.78 28.13 29.32 16.5 13.94 27.56 39.41
```

```
power 0.0
dt 40.0
%-----%
% cycle 17
%-----%
```

```
STATE COOL : void = 68.3 69.6 67.0 65.0 65.6 66.0 65.6 61.5 62.2 50.0
power 34.116 44.772 43.498 44.863 38.056 42.015 39.485 30.967 23.969 23.614
dt 9.49 28.94 27.3 28.88 28.37 28.27 27.34 27.89 4.5 64.01
```

```
power 0.0
dt 14.0
%-----%
% cycle 18
%-----%
```

```
STATE COOL : void = 78.1 76.8 75.6 75.0 74.1 73.5 72.9 71.8 70.3 67.9 65.6 70.4 70.4 53.8
power 29.047 38.22 38.329 45.655 37.137 40.55 39.312 43.998 41.96 40.249 45.573 54.109 38.866
39.694
dt 3.72 8.47 28.17 26.01 29.07 26.63 30.21 24.54 28.3 29.51 26.06 27.93 2.78 81.6
```

```
power 0.0
dt 12.0
%-----%
% cycle 19
%-----%
```

```
STATE COOL : void = 53.8 53.6 52.9 51.6 51.0 49.4 48.8 47.2 45.9 40.6 38.0 31.9 30.1 19.2 13.4
power 13.659 19.893 26.053 19.064 18.71 18.118 17.881 21.904 21.458 18.946 19.838 22.377 18.791
17.681 14.842
dt 31.62 32.56 16.58 28.32 23.08 29.8 12.08 24.64 25.15 28.49 27.22 28.95 22.99 24.42 29.1
```

```
power 0.0
dt 35.0
%-----%
% cycle 20
%-----%
```

```
STATE COOL : void = 44.0 43.6 42.2 41.1 40.4 38.4 36.5 34.5 31.2 25.8 19.0 18.8
power 15.334 15.006 18.491 19.292 14.251 13.932 23.032 13.495 21.057 15.261 11.339 8.59
dt 7.04 21.58 29.2 22.39 30.3 31.01 23.44 32.0 25.64 28.3 9.52 12.57
```

```
power 0.0 0.0 0.0 0.0 0.0 0.0
dt 1479.0 1.0 15.0 61.0 58.0 85.0
```

end history

end

Table C.4 Polaris Input File for the Fukushima Daini 1 Assembly 2F1ZN2 (ATRIUM9)

```
=polaris
title "Atrium-9 model "
lib "xn56v7.1"
sys BWR
geom FuelNode : ASSM 9 1.45
channel COOL
hgap 0.65 : MOD.1
box 0.25 0.87376 6.7
opt KEFF UpscatterSuperGroup=1
shield ALL=N FUEL=P GAD=P
deplete FUEL=YES GAD=YES
opt CRITSPEC Method="P1"

mat FUEL.1 : uo2_f100 temp=900 dens=10.63
  comp uo2_f100 : UOX 4.9

mat FUEL.2 : uo2_f102 temp=900 dens=10.63
  comp uo2_f102 :UOX 4.2
mat FUEL.21 : uo2_f102 temp=900 dens=10.63
mat FUEL.22 : uo2_f102 temp=900 dens=10.63

mat FUEL.3 : uo2_f103 temp=900 dens=10.63
  comp uo2_f103 : UOX 3.6
mat FUEL.31 : uo2_f103 temp=900 dens=10.63

mat FUEL.4 : uo2_f104 temp=900 dens=10.63
  comp uo2_f104 : UOX 3.0
mat FUEL.41 : uo2_f104 temp=900 dens=10.63

mat FUEL.5 :uo2_f105 temp=900 dens=10.63
  comp uo2_f105 : UOX 2.1

mat GAD.1 : uo2gd_f50 temp=900 dens=10.38
  comp uox34 : UOX 3.0
  comp uo2gd_f50 : WT GD203=5.0 uox34=-100

mat GAP.1 : he_GAP temp=558.15
  comp he_GAP : CONC
    2003=1.50456E-11
    2004=1.50456E-05

mat COOL.1 : H2O temp=558.15 :void=14
mat MOD.1 : H2O temp=558.15 :void=0

mat FUEL.100 : uo2_f100 temp=900 dens=10.63
mat GAD.100 : uo2gd_f50 temp=900 dens=10.38

pin C2 : 0.47000 0.49000 0.55000
        : GAD.100 gap.1 clad.1
pin C3 : 0.47000 0.49000 0.55000
        : FUEL.100 gap.1 clad.1

pin 1 : 0.47000 0.49000 0.55000
       : FUEL.1 gap.1 clad.1
pin 2 : 0.47000 0.49000 0.55000
       : FUEL.2 gap.1 clad.1
pin 3 : 0.47000 0.49000 0.55000
       : FUEL.3 gap.1 clad.1
pin 4 : 0.47000 0.49000 0.55000
```

```

      : FUEL.4      gap.1      clad.1
pin 5 : 0.47000    0.49000    0.55000
      : FUEL.5      gap.1      clad.1
pin 9 : 0.47000    0.49000    0.55000
      : GAD.1       gap.1      clad.1
pin 21 : 0.47000   0.49000   0.55000
      : FUEL.21     gap.1      clad.1
pin 22 : 0.47000   0.49000   0.55000
      : FUEL.22     gap.1      clad.1
pin 41 : 0.47000   0.49000   0.55000
      : FUEL.41     gap.1      clad.1
pin 31 : 0.47000   0.49000   0.55000
      : FUEL.31     gap.1      clad.1
pin W 3.0 : 1.8425 1.925 : MOD.1 CAN.1 : SQR SQR

```

```

pinmap 5
4      3
3 C2  C3
2 22  21  W
2 9   21  W  W
2 22  21  W  W  W
3 9   1  21  21  21  1
4 3   9  22  9  22  9  3
5 4   3  2  2  2  3  4  5

```

```

mesh MOD : nf=3 nd=4 nx=6 ny=6 ns=8 nr=4
mesh FUEL : nr=3 ns=8
mesh GAD : nr=5 ns=8
%mesh CLAD : ns=8
mesh TUBE : ns=8

```

```

state ALL : temp=559
          FUEL : temp=900
          GAD : temp=900
          MOD : void=0
          COOL :void=14

```

```

%-----%
% Irradiation Report of Fuel Samples of BWR 9x9-9 Fuel
% Japan Nuclear Energy Safety Organizaion Toru YAMAMOTO (JNES 2014)
%-----%

```

```

basis ALL=no GAD.100=yes
read history

```

```

STATE COOL : void = 67.6 67.6 67.6 69.1 69.1 69.2 69.2 70.2 70.2 71.2 71.2 72.5 72.5 73.6 73.6
73.6
power 17.019 18.907 18.907 19.584 19.584 20.291 20.291 20.412 20.412 20.584 20.584 20.432
20.432 20.17 20.17 20.17
dt 4.0 16.0 16.0 17.5 17.5 21.0 21.0 16.0 16.0 15.5 15.5 17.5 17.5 17.5 17.5 12.0
power 0.0
dt 6.0

```

```

STATE COOL : void = 74.2 74.3 74.3 74.0 74.0 74.4 74.4 73.2 73.2 73.2
power 16.887 20.432 20.432 21.21 21.21 22.745 22.745 24.876 24.876 24.876
dt 7.0 15.5 15.5 16.0 16.0 16.5 16.5 18.5 18.5 18.0
power 0.0
dt 40.0

```

```

STATE COOL : void = 77.0 77.0
power 16.998 16.998

```

```

dt      8.0 26.0
power   0.0
dt      71.0

STATE COOL : void = 76.5 76.3 76.3 76.4 76.4 76.5 76.5 76.6 76.6 76.8 76.8 76.9 76.9 76.8 76.3
76.5 76.5
power   61.246 25.28 25.28 25.583 25.583 25.886 25.886 25.704 25.704 25.523 25.523 25.25 25.25
25.068 25.381 26.078 26.078
dt      5.0 12.0 12.0 16.0 16.0 15.5 15.5 16.0 16.0 19.0 19.0 16.0 16.0 31.0 28.0 24.0 28.0

power   0.0
dt      86.0

STATE COOL : void = 72.9 73.3 74.3 73.4 73.7 73.8 73.6 73.4 72.9 73.0 73.0 71.2 71.4 70.8 70.8
68.8 68.8
power   24.947 24.402 24.816 24.886 24.573 24.977 25.149 25.068 25.119 25.644 25.644 25.725
26.826 28.411 28.411 28.401 28.401
dt      6.0 31.0 32.0 17.0 32.0 31.0 32.0 35.0 31.0 21.0 21.0 32.0 28.0 19.0 19.0 25.0 11.0

power   0.0
dt      3537.0
power   0.0
dt      15.0
power   0.0
dt      347.0
power   0.0
dt      3.0
power   0.0
dt      4.0
power   0.0
dt      347.0

end history

end

```

Table C.5 Polaris Input File for Fukushima Daini-2 Assembly 2F2DN23 (8 × 8-2)

```
=polaris
title "Fukushima Daini -2 Assembly model "
lib "xn56v7.1"
sys BWR
geom FuelNode : ASSM 8 1.625
channel COOL
hGAP 0.6629 0.6629 : MOD.1 MOD.1

box hspan=6.70305 rad=0.9652 thick=0.2032

opt KEFF UpscatterSuperGroup=1
deplete ALL=false FUEL=true GAD=true
shield ALL=N FUEL=P GAD=R
basis ALL=no GAD.100=yes

mat FUEL.1 : uo2_f100 temp=900 dens=10.42
  comp uvec100 : WT scale=PCT
    U234=0.04
    U235=3.910
    U238=96.05
  comp uo2_f100 : FORM uvec100=1 O=2

mat FUEL.2 : uo2_f102 temp=900 dens=10.42
  comp uvec102 : WT scale=PCT
    U234=0.031
    U235=3.448
    U238=96.521
  comp uo2_f102 : FORM uvec102=1 O=2

mat FUEL.3 : uo2_f103 temp=900 dens=10.42
  comp uvec103 : WT scale=PCT
    U234=0.03
    U235=3.405
    U238=96.565
  comp uo2_f103 : FORM uvec103=1 O=2

mat FUEL.4 : uo2_f104 temp=900 dens=10.42
  comp uvec104 : WT scale=PCT
    U234=0.026
    U235=2.903
    U238=97.071
  comp uo2_f104 : FORM uvec104=1 O=2

mat FUEL.5 :uo2_f105 temp=900 dens=10.42
  comp uvec105 : WT scale=PCT
    U234=0.018
    U235=1.997
    U238=97.985
  comp uo2_f105 : FORM uvec105=1 O=2

mat GAD.6 : uo2gd_f50 temp=900 dens=10.23
  comp uox341 : UOX 3.41
  comp uo2gd_f50 : WT GD203=4.5 uox341=-100
mat GAD.100 : uo2gd_f50 temp=900 dens=10.23

mat GAP.1 : he_GAP temp=559.15
  comp he_GAP : CONC
    2003=1.50456E-11
```


Table C.6 Polaris Input File for Fukushima Daini-2 Assembly 2F2D1 (8 × 8-4)

```

=polaris
title "Fukushima Daini -2 Assembly model B3"
lib "xn56v7.1"

sys BWR
geom FuelNode : ASSM 8 1.625
channel COOL
hGAP 0.6629 0.6629 : MOD.1 MOD.1

box hspan=6.70305 rad=0.9652 thick=0.2032

opt KEFF UpscatterSuperGroup=1

shield ALL=N FUEL=P GAD=R
basis ALL=no GAD.100=yes

DEplete FUEL=yes GAD=yes

mat FUEL.1 : uo2_f100 temp=900 dens=10.61
  comp uo2_f100 : UOX 4.5

mat FUEL.2 : uo2_f102 temp=900 dens=10.61
  comp uo2_f102 :UOX 3.9

mat FUEL.3 : uo2_f103 temp=900 dens=10.61
  comp uo2_f103 : UOX 3.4

mat FUEL.4 : uo2_f104 temp=900 dens=10.61
  comp uo2_f104 : UOX 2.9

mat FUEL.5 :uo2_f105 temp=900 dens=10.61
  comp uo2_f105 : UOX 2.0

mat GAD.6 : uo2gd_f50 temp=900 dens=10.48
  comp uox341 : UOX 3.41
  comp uo2gd_f50 : WT GD203=4.5 uox341=-100

mat GAD.100 : uo2gd_f50 temp=900 dens=10.48

mat GAP.1 : he_GAP temp=559
  comp he_GAP : CONC
    2003=1.50456E-11
    2004=1.50456E-05
mat COOL.1 : H2O temp=559 :void=60.48

mat MOD.1 : H2O temp=559 :void=0

%<specialfield1>
%<specialfield3>

pin B : 0.519 0.529 0.615 :GAD.100 GAP.1 CLAD.1
pin 1 : 0.519 0.529 0.615 :FUEL.1 GAP.1 CLAD.1
pin 2 : 0.519 0.529 0.615 :FUEL.2 GAP.1 CLAD.1
pin 3 : 0.519 0.529 0.615 :FUEL.3 GAP.1 CLAD.1
pin 4 : 0.519 0.529 0.615 :FUEL.4 GAP.1 CLAD.1
pin 5 : 0.519 0.529 0.615 :FUEL.5 GAP.1 CLAD.1
pin G : 0.519 0.529 0.615 :GAD.6 GAP.1 CLAD.1

pin W 2 : 1.623 1.7 : MOD.1 CAN.1

```

```

pinmap 5
      4 2
      3 B 1
      3 2 4 W
      3 2 4 W W
      3 G 1 4 4 1
      4 2 G 2 2 G 2
      5 4 3 3 3 3 4 5

mesh COOL : nx=9 ny=9 ns=16 nr=2
%<specialfield2>
mesh MOD : nf=4 nd=5 nx=10 ny=10 ns=16 nr=4
mesh FUEL : nr=3 ns=16
mesh GAD : nr=7 ns=16
%mesh CLAD : ns=16
mesh TUBE : ns=16

state
  ALL : temp=559
  FUEL : temp=900
  GAD : temp=900
  MOD : temp=559 void=0
  COOL : temp=559 void=60.48

read history
power 32.58 33.07 33.07 33.07 33.07 33.07 33.07 33.07 33.07 33.07 33.07 32.92 32.92 32.92 32.92
32.92 32.92 32.60 32.60 32.60 32.60 32.60 32.60 32.60 32.61 32.61 32.61 32.61 32.61 32.61 32.61
0.00
dt 4.6 14.0 14.0 14.0 14.0 14.0 14.0 14.0 14.0 14.0 14.0 12.6 12.6 12.6 12.6 12.6 12.6 13.8 13.8
13.8 13.8 13.8 13.8 14.4 14.4 14.4 14.4 14.4 14.4 14.4 14.4 118.0

power 30.20 30.20 30.20 30.20 29.72 29.72 29.72 29.72 29.72 29.72 29.72 29.72 29.72 29.72 29.09
29.09 29.09 29.09 29.09 29.09 29.09 29.09 29.09 28.93 28.93 28.93 28.93 28.93 28.93 28.93
0.00
dt 13.3 13.3 13.3 13.3 11.5 11.5 11.5 11.5 11.5 11.5 11.5 11.5 11.5 11.5 14.4 14.4 14.4 14.4
14.4 14.4 14.4 14.4 14.4 14.9 14.9 14.9 14.9 14.9 14.9 14.9 82.0

power 26.04 26.04 26.04 26.04 26.04 24.12 24.12 24.12 24.12 24.12 24.12 24.12 24.12 24.12 24.12
22.67 22.67 22.67 22.67 22.67 22.67 0.00 0.00
dt 22.8 22.8 22.8 22.8 22.8 12.9 12.9 12.9 12.9 12.9 12.9 12.9 12.9 12.9 20.5 20.5 20.5
20.5 20.5 20.5 990.0 60.0

end history

end

```

Table C.7 Polaris Input File for Leibstadt Assembly AIA003 (SVEA96 Cominant Lattice)

```
=polaris
title "Leib N4 DOM"

lib "xn56v7.1"
sys BWR

%%%%%%%%%%%%%%%%%%%%%%%%%%%%%%%%%%%%%%%%%%%%%%%%%%%%%%%%%%%%%%%%%%%%%%%%
% options
%%%%%%%%%%%%%%%%%%%%%%%%%%%%%%%%%%%%%%%%%%%%%%%%%%%%%%%%%%%%%%%%%%%%%%%%
shield ALL=N FUEL=P GAD=R
opt KEFF UpscatterSuperGroup=1
basis ALL=no FUEL.9=yes
deplete FUEL=yes GAD=yes
%%%%%%%%%%%%%%%%%%%%%%%%%%%%%%%%%%%%%%%%%%%%%%%%%%%%%%%%%%%%%%%%%%%%%%%%
% materials
%%%%%%%%%%%%%%%%%%%%%%%%%%%%%%%%%%%%%%%%%%%%%%%%%%%%%%%%%%%%%%%%%%%%%%%%
[

]
%%%%%%%%%%%%%%%%%%%%%%%%%%%%%%%%%%%%%%%%%%%%%%%%%%%%%%%%%%%%%%%%%%%%%%%%
% geometry
%%%%%%%%%%%%%%%%%%%%%%%%%%%%%%%%%%%%%%%%%%%%%%%%%%%%%%%%%%%%%%%%%%%%%%%%
geom myBWR : ASSM 10 [ ]
hgap 0.69 0.69 : MOD.1 MOD.1
%: MOD.2 MOD.1
% box thichness, radius, half width
box [ ]

pin 1 : [0.4095 0.418 0.481] : FUEL.1 GAP.1 CLAD.1
pin 2 : 0.4095 0.418 0.481 : FUEL.2 GAP.1 CLAD.1
pin 3 : 0.4095 0.418 0.481 : FUEL.3 GAP.1 CLAD.1
pin 4 : 0.4095 0.418 0.481 : GAD.4 GAP.1 CLAD.1
pin 5 : 0.4095 0.418 0.481 : FUEL.5 GAP.1 CLAD.1
pin 6 : 0.4095 0.418 0.481 : FUEL.6 GAP.1 CLAD.1
pin 7 : [ ] : GAD.7 GAP.1 CLAD.1
pin 8 : [ ] : FUEL.8 GAP.1 CLAD.1
pin 9 : [ ] : FUEL.9 GAP.1 CLAD.1
pin E : [ ] : COOL.1 : SQR
```

```

mesh COOL.1 : nx=9 ny=9 nr=3
mesh FUEL : nr=2 ns=16
mesh GAD : nr=6 ns=16
mesh MOD.1 : nf=3 nd=4 nx=6 ny=6 ns=16 nr=4
mesh MOD.2 : nf=3 nd=5

```

```

pinmap
1
2 2
3 4 6
3 5 6 7
2 6 9 8 E
2 6 9 8 E E
3 5 6 7 8 8 7
3 4 6 6 9 9 6 6
2 2 4 5 6 6 5 4 2
1 2 3 3 2 2 3 3 2 1

```

```

%cross halfwidth=0.0
%
cross [
1a 1b 1c 2c 2b 2a halfwidth
]
: 1 1 1 4 1 1 5
5 1 1 4 1 1 1

```

```

dxmap
-.[

```

```

]
dymap
-.[

```

```

% state
%%%%%%%%%%%%%%%%%%%%%%%%%%%%%%%%%%%%%%%%%%%%%%%%%%%%%%%%%%%%%%%%%%%%%%%%
state ALL : temp=560
FUEL : temp=900
GAD : temp=900
MOD : void=0
COOL : void=10

```

```

read history
%cyc 15
STATE COOL : void = 0.23 0.08 0.92 0.39 3.09 2.24 1.91 8.78 14.16 11.69 6.55 1.3 0.19 0
COOL : temp=560 FUEL : temp=816 GAD : temp=816
power 0 15.65 24.07 26.01 27.21 31.01 29.67 32.83 40.13 40.99 36.52 28.22 19.98 0
dt 1 12 34 27 13 31 33 21 36 34 36 41 32 24

```

```

%cyc16
STATE COOL : void = 1.88 22.76 21.65 22.73 24.9 20.57 10.99 4.05 0.82 0 0
COOL : temp=561.7 FUEL : temp=924.7 GAD : temp=924.7

```

```
power 18.73 41.24 48.24 47.47 48.60 49.32 43.96 36.06 28.97 20.89 0.00
dt 28 36 36 33 36 36 34 34 30 32 21
```

```
%cyc17
```

```
STATE COOL : void = 15.94 11.74 19.43 18.72 19.76 16.67 17.89 19.3 14.62 10.35 3.44 1.29 0
COOL : temp=562 FUEL : temp=944 GAD : temp=944
power 25.7 41.1 41.8 45.2 45.6 43.8 45.8 45.8 43.3 39.4 34.5 25.3 0.0
dt 17 39 30 35 35 14 36 34 22 27 35 25 21
```

```
%cyc18
```

```
STATE COOL : void = 6.55 4.13 4.42 3.45 3.09 2.61 1.59 0.07 1.27 0 0 0
COOL : temp=559 FUEL : temp=838 GAD : temp=838
power 31.01 34.97 32.86 32.94 32.03 31.40 30.43 25.76 23.66 23.45 18.28 0
dt 24 34 28 29 36 28 33 42 28 36 24 15
```

```
%cyc19
```

```
STATE COOL : void = 0 0 0 0 0 0 0 0 0 0 0 0 0
COOL : temp=554 FUEL : temp=731 GAD : temp=731
power 18.10 22.19 20.85 22.35 22.28 22.92 23.06 22.59 19.81 15.84 12.82 12.13 10.08 0
dt 18 39 38 27 27 16 12 36 35 40 24 14 23 21
```

```
%cyc20
```

```
STATE COOL : void = 0 0 0 0 0 0 0 0 0 0 0
COOL : temp=554 FUEL : temp=695 GAD : temp=695
power 11.05 15.21 14.40 13.16 12.68 12.36 11.81 10.69 8.47 8.52 6.43 0
dt 16 22 36 40 36 38 39 36 23 32 32 42
```

```
%cyc21
```

```
STATE COOL : void = 0.07 0 0 0 0 0 0
COOL : temp=556 FUEL : temp=687 GAD : temp=687
power 6.59 11.19 10.99 10.66 10.61 10.44 10.44 10.99
dt 10 30 33 36 21 29 27 5
```

```
power 0
dt 1739
end history
```

```
end
```

Table C.8 Polaris Input File for Limerick Assembly YJ1433 (GE11)

```

=polaris
title "2-D depletion based on Limerick Unit1 BWR, GE11 9x9 Assembly YJ1433 "
lib "xn56v7.1"
sys BWR
geom FuelNode : ASSM 9 [           ]
channel COOL
hgap [           ] : MOD.1 MOD.1
box hspan=[
                                     ]

opt KEFF UpscatterSuperGroup=1

shield ALL=N FUEL=P GAD=R

deplete FUEL=YES GAD=YES
opt CRITSPEC Method="P1"

mat CAN.1 : ZIRC2 temp=560

mat CLAD.1 : ZIRC2 temp=560

mat [

                                     ]

mat COOL.1 : H2O temp=560 : dens=1.0
mat MOD.1 : H2O temp=560 : void=0

pin  1 :    0.4877    0.559 :    FUEL.22 CLAD.1
pin  2 :    0.4877    0.559 :    FUEL.28 CLAD.1
pin  3 :    0.4877    0.559 :    FUEL.34 CLAD.1
pin  4 :    0.4877    0.559 :    FUEL.39 CLAD.1
pin  5 :    0.4877    0.559 :    FUEL.36 CLAD.1

pin  7 :    0.4877    0.559 :    GAD.1   CLAD.1
pin  A :    0.4877    0.559 :    FUEL.100 CLAD.1
pin W1 [           ] :    MOD.1   can.1   COOL.1

pinmap  1
        2  2
        3  4  4
        4  7  4  4
        4  4  4  W1 _
        4  7  5  W1 W1 4
        3  4  5  5  4  4  7

```

```
2 2 4 7 A 7 4 2
1 2 3 4 4 4 5 2 1
```

```
mesh COOL : nx=9 ny=9 ns=16 nr=2
mesh COOL.2 : nx=9 ny=9 ns=16 nr=4
mesh MOD : nf=4 nd=5 nx=10 ny=10 ns=16 nr=4
mesh MOD.2 : ns=4 nr=1
mesh FUEL : nr=3 ns=16
mesh GAD : nr=7 ns=16
%mesh CLAD : ns=16
mesh TUBE : ns=16
```

```
state ALL : temp=560
          FUEL : temp=1100
          GAD : temp=1100
          COOL : temp=575 dens=0.3
```

```
%-----%
%-----%
```

```
basis ALL=no FUEL.100=yes
read history
```

```
%power is reduced by 1.0 void is reduced by 1.0
```

```
STATE COOL : dens = 0.3756 0.3294 0.3294 0.3305 0.3305 0.3673 0.3673 0.3298 0.3508 0.403 0.4777
0.4777
power 27.832 28.364 28.364 29.381 29.381 29.271 29.271 33.895 31.112 35.509 29.422 0.0
dt 73.0 45.5 45.5 45.5 45.5 45.5 55.0 53.0 50.0 67.0 38.0
%
```

```
STATE COOL : dens = 0.2614 0.2546 0.2723 0.2723 0.2926 0.2978 0.3076 0.3339 0.3181 0.3557
0.3587 0.3587 0.4049 0.4856 0.4856
power 37.768 35.744 34.256 34.256 33.12 33.1 29.463 31.787 28.507 31.299 21.042 21.042 30.618
28.601 0.0
dt 57.0 65.0 42.5 42.5 37.0 67.0 37.0 67.0 35.0 42.0 43.0 43.0 60.0 45.0 27.0
%
```

```
STATE COOL : dens = 0.3478 0.3279 0.3358 0.3358 0.3575 0.3609 0.4173 0.4345 0.4135 0.3756 0.403
0.4909
power 24.239 28.121 28.964 28.964 27.857 29.895 27.207 22.966 21.894 24.292 23.147 18.596
dt 57.0 78.0 60.5 60.5 71.0 74.0 71.0 81.0 41.0 48.0 48.0 63.0
power 0.0 0.0 0.0
dt 1518.0 13.0 33.0
```

```
end history
end
```


BIBLIOGRAPHIC DATA SHEET

(See instructions on the reverse)

**NUREG/CR-7251
ORNL/TM-2018/782**

2. TITLE AND SUBTITLE

**Margins for Uncertainty in the Predicted Spent Fuel Isotopic Inventories
for BWR Burnup Credit**

3. DATE REPORT PUBLISHED

MONTH

December

YEAR

2018

4. FIN OR GRANT NUMBER

5. AUTHOR(S)

Ian Gauld, Ugur Mertuyrek

6. TYPE OF REPORT

Technical

7. PERIOD COVERED (Inclusive Dates)

8. PERFORMING ORGANIZATION - NAME AND ADDRESS (If NRC, provide Division, Office or Region, U. S. Nuclear Regulatory Commission, and mailing address; if contractor, provide name and mailing address.)

Oak Ridge National Laboratory
Managed by UT-Battelle, LLC
Oak Ridge, TN 37831-6170

9. SPONSORING ORGANIZATION - NAME AND ADDRESS (If NRC, type "Same as above", if contractor, provide NRC Division, Office or Region, U. S. Nuclear Regulatory Commission, and mailing address.)

Division of Systems Analysis
Office of Nuclear Regulatory Research
U.S. Nuclear Regulatory Commission
Washington, D.C. 20555-0001

10. SUPPLEMENTARY NOTES

11. ABSTRACT (200 words or less)

This report describes research to develop a technical basis to expand burnup credit to boiling water reactors (BWRs). One of the largest components of uncertainty in burnup credit analyses is the predicted isotopic inventories of spent fuel as applied to the criticality safety analysis application model. The analysis of BWR fuel inventories is challenging due to the complexity of BWR assembly designs, the lack of publicly available radiochemical assay measurements, and limited access to documentation on fuel design and operating conditions. This study has compiled and evaluated experimental data on measured nuclide concentrations in commercial spent fuel for more than 75 fuel samples that cover a wide range of modern assembly designs and operating conditions. These data were applied to predict the net effect of isotopic uncertainties on the effective neutron multiplication factor for a representative spent nuclear fuel storage system. The experimental data, uncertainty analysis methodology, and results for a dry storage cask application system are described. The results are applicable to BWR burnup credit beyond peak reactivity where any initial gadolinium present in the fuel has been fully depleted.

12. KEY WORDS/DESCRIPTORS (List words or phrases that will assist researchers in locating the report.)

boiling water reactor
burnup credit
nuclide uncertainty analysis
SCALE
spent nuclear fuel
isotopic validation

13. AVAILABILITY STATEMENT

unlimited

14. SECURITY CLASSIFICATION

(This Page)

unclassified

(This Report)

unclassified

15. NUMBER OF PAGES

16. PRICE



Federal Recycling Program



UNITED STATES
NUCLEAR REGULATORY COMMISSION
WASHINGTON, DC 20555-0001

OFFICIAL BUSINESS



@NRCgov



NUREG/CR-7251

Margins for Uncertainty in the Predicted Spent Fuel Isotopic Inventories for BWR Burnup Credit

December 2018